ASPECTS OF UNDERGROUND DISPOSAL OF RADIOACTIVE WASTE IN ROCK SALT

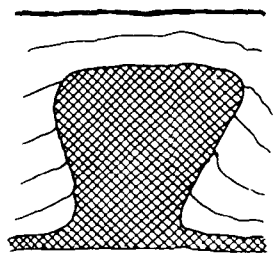

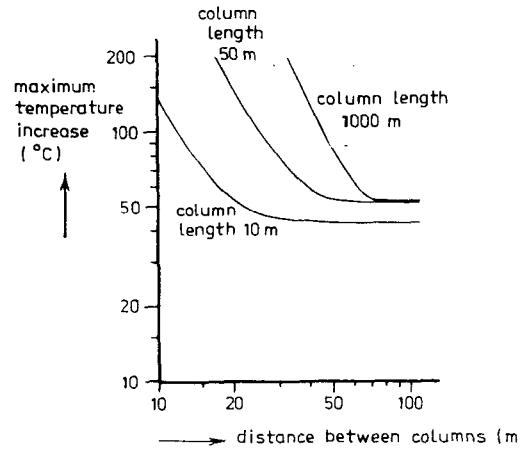

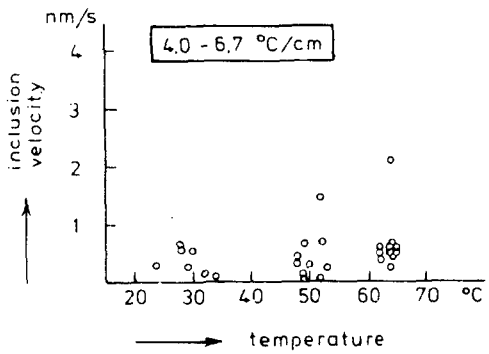

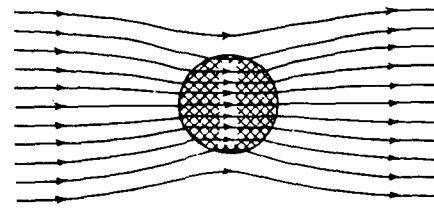

W.M.G.T. van den Broek

ASPECTS OF UNDERGROUND DISPOSAL OF RADIOACTIVE WASTE IN ROCK SALT

CIP-GEGEVENS KONINKLIJKE BIBLIOTHEEK, DEN HAAG

Broek, W.M.G.T. van den

Aspects of underground disposal of radioactive waste in rock salt / W.M.G.T. van den Broek. - [S.l. : s.n.]. - Ill.
Proefschrift Delft. - Met lit. opg.
ISBN 90-9002816-1
SISO 644.5 UDC 628.396:628.4.047(043.3)
Trefw.: radioactieve afvalstoffen ; opslag.

Druk: ALEVO - Delft

ASPECTS OF UNDERGROUND DISPOSAL OF RADIOACTIVE WASTE IN ROCK SALT

PROEFSCHRIFT

ter verkrijging van de graad van doctor
aan de Technische Universiteit Delft,
op gezag van de Rector Magnificus, prof. drs. P.A. Schenck,
in het openbaar te verdedigen ten overstaan van een
commissie door het College van Dekanen daartoe aangewezen,
op donderdag 20 april 1989 te 14.00 uur

door

Wilhelmus Maria Gerardus Theodorus van den Broek
natuurkundig ingenieur
geboren te Heerlen

Dit proefschrift is goedgekeurd
door de promotor prof.dr.ir. J. Hagoort.

STELLINGEN

behorende bij het proefschrift "Aspects of underground disposal of radioactive waste in rock salt" van W.M.G.T. van den Broek.

1. Een verantwoorde methode voor berging van uit Nederland afkomstig radio-actief afval dient op den duur beschikbaar te zijn, onafhankelijk van de vraag of men doorgaat met de opwekking van elektriciteit door middel van kernenergie.

2. Aan de ondergrondse berging van radio-actief afval dienen hoge veiligheidseisen te worden gesteld; men dient echter te beseffen dat absolute veiligheid niet bestaat.

3. Het pas definitief vastleggen van vorm en afmetingen waarin radio-actief afval zal worden geborgen nadàt voor een specifieke bergingsmethode is gekozen zal de efficiëntie van de berging ten goede komen.

4. Diepgelegen zoutholten worden niet in beschouwingen over berging van radio-actief afval in steenzout betrokken omdat deze zoutholten, bedreven onder atmosferische omstandigheden, zeer snel worden dichtgedrukt. Echter juist van dit dichtdrukken zou gebruik kunnen worden gemaakt om een snelle en goede isolatie van het afval ten opzichte van de biosfeer te waarborgen.
(dit proefschrift, hoofdstuk 3)

5. Het kan voordeel bieden om ondergrondse berging van kernsplijtingsafval in steenzout te laten voorafgaan door een periode van enige tientallen jaren van bovengrondse opslag.
(dit proefschrift, hoofdstukken 4 en 8)

6. De beschikbaarheid van een verantwoorde methode voor berging van kernsplijtingsafval houdt in dat een verantwoorde methode voor berging van het overige radio-actieve afval eveneens beschikbaar is.

7. Voor de beoordeling van de veiligheid van berging van radio-actief afval dient de maximale omvang van de effecten, veroorzaakt door de bergingsoperatie en de eigenschappen van het afval, te kunnen worden voorspeld.
(dit proefschrift, hoofdstuk 8)

8. Ook niet-nucleaire vormen van opwekking van elektriciteit brengen risico's en/of nadelen met zich mee.

9. Bij de opslag van energie in verband met het gelijkmatiger belasten van Nederlandse elektriciteitscentrales dient ondergrondse opslag van energie (in de vorm van opgepompte verzadigde pekel) in zoutholten, mede vanwege het zeer beperkte bovengrondse ruimtebeslag, serieus te worden overwogen.
(Quist, B.B., Holscher, H. and Verschuur, E.: Energy storage systems for electrical energy, Solution Mining Research Institute Autumn Meeting, Amsterdam, September 1986.)
(Grupping, A.W.: BOPAC bekeken, De Ingenieur, 98 (oktober 1986) 36.)

10. De door Hume en Shakoor gepresenteerde, aan Dreyer ontleende, schuifspanningen in de kruipkrommen van steenzout zijn op een onjuiste wijze omgerekend van kp/cm^2 (kilogramkracht per vierkante centimeter) naar GPa (gigapascal).
(Hume, H.R. en Shakoor, A.: Physical properties data for rock salt, chapter 3 (Mechanical properties), NBS Monograph 167, U.S. Department of Commerce, Washington, 1981.)
(Dreyer, W.: The science of rock mechanics, Part 1 (The strength properties of rocks), Trans Tech Publications, Clausthal-Zellerfeld, 1972.)

11. Bij het ont-oliën van water door middel van plaatseparatie wordt, bij een vlakke oliedruppelgrootte-karakteristiek, nog circa éénderde deel van de oliedruppels met een diameter kleiner dan de kritische druppeldiameter afgescheiden.
(Van den Broek, W.M.G.T.: Some theoretical aspects of de-oiling of water by plate separation, Delft Prog. Rep., 13 (1988/1989) 87.)

12. Voor het ont-oliën van water door middel van gasflotatie zijn zeer kleine gasbelletjes niet bruikbaar.

13. De beschikbaarheid van complexe rekenprogramma's voor de oplossing van fysisch-mathematische problemen maakt de kennis van analytische benaderingen niet overbodig.

14. De mooiste automobielen van deze eeuw werden gebouwd in de jaren dertig, met de jaren vijftig als goede tweede.

15. Het schrijven van het woord "bommelding" als "bom-melding" leidt tot een verbetering van de leesbaarheid, in het bijzonder voor lezers van stripverhalen.

16. Eén van de voordelen van het daadwerkelijk promoveren is, dat de irritante vraag "En, hoe staat het met je promotie?" je niet meer zal worden gesteld.

aan Hannie
en Eveline

CONTENTS

Contents (continued) page

INTRODUCTION

Nuclear power plants, hospitals, laboratories and the industry produce radioactive waste. Several components of the waste remain radioactive for thousands of years or more. The waste must therefore be isolated from the biosphere for a very long time. By far the most studied isolation method is disposal by burial in a deep earth formation.

Part of the radioactive waste, notably the high-level nuclear waste (HLW), generates heat. To prevent an excessive increase in temperature in a potential host formation, the latter must have a relatively high thermal conductivity. Furthermore, radioactive components may at some point in time come in contact with ground-water. Therefore a potential host formation must in addition have an extremely low permeability, so that ground-water influx and hence any spreading of radioactivity by means of ground-water will be minimal.

The subject of this thesis concerns disposal of radioactive waste in underground rock-salt formations. Rock salt is one of the few potential host formations for accomodating radioactive waste; it has a relatively high thermal conductivity and is practically impermeable. Other potential host formations are granite and clay. Rock salt has been chosen in this study because it has better conductivity and permeability characteristics than the other two rock types, and occurs extensively underground in the Netherlands. As to salt characteristics and expected volumes of the radioactive waste the thesis is based on the situation in the Netherlands, where future extension of the nuclear power electricity supply up to a total capacity of 3500 MWe is being considered. Many of the considerations and studied effects are, however, not particularly related to the waste volume and salt formation type, and several results are therefore more widely applicable.

State of the art

Research on disposal of radioactive waste pertains to:

Characteristics and volume of the waste

Radioactive waste is usually made available for disposal in a few different forms, viz.: as cylindrical stainless-steel canisters containing the highly active waste vitrified with glass (the HLW) and, furthermore, in steel vessels or as concrete blocks in case of wastes of

lower activity. In each type a large variety of components is present. The characteristics of the several types of waste concentrate are sufficiently well known.

Properties of salt formations

The extension of the underground salt formations in the Netherlands and the Dutch continental shelf is well-known. Some salt formations have been thoroughly investigated in connection with actual or proposed mining activities. Of other formations often no composition data are known. Sufficient overall knowledge is present, however, to estimate a few relevant properties of rock salt, as for instance the thermal properties. Rock-mechanical properties vary considerably with salt type. From measurements in the laboratory a wealth of data on salt deformation is available. It remains to be seen how far these data hold for deformations at geological rates. As to radiation damage of salt, data on structural and compositional changes are restricted. Such changes have been shown, however, to be strongly dependent on salt type and on radiation level.

Mining and disposal techniques

Two options are available for the disposal of radioactive waste in salt formations, viz.: (i) a salt mine comprising (dry) bore holes and excavated bunkers and (ii) bore holes drilled from the surface for the waste canisters in combination with a cavity washed out at a bore-hole bottom in the salt for the other waste concentrates. The required mining and drilling techniques have been put into practice numerous times for other ends than radioactive waste disposal. Adaptation of these techniques for disposal purposes seems feasible. Specific problems connected with waste disposal operations (protection against radiation during transport of the waste, handling of sizeable waste packs) can in principle be solved.

Interaction with subsurface rock material

The radioactive waste interacts with the rock material in a number of ways:

- The heat generation of some waste components will result in a significant underground temperature disturbance. The resulting increase in temperature can be predicted with sufficient accuracy.
- The underground heat regime may induce brine inclusions in the salt to migrate toward the waste canisters and possibly cause damage to the

HLW-canisters, for example by corrosive attack. There are indications that the migration phenomenon is of limited importance.

- Mining operations as well as the placement of heat radiating radioactive waste may activate movements in the salt. Salt movements are since long the object of study. Sufficient knowledge is available to be able to predict salt movements for the coming few thousand years.
- The disposal of the waste might cause radiation damage in the salt, forming colloidal sodium and free chlorine molecules. The extent of radiation damage, if any, of the salt at the radiation level pertaining to waste disposal situations, cannot yet reliably be predicted.

Protecting barriers between waste and biosphere

Placement of durable barriers between the waste and the biosphere may keep the waste isolated from the biosphere for a very long time. As protecting barriers can be mentioned: the matrix material in which the waste is embedded (e.g. glass), the stainless-steel wall of the waste canisters, the salt formation itself and the formations around the salt. Not all barriers have to be equally resistant, the presence of one very strong barrier can outweigh the other barriers.

Problem areas

From the above it is evident that there are a number of problem areas. Some important items are:

- Achieving optimum distribution of the waste components over the different types of waste concentrate.
- Adaptation of available mining techniques specifically for the disposal of radioactive waste.
- Extent and effect of migration of brine inclusions.
- Long term salt movements.
- Extent of and consequences of radiation damage of salt.

A considerable part of this thesis deals with these problem areas and related aspects.

Objectives

The general objective of this study is to add relevant data and knowledge to the already available know-how on disposal of radioactive waste in rock salt.

Specific objectives are:

- Calculation of the increases in temperature in the rock salt resulting from the HLW-disposal for a number of disposal configurations, and an analysis of the influence of impurities in rock salt on these increases.
- Collection of experimental data on migration of brine inclusions in sodium chloride and calculation of the maximum amount of brine that can be expected to assemble around a HLW-canister under practical disposal circumstances.
- Investigation of means of influencing the distribution of the various specific radioactive components over the several types of waste concentrate, such as to arrive at optimum conditions for the disposal operation. One such condition pertains to the dimensions of the waste concentrates, other conditions to heat generation, radiation intensity etc.
- Study of the protective quality of the barrier formed by melting together the high-level nuclear waste with glass.

Organization of the thesis

The thesis comprises eight chapters, which can be read separately.

The first three chapters review available know-how in relation to the subject of this thesis. Successively are discussed: radioactive waste (forms, amounts, properties), salt formations (types, amounts, properties) and mining techniques (types, advantages and disadvantages). These chapters are based on the literature in the respective fields.

Chapter 4 treats the increase in temperature due to the heat generation by the HLW. While most other authors give calculations for disposal at fixed spacings of the bore holes only, this chapter offers a more general treatment of the increase in temperature. This allows us to predict this increase for any variety of disposal pattern. The chapter concludes with an analysis of the influence of impurities in rock salt on the increase in temperature.

Chapter 5 deals with the possible thermal migration of brine inclusions in the rock salt in the direction of the HLW heat source. Such brine inclusions might exert aggressive action when contacting the buried waste canisters. This chapter describes our experiments on migration and their results. We present a rather simple theoretical model which gives a reasonable description of the migration mechanism. As an outcome of this work an estimate can be given of the maximum amount of brine that would

migrate toward the waste under disposal circumstances. The experimental migration data were obtained using sodium chloride single crystals, but it can be argued that propagation velocities of brine inclusions in natural rock salt will be of the same order of magnitude.

High-level nuclear waste is the most radioactive type of waste concentrate to be dealt with. This waste is a combination of a large number of components with varying properties. A new concept proposed by the author is to separate this HLW into two waste categories. The advantage of this concept lies in the typical properties of these two waste categories: one category contains the (short-living) heat-generating components, the other category contains the long-living components, with negligible heat-generation rate. Because of these differing properties, disposal of the HLW, when split in separate parts, can be carried out more effectively. Chapter 6 gives a first analysis of the advantages of this concept and discusses consequences for the processing of the HLW prior to disposal.

One of the barriers between the radioactive waste and the biosphere is the glass matrix with which the HLW is vitrified. This barrier has received only little attention in the past. In chapter 7 the effect of the glass as a single barrier is analysed. To this end it was assumed that all other barriers (the salt included) had become ineffective c.q. had disappeared. The effect of the glass barrier was studied by determining the radioactive contamination of the ground-water as a result of the slow dissolution of the glass.

The last chapter, chapter 8, gives a combined treatment of some relevant aspects of disposal of high-level nuclear waste in rock salt. Here the main conclusion of the thesis is presented. The chapter is concluded with a number of recommendations for further study.

Chapter One

RADIOACTIVE WASTE

Abstract

Radioactive waste comprises low-active solid waste, LAW, medium-active solid waste, MAW, high-active solid waste, HAW, and the waste resulting from the reprocessing of the spent fuel elements, high-level nuclear waste, HLW. Most of the LAW, MAW and HAW is mixed with cement and contained in steel drums. HLW is mixed with glass, vitrified and in this way incorporated in glass cylinders; these cylinders are subsequently contained in stainless-steel canisters.

Estimates of yearly and total amounts of radioactive waste for a 3500 MWe nuclear power plant scheme are presented. The radioactive waste from national hospitals and laboratories is also taken into account.

1.1 Introduction

Radioactive waste is produced in solid, liquid and gaseous form. Liquid and gaseous wastes of very low radioactivity are usually (mostly after dilution) discharged into the open environment (Vrijen [1]). The remaining liquid and gaseous wastes are solidified, or are burned. In this last case most of the radioactive components are captured in filters present in the flue stack. Thus the larger part of the radioactive waste is in, or is converted into, solid form. We restrict ourselves to the solid and solidified radioactive waste.

1.2 Waste classification

There are different ways to classify radioactive waste:

- according to type of radiation (α-, β-, γ-radiation);
- according to the half-lifes of the radioactive components (short-living, long-living components);
- according to source (hospitals, laboratories, nuclear power plants);
- according to surface dose-equivalent rate.

This last classification is most frequently used, and will also be used here. The following waste classes are distinguished [1]:

- Low-active solid waste, LAW (in Dutch: laag-actief vast afval, LAVA), surface dose-equivalent rate below 200 mrem/h[†].
- Medium-active solid waste, MAW (in Dutch: middel-actief vast afval, MAVA), surface dose-equivalent rate between 200 and 2000 mrem/h.
- High-active solid waste, surface dose-equivalent rate above 2000 mrem/h. This last waste class can be subdivided:
- High-active waste with a relatively low heat production, HAW (in Dutch: hoog-actief vast afval, HAVA).
- Heat generating high-active waste: the waste resulting from the reprocessing of the spent fuel elements. For this waste type the term "high-level nuclear waste", HLW, will be used (in Dutch: kernsplijtingsafval, KSA).

Reprocessing of the spent fuel elements, whereby the useful components (uranium, plutonium) are separated from the other components (among others: fission products) does not form a necessary part of the management of nuclear fuel and nuclear waste. An alternative for reprocessing is to dispose of the spent fuel as radioactive waste. However, this alternative leads to inefficient use of nuclear fuel and is not practised in the Netherlands. We therefore do not take this alternative into account.

1.3 Waste forms

Radioactive waste in its original form is not very suited for storage or disposal. Most of the low-, medium- and high-active waste is therefore compressed, mixed with cement, and contained in steel drums. An exception is radioactive waste with short-living components; this waste becomes ordinary (non-radioactive) waste within an acceptable time, and can be treated as such [3].

According to Codee [3] two types of containers for LAW, MAW and HAW will be used in the Netherlands. Hamstra [4] gives five container types and the

[†] The "rem" is a unit for absorbed radiation energy, whereby also the biological effects are taken into account: 1 rem = 10^{-2} q J/kg with q the "quality factor" referring to biological perception; q lies between 1 and 20, dependent on the radiation type [2].

Van Hattem en Blankevoort report [5] considers nine container types. The volumes of these containers vary between 0.2 and 2.2 m^3, the diameters between 43 and 125 cm.

A separate waste category is the waste resulting from the dismantling of nuclear power plants. A special characteristic of this waste is, that it will contain very large construction elements. For any disposal method very large structures are unsuited, and these elements will have to be broken down to smaller pieces. According to Hamstra [4] these smaller pieces will still be of considerable size: $2.3 \times 2.3 \times 4.6 = 24\ m^3$. A further reduction in size is of course possible and probably recommendable: the advantages (better transport possibilities, fewer restrictions imposed on the disposal facility) will have to be carefully placed against the drawbacks (among others: extra energy, and thus extra costs).

The high-level nuclear waste, HLW, is kept in liquid form, in the reprocessing plant for about 10 years. In this period several of the heat producing components decay to less active or to stable components. After this the HLW is mixed with glass and vitrified, in a cylindrical form. Finally, the glass cylinders are packed in stainless-steel canisters. These processes will be carried out outside the Netherlands, in France and in Great Britain.

The dimensions of the HLW disposal elements in final form are not yet standardized. At first canisters with a diameter of the order of 20 cm were considered [6,7]. However, nowadays 43 cm is the most frequently used diameter in waste disposal analyses [4,5].

1.4 Amounts of waste in the Netherlands

The amounts of waste depend on the capacity and the operation period of the nuclear power plants. We will base ourselves on the Dutch 3500 MWe nuclear power plant scheme [8], i.e. an extension with 3000 MWe of the existing nuclear power capacity of 500 MWe; we will assume a 40 years operation period of the nuclear power plants.

Van Erpers Royaards [9] estimates the amounts of LAW, MAW and HAW for the two existing nuclear power plants to be about 1040 m^3 per year, and for three future 1000 MWe nuclear power plants about 3750 m^3 per year. Apart from nuclear power plants also hospitals and laboratories produce radioactive waste, viz: about 1000 m^3 per year [3].

Table 1.1 Yearly and total amounts of radioactive waste for the Dutch 3500 MWe nuclear power plant scheme, 40 years in operation, including the waste from hospitals and laboratories.
Assumed period for hospitals and laboratories: 100 years.

waste type	volume (m^3)		number of canisters	
	yearly	total	yearly	total
LAW, MAW and HAW:				
- from nuclear power plants	4,800	192,000		
- from dismantling of nuclear power plants		70,000		
- from hospitals and laboratories	1,000	100,000		
total LAW, MAW and HAW	5,800	362,000		
high-level nuclear waste, HLW:				
- in case of 50 l canisters	8.8	350	175	7,000
- in case of 200 l canisters	8.8	350	44	1,750

The figures for the amount of vitrified HLW vary. An average value from four references [10-13] is 2.5 m^3 per 1000 MWe.year. The Van Hattum and Blankevoort report [5] gives 3.5 m^3 per 1000 MWe.year. According to Van Erpers Royaards [9] the amount of HLW is still larger, 5 m^3 per 1000 MWe.year. We shall base ourselves on the first figure, 2.5 m^3 HLW per 1000 MWe.year, bearing in mind that this figure might be an underestimation.

After 40 years operation the dismantling of the nuclear power plants also yields radioactive waste. Estimates vary between less than 10,000 m^3 up to 30,000 m^3 per 1000 MWe [14]. Rather arbitrarily we will use a figure of 20,000 m^3 per 1000 MWe.

Table 1.1 summerizes the yearly and total amounts of radioactive waste. For the waste from hospitals and laboratories a 100 year period was taken.

1.5 Waste properties and composition

Quantitative data on the heat generation of HLW as a function of time are required for calculating the increases in temperature. Such data are given in the corresponding chapter of this thesis, chapter 4. Similarly data on the composition of HLW are essential for evaluation of the consequences of

the several separation schemes for this waste type. Information about this composition is presented in chapter 6.

LAW, MAW and HAW consist of a large variety of materials, from lightly contaminated clothing to filters used for waste-water purification [13]. The concentration of the radioactive components is much lower than in HLW. Precise knowledge of the composition is not essential for the subjects treated in this thesis.

With regard to the properties of LAW, MAW and HAW: the most important property is the surface dose-equivalent rate. The variation of this property was already given. The heat generation is negligible, compared with that of HLW (except for a single HAW category [5]). The only characteristic in which LAW, MAW and HAW surpass HLW is the amount of waste.

1.6 Discussion and conclusions

1. The amounts of radioactive waste presented in this chapter were calculated for a typical nuclear power plant scheme for the Netherlands. For other nuclear power plant schemes the waste amounts can easily be derived from the presented data.
2. The presented amounts of waste must not be treated as absolute figures; a reasonable margin should be taken into account. This holds especially for the figures on dismantling of nuclear power plants and for the amount of HLW.
3. An analysis to determine which waste dimensions are the optimal ones has still to be made. For this analysis the complete waste processing and disposal operation has to be considered. Specific dimensions mentioned in this chapter (HLW-canister diameters, dimensions of the waste from dismantling) must therefore be considered as provisional, not final.

List of symbols

q quality factor for the biological effects of radiation

List of abbreviations

HAVA hoog-actief vast afval (= HAW)
HAW high-active solid waste

HLW high-level nuclear waste

KSA kernsplijtingsafval (= HLW)

LAVA laag-actief vast afval (= LAW)

LAW low-active solid waste

MAVA middel-actief vast afval (= MAW)

MAW medium-active solid waste

MWe megaWatt (electric)

References

1. Vrijen, J.: Interim opslagfaciliteit voor laag- en middel-radioactief afval, Symposium Radioactief afval in Nederland, Koninklijk Instituut van Ingenieurs, The Hague, 1984.
2. Weber, J. and Rasmussen, C.E.: Stralingsbescherming, Delftse Uitgevers Maatschappij, Delft, 1985.
3. Codee, H.D.K.: Radioactief afval, Symposium Radioactief afval in Nederland, Koninklijk Instituut van Ingenieurs, The Hague, 1984.
4. Hamstra, J.: Doelstellingen en randvoorwaarden inzake het ondergronds in een zoutformatie opbergen van het Nederlandse nucleaire afval, Report Commissie Opberging te Land, OPLA 84-78, Ministry of Economic Affairs, The Hague, 1984.
   See also: Voorstel voor een programma van onderzoek inzake geologische opberging van radioactief afval in Nederland, Report Commissie Opberging te Land, Ministry of Economic Affairs, The Hague, 1984.
5. Locatie-onafhankelijke studie inzake de aanleg, bedrijfsvoering en afsluiting van mogelijke faciliteiten voor de definitieve opberging van radioactief afval in steenzoutformaties in Nederland, Van Hattum en Blankevoort/Koninklijke Volker Stevin, Beverwijk, 1986.
6. Hamstra, J. and Kevenaar, J.W.A.M.: Temperature calculations on different configurations for disposal of high-level reprocessing waste in a salt dome model, Report Netherlands Energy Research Foundation, ECN-42, 1978.
7. Ploumen, P.: Numerische Langzeitberechnung dreidimensionaler Temperaturfelde mit Hilfe eines speziellen Finite-element-verfahrens am Beispiel der Endlagerung hochradioaktiver Abfälle im Salzgestein, Thesis Rheinisch-Westfälischen Technische Hochschule Aachen, 1980.
8. Energienota, Ministry of Economic Affairs, The Hague, 1974.
9. Van Erpers Royaards, R.: Kernafval, Kluwer, Deventer, 1982.
10. Ploumen, P. and Strickmann, G.: Berechnung der zeitlichen und raümlichen Temperaturverteilung bei der säkularen Lagerung hochradioaktiver Abfälle in Salzstöcken, Report Rheinisch-Westfalische Technische Hochschule Aachen, 1977.
11. Hamstra, J.: Kanttekeningen bij het rekenen aan opberging van vastgemaakt KSA in een zoutkoepel, Report Netherlands Energy Research Foundation, Petten, 1976.
12. Demmenie, C.A.: Het opbergen van KSA-cylinders in boorgaten, Report Delft University of Technology, 1976.
13. Dietz, D.N.: De berging ondergronds van radio-actief afval, AO 1680, Stichting IVIO, Lelystad, 1977.
14. Maatschappelijke Discussie Energiebeleid: Analytische Verslagen van de Controversezittingen in het kader van de Informatiefase, Stuurgroep Maatschappelijke Discussie Energiebeleid, The Hague, 1984.

Chapter Two

SALT FORMATIONS

Abstract

Most of the Dutch salt is Zechstein salt, 200-250 million years old. The salt formations beneath the main land (NE-Netherlands) are well-known. It is less known that about 80 % of the Dutch salt lies beneath the Dutch part of the continental shelf.

The composition of the rock salt varies. In most cases 90-99 % halite (NaCl) is present; the rest of the salt consists of impurities, almost exclusively other salts with anhydrite ($CaSO_4$) as the most important impurity.

In many places the original salt layer has been deformed to salt pillows and salt domes. The velocities connected with these halokinetic processes are at most 0.25 mm/year. Movements to be expected in undisturbed salt layers or in already formed salt pillows or salt domes will be very much smaller, or even absent.

An important property of rock salt, in connection with radioactive waste disposal, is its permeability: at some depth rock salt can be considered impermeable under in-situ circumstances.

2.1 Origin and age of salt deposits

Salt deposits have been formed through evaporation of sea water. The salt deposition process can be described with the shallow basin model [1-4], see figure 2.1. Consider a shallow basin filled with sea water. The basin is connected with the sea via a channel above a bar that separates sea and basin. The basin is supposed to be located in a warm climate, with a high water evaporation rate. Loss of basin water by evaporation is compensated by influx of fresh sea water containing salt. Since the water in the basin evaporates, there is a net transport of salt to the basin: the basin water becomes more and more concentrated. Eventually salt will precipitate and the basin will be filled with salt.

The shallow basin model is a relatively simple model. It explains the deposition mechanism. It does not explain why some salt formations have original thicknesses of 1000 m or more. A possible explanation might be the

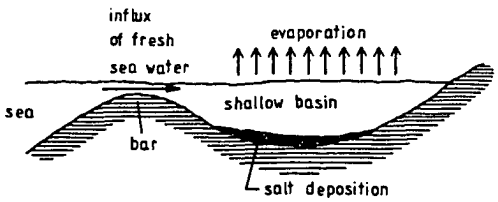

Figure 2.1 Shallow basin salt-deposition model.

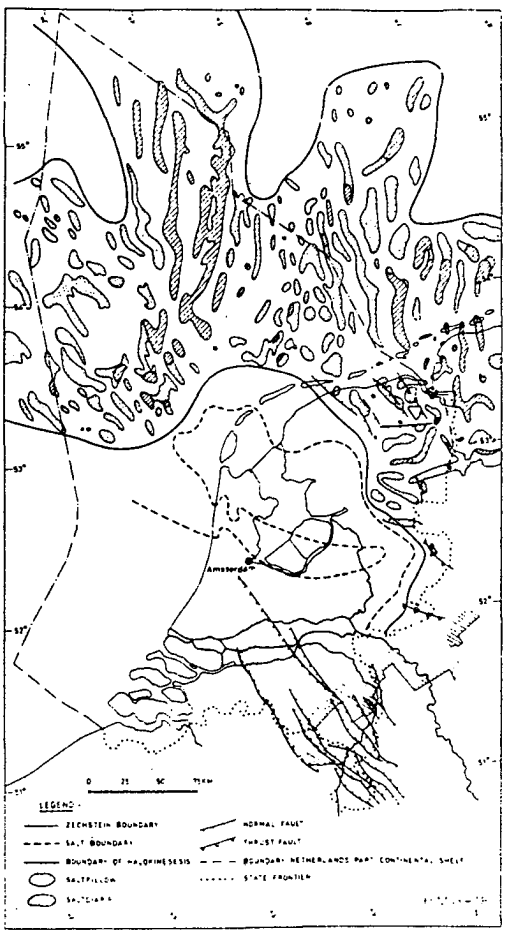

Figure 2.2 Extension of the Zechstein basin under the Netherlands and under the Dutch part of the continental shelf.
Source: Harsveldt [8], based on a figure by Heybroek et al. [9].

simultaneous occurrence of slow subsidence of the basin floor during salt deposition [5]. An alternative explanation is stratification: the occurrence of layers of brine with increasing density (and salt concentration) with increasing depth. It can be shown that under these circumstances salt can also be deposited in deep basins (see the description of the "deep basin model" by Schmalz [5]).

Eby [6] and Borchert and Muir [7] give data on the distribution and age of the salt deposits of the world. Some salt deposits (in Siberia, Ethiopia and Iran) are very old, about half a billion years or more. However, many deposits are younger. The larger part of the Dutch salt is Zechstein salt, 200-250 million years old. The Zechstein salt covers the area North Germany, Northern Netherlands, North Sea, East England. Figure 2.2 gives the presence on Dutch territory (on shore as well as offshore). Furthermore there is somewhat younger salt, of Triassic origin, in the Eastern Netherlands.

Another important salt deposit is the Gulf Coast salt (south-eastern USA, extending into the Gulf of Mexico). The salt here is 150-200 million years old [1,10]. This area is of importance because of the many mining activities and because of the literature and data available on this deposit.

Salt deposition is of course not restricted to the past, also nowadays salt deposits are formed. An example is the deposition process in the Dead Sea [11].

2.2 Composition of rock salt

Evaporation of entrapped marine water causes successive precipitation of several salts. This process has been described in literature [7,12-15].

The salts to precipitate first are carbonates (calcite, dolomite) and gypsum. Precipitation of sodium chloride (halite) starts when the concentrations of the different components in sea water have become about 10 times as large as their respective concentrations in present-day sea water.

In the halite precipitation process two phases can be distinguished:

Phase A

For a concentration factor (relative to the original volume of sea water) between 10 and 60, halite precipitates simultaneously with calcium sulphate (calcium sulphate in the form of gypsum, or anhydrite, or polyhalite). In this phase the bulk of the halite is precipitated.

Phase B

For a concentration factor of more than 60, magnesium salts (kieserite, bischofite), potassium chloride (sylvite) and/or magnesium-potassium double salts (carnallite, kainite) precipitate along with the rest of the halite.

Several factors influence the precipitation process, and they are different for each salt deposit: temperature, pressure, sea-water composition. This last factor is not a universal constant, but depends on the considered location and geological period.

The salts mentioned do not form the complete list of materials that can be present in rock salt. According to Lotze [12] small amounts of mainly hematite, quartz and clay minerals can also be present. These materials, often present as solids in the evaporating sea-water, can be entrapped in the growing rock-salt formation. The same applies to the sea water itself: also small amounts of brine are found entrapped in rock salt (see also chapter 5).

Summarizing, the most important materials that can be found in rock-salt formations are:

halite	$NaCl$
calcite	$CaCO_3$
dolomite	$CaCO_3.MgCO_3$
gypsum	$CaSO_4.2H_2O$
anhydrite	$CaSO_4$
polyhalite	$K_2SO_4.MgSO_4.2CaSO_4.2H_2O$
kieserite	$MgSO_4.H_2O$
bischofite	$MgCl_2.6H_2O$
sylvite	KCl
carnallite	$KCl.MgCl_2.6H_2O$
kainite	$KCl.MgSO_4.3H_2O$
hematite	Fe_2O_3
quartz	SiO_2
brine	H_2O (plus dissolved salts)
clay minerals	

What is the concentration of these materials in rock salt, in particular what is the halite concentration?

Analysis of the composition of sea-water gives some information about the halite concentration on a large scale. Complete evaporation of present-day

sea-water yields an overall halite concentration in the salt of about 70 weight % [16]. The composition of sea-water, however, has changed in the course of time. Complete evaporation of NW-European sea-water in the Zechstein period (data by Ruchin [17]) would yield a halite concentration in the salt of about 84 weight % [16].

These halite concentrations, however, do not provide more than a rough indication of the real halite concentration in rock salt. In many cases a full evaporation cycle was not completed. This implies that the halite concentration will generally be higher than 70 or 84 weight % respectively: these numbers are lower limits for the halite concentration. Even for a full evaporation cycle there will be regions in the rock salt where the halite concentration is very high. During phase A halite is by far the most important precipitating salt.

In the literature halite concentrations of about 99 weight % are mentioned [12,18,19]. Most rock-salt formations, however, have halite concentrations between 90 and 99 weight %. A typical value for the halite concentration is 95 %; it was observed that domal salt has a somewhat higher halite concentration than the salt of bedded deposits [19].

The concentration of the impurities will generally be 1-10 weight %. In very pure rock salt the most important impurities are frequently anhydrite and clay. Especially anhydrite occurs as an important impurity in most salt formations. No simple rules can be given for the occurrence of the other impurities, their presence and concentration depend on the specific conditions during and after the formation of the considered salt deposit.

2.3 Development and stability of salt formations

A salt deposit can become buried under sediments of the successive geological periods. These sediments generally have a higher specific mass than the salt, a relatively light material. Salt can be described as an extremely viscous liquid. The system of a light (viscous) liquid beneath heavier sediments is in principle unstable. In many places the original salt deposit layers have been deformed in the course of time and have broken through the overlying strata. This led to the formation of salt domes. In many cases deformation occurred without a breakthrough; here the salt layers have an increased thickness and we speak of salt pillows. Figure 2.3 gives

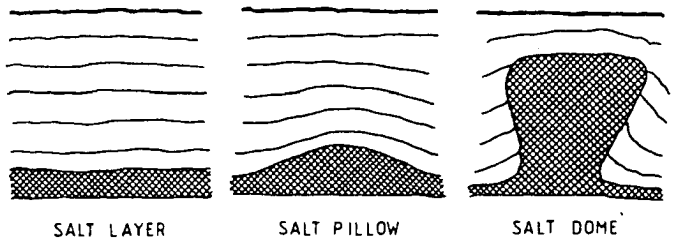

Figure 2.3 Schematic representation of the three types of salt formations and the positions of the overlying strata.

the three types of salt formations: layer, pillow and dome. The salt deformation phenomenon is known as "halokinesis" [20].

The formation of salt pillows and domes did not always occur. It was observed that the original salt layer as well as the overlying sediment must have a certain thickness (of the order of 300 and 1000 m respectively - see Trusheim [21,22]) before halokinesis can take place.

During salt dome formation the rising salt may have come into contact with flowing ground-water. Salt is very soluble and this contact would subsequently have led to salt dissolution and transport away from the dome. However, some impurities in the salt - especially calcium sulphate - have low solubilities and would therefore have remained behind. That is the reason why many salt domes are capped by a (cap)rock on top, mainly consisting of anhydrite or gypsum.

The existence of the halokinesis phenomenon implies that a salt formation is in principle unstable. However, on a geological time scale stable formations do not exist. What matters is which deformation velocities may occur in practice. The velocities for an undisturbed salt layer are extremely small. The same applies for salt pillows and salt domes once they have been formed. The largest velocities will occur during the growing phase of a salt dome (or a salt pillow). Even then the velocities are very small. The largest velocities to be expected for Dutch salt in the growing phase are 0.25 mm/year [23]. High-level nuclear waste (HLW), the most active type of radioactive waste type, remains very toxic for a period of well over a million years (see chapter 7). Combination with the mentioned salt velocity yields that salt displacements of several hundred meters during the period of HLW-toxicity cannot be excluded.

2.4 Porosity and permeability of rock salt

For this thesis a number of physical properties of rock salt are of importance. Here the porosity and permeability will be discussed. Data on other relevant properties will be presented in the corresponding chapters (e.g. thermal properties in chapter 4).

Laboratory measurements of the porosity of rock salt yield values of about one to a few % (0.62-7.17 % (Aufricht and Howard [24]); 0.59-1.71 % (Reynolds and Gloyna [25])). Permeability data measured in the laboratory differ many orders of magnitude (0.0001-795 millidarcy [24]). However, one may question the validity of these figures, because "standard permeability tests on rock-salt cores are usually of no use, since the cores are damaged when taken out of their tri-axial in-situ stress field; such damage may be caused by stress relief deformation that results in intergranular loosening" (Baar [26]). In-situ tests may only be better to some degree, for also for these types of tests the original stress field must be disturbed.

More information on the permeability can be obtained from observations made during mining activities in rock salt. On the one hand the presence of pockets of entrapped gas [19,26] indicates that impermeable regions in rock salt may exist. On the other hand seeps and drips are known to be present in salt mines [19], and this may indicate permeability. Moreover, tests in a salt mine yielded permeabilities to gasoline of 0-6 millidarcy, with an average value of 0.3 millidarcy [24].

According to Lorentz et al. [19] "the permeability of halite is effectively zero when the pressure is sufficient to deform the halite plastically and close off the passageways at crystal interfaces". This conclusion is shared by Baar [26] and Hofrichter [27]. The presence of permeability as indicated by seeps and drips, or by the loss of stored gasoline, must therefore be ascribed to the changes in the rock salt due to mining activities. Permeability in rock salt may also be caused by permeable impurities, e.g. anhydrite [19]. Generally speaking, however, in-situ rock salt - under sufficient overburden pressure - is impermeable.

2.5 Salt formations in the Netherlands

The information given in this paragraph is derived from publications by Coelewij et al. [28], Harsveldt [8,29], Heybroek et al. [9], Van Montfrans

Table 2.1 Estimated areas of Dutch salt, divided in "land-salt" and "sea-salt", and distinguishing between halokinetic salt and thin salt layers. The areas are derived from figure 2.2.

salt type	land-salt		sea-salt		land- and sea-salt	
	(km^2)	(% of total salt area)	(km^2)	(% of total salt area)	(km^2)	(% of total salt area)
halokinetic salt	7,000	12	36,000	62	43,000	74
thin salt layers	5,000	9	10,000	17	15,000	26
total	12,000	21	46,000	79	58,000	100

[30], Mulder [31,32], Pannekoek [33], Rutten [34], Thiadens [3], Wassmann [35] and Van Wijhe et al. [36].

Figure 2.2 shows the extension of the Zechstein salt in the Netherlands and in the Dutch part of the continental shelf. The salt pillows and salt domes are restricted to the NE-part of the Netherlands and Northern part of the continental shelf. The total area of salt deposition is larger than the region mentioned: bordering the halokinesis region layer-salt is present. A peculiar extension of this salt is the tongue of some 20 km width, emerging from the North Sea and ending on the Veluwe, with a thickness of up to 200 m. The depth of the base Zechstein varies: about 3000-4000 m in the NE-Netherlands and on the continental shelf, less deep for the remaining salt.

The salt of the NE-Netherlands is the best known. In Twente rock salt is mined by Akzo Zout Chemie Nederland BV. Incidentally, this salt is not Zechstein salt but Triassic salt, about 200 million years old. The salt domes in the Groningen-Drenthe area have gained the most attention in discussions on radioactive waste disposal. However, these salt domes constitute only a limited number of the salt formations beneath the Netherlands and the Dutch continental shelf.

If we divide the Dutch salt in "land-salt" and "sea-salt" and make a distinction between thin layers (the region between the interrupted and uninterrupted lines in figure 2.2) and halokinetic salt, then we find data as presented in table 2.1. From this table we learn that only a fifth part of the Dutch salt is land-salt and that more than half of this salt consists

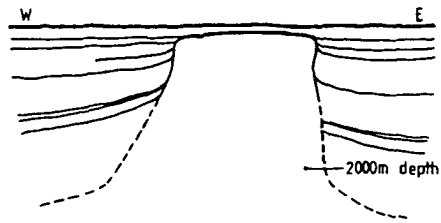

Figure 2.4 Profile of the Schoonlo salt dome in the Netherlands. Source: Mulder [33].

of halokinetic salt, thus salt with an originally thick mother layer. Four-fifth of the Dutch salt is sea-salt, and the amount of halokinetic sea-salt is five times the amount of halokinetic land-salt.

One of the best documented Dutch salt domes is the Schoonlo dome (figure 2.4). This relatively young dome was formed about 40 million years ago. The salt of this dome is mostly colorless or white. The grain size of the rock-salt crystals varies between coarse and fine. Small anhydrite bands are present and also some potassium salt.

In some places potassium salts are present in larger amounts, together with magnesium and potassium-magnesium salts. These amounts can be so large that mining of these salts is economically attractive. In the Veendam area these salts (mainly bischofite and carnallite) are mined by means of solution mining.

2.6 Conclusions

1. The Zechstein salt of Western Europe was formed 200-250 million years ago. Since then thick salt layers have in many places been deformed to salt pillows and salt domes.
2. Generally rock salt consists of 90-99 % halite; the rest of the salt consists mainly of other salts, with anhydrite as the most important impurity.
3. The deformation processes in salt are caused by the difference in density between the salt and the, heavier, overlying strata.

4. The deformation velocities in rock salt are very small. The value 0.25 mm/year can be taken as the largest velocity that can occur in halokinetic deformation processes in Dutch salt.
5. Deep-lying rock salt can generally be considered as impermeable.
6. Underlying the NE-part of the Netherlands and the Northern part of the Dutch continental shelf about 60,000 km^2 salt is present. 80 % of this salt lies beneath the sea.

List of abbreviations

HLW high-level nuclear waste

References

1. Hanna, M.A.: Salt domes: favorite home for oil, Oil and Gas Journal, 57 (2.2.1959) 138.
2. Raup, O.B.: Brine mixing; an additional mechanism for formation of basin evaporites, Bull. Amer. Assoc. Petr. Geol., 54 (1970) 2246.
3. Thiadens, A.A.: Het zout der aarde, hoofdstuk III (geologie van het zout), N.V. Kon. Ned. Zout Industrie, Hengelo, 1968.
4. Pannekoek, A.J. and Van Straaten, L.M.J.U. (editors): Algemene Geologie (third edition), Wolters-Noordhoff, Groningen, 1982.
5. Schmalz, R.F.: Deep-water evaporite deposition: a genetic model, Bull. Amer. Assoc. Petrol. Geol., 53 (1969) 798.
6. Eby, J.B.: Salt dome interest centers on Gulf Coast, World Oil, 143 (October 1956) 143.
7. Borchert, H. and Muir, R.O.: Salt deposits, D. van Nostrand, London, 1964.
8. Harsveldt, H.M.: Salt resources in the Netherlands, Geologica Ultraiectina Special Publication No. 1 (August 1980) 29.
9. Heybroek, P., Haanstra, U. and Erdman, D.A.: Observations on the geology of the North Sea area, Proceedings Seventh World Petroleum Congress, Vol. 2 (1967) 905.
10. Kupfer, D.H.: Shear zones inside Gulf Coast salt stocks help to deliniate spines of movement, Bull. Amer. Assoc. Petrol. Geol., 60 (1976) 1434.
11. Zak, I.: The geochemical evolution of the Dead Sea, Proceedings Fifth Symposium on Salt, Vol. 1, 181, The Northern Ohio Geological Society, Cleveland, 1978.
12. Lotze, F.: Steinsalz und Kalisalze (I. Teil, Zweite Auflage), Borntraeger, Berlin, 1957.
13. Füchtbauer, H. and Müller, G.: Sedimente und Sedimentgesteine, E. Schweizerbart'sche Verlagsbuchhandlung, Stuttgart, 1970.
14. Braitsch, O.: Salt deposits, Springer, Berlin, 1971.
15. Jendersie, H.: Kali- und Steinsalzbergbau (Band II), Deutscher Verlag fürGrundstoffenindustrie, Leipzig, 1969.
16. Van den Broek, W.M.G.T.: Impurities in rock-salt; consequences for the temperature increases at the disposal of high-level nuclear waste, Report Delft University of Technology, 1982.
17. Ruchin, L.B.: Grundzüge der Lithologie, Akademie-Verlag, Berlin, 1958.

18. Erhardt, K.: Exploration eines neuen Baufeldes im Grubenbetrieb des Steinsalzbergwerkes Braunschweig-Lüneburg der Kali und Salz AG, Proceedings Fifth Symposium on Salt, Vol. 1, 231, The Northern Ohio Geological society, Inc., 1980.
19. Lorenz, J., Haas Jr., J.L., Clynne, M.A., Potter III, R.W. and Schafer, C.M.: Physical properties data for rock salt (chapter I: geology, mineralogy and some geophysical and geochemical properties of salt deposits), National Bureau of Standards Monograph 167, Washington, D.C., 1981.
20. Richter-Bernburg, G. and Schott, W.: Die nordwestdeutschen Salzstöcke und ihre Bedeutung für die Bildung von Erdöl-Lagerstätten, Erdöl und Kohle, 12 (1959) 294.
21. Trusheim, F.: Uber Halokinese und ihre Bedeutung für die strukturelle Entwicklung Norddeutschland, Zeits. Deutsch. Geol. Ges., 109 (1957) 111.
22. Trusheim, F.: Mechanism of salt migration in Northern Germany, Bull. Amer. Assoc. Petrol. Geol., 44 (1960) 1519.
23. Rapport over de mogelijkheden van opslag van radioactieve afvalstoffen in zoutvoorkomens in Nederland, Interdepartementale Commissie voor de Kernenergie, Ministry of Economic Affairs, The Hague, 1979.
24. Aufricht, W.R. and Howard, K.C.: Salt characteristics as they affect storage of hydrocarbons, Journal of Petroleum Technology, 13 (1961) 733.
25. Reynolds, T.D. and Gloyna, E.F.: Permeability of rock salt and creep of underground cavities, U.S. Atomic Energy Commission Report TD-12383 (as cited in Robertson, E.C.: Physical properties of evaporite minerals, U.S. Geological Survey Report TE1-821, 1962).
26. Baar, C.A.: Applied salt-rock mechanics (I. The in-situ behavior of salt rocks), Elsevier, Amsterdam, 1977.
27. Hofrichter, E.: Zur Frage der Porosität und Permeabilität von Salzgesteinen, Erdoel-Erdgas Zeitschrift, 92 (March 1976) 77.
28. Coelewij, P.A.J., Haug, G.M.W. and Van Kuijk, H.: Magnesium-salt exploration in the Northeastern Netherlands, Geologie en Mijnbouw, 57 (1978) 487.
29. Harsveldt, H.M.: Salt resources in the Netherlands as surveyed mainly by AKZO, Proceedings Fifth Symposium on Salt, Vol. 1, 65, The Northern Ohio Geological Society, Cleveland, 1978.
30. Van Montfrans, H.M.: Enkele geologische gegevens voor het opstellen van een voorlopig model ten dienste van de risico-analyse van het opbergen van radio-actief afval in een zoutkoepel in N.O. Nederland, Interdepartementale Commissie voor de Kernenergie, Bijlagen bij het rapport over de mogelijkheden van opslag van radio-actieve afvalstoffen in zoutvoorkomens in Nederland, The Hague, 1979.
31. Mulder, A.J.: De zoutpijler Schoonlo, Geologie en Mijnbouw, 10 (May 1948) 117.
32. Mulder, A.J.: De zoutpijler van Schoonlo, Geologie en Mijnbouw, 12 (June 1950) 169.
33. Pannekoek, A.J.: Anhydriet en gips in Nederland (geologische inleiding), Geologie en Mijnbouw, 14 (March 1952) 69.
34. Rutten, M.G.: Continental origin of fossile salt layers, Geologie en Mijnbouw, 16 (March 1954) 61.
35. Wassmann, Th.: Mining subsidence in Twente (East Netherlands), Geologie en Mijnbouw, 59 (1980) 225.
36. Van Wijhe, D.H., Lutz, M. and Kaasschieter, J.P.H.: The Rotliegend in the Netherlands and its gas accumulations, Geologie en Mijnbouw, 59 (1980) 3.

Chapter Three

MINING TECHNIQUES IN ROCK SALT

Abstract

Two options for disposal of radioactive waste in rock salt are available: (i) a salt mine repository wherein all waste types can be buried, and (ii) the combination of bore holes in the salt drilled from the surface, for the high-level nuclear waste, with a salt cavity for the other radioactive waste.

General knowledge and experience is available for both disposal options. Most of the research on disposal, however, has been concentrated on the salt mine. Consequently, much specific experience has been collected here. The bore holes/cavity option has however some important advantages such as a wider choice in potential salt formations and relatively low costs. Therefore this option deserves more attention than it has received until now.

3.1 Introduction

Three mining techniques are available for disposal of radioactive waste in rock salt:

- salt mine construction;
- bore-hole drilling;
- solution mining.

These techniques provide for two disposal options:

1. The conventional salt mine, or salt mine repository, which can accommodate all types of radioactive waste.
2. The combination of bore holes in the salt, drilled from the surface, for the high-level nuclear waste (HLW), with a salt cavity for the low-active solid waste (LAW), medium-active solid waste (MAW) and high-active solid waste (HAW).

Figure 3.1 gives schematic views of both options.

We shall give a short description of each technique and shall discuss some properties of the two disposal options.

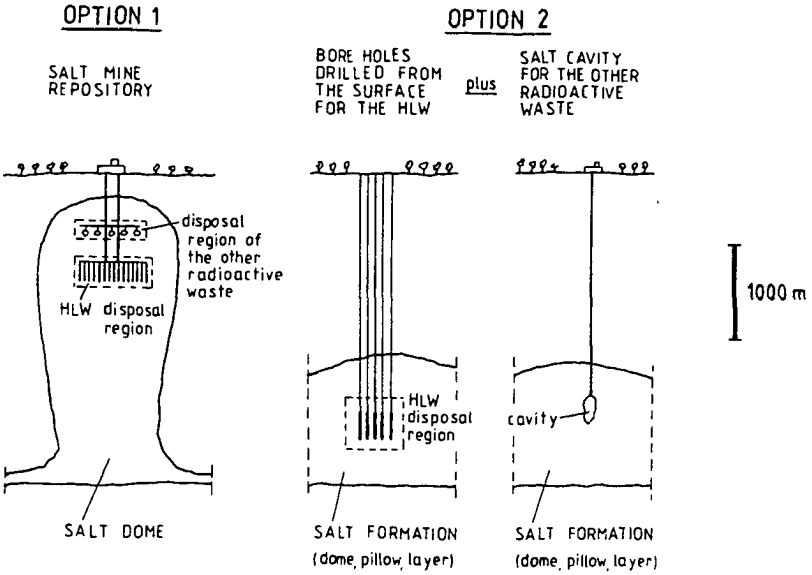

Figure 3.1 Schematic views of the two options for radioactive waste disposal.

3.2 Conventional salt mine

Conventional mining is the oldest of the available techniques. Quite a number of salt mines, for the production of rock salt or of potassium salts, exist or have existed and much knowledge and experience has been gathered. Conventional mining primarily aimed at disposal of radioactive waste has not been carried out yet, although some plans are in an advanced stage (e.g. Gorleben, Federal Republic of Germany, FRG). Abandoned salt mines have been used (Lyons salt mine, Kansas, USA) or are still in use (Asse salt mine, FRG) as sites for in-situ experiments on radioactive waste disposal.

Hamstra and Velzeboer [1] made a design of a salt repository for radioactive waste, to be mined in a medium-sized salt dome. We shall use this design as our example of the first disposal option, the conventional salt mine. Important characteristics of the repository of Hamstra and Velzeboer are:

1. The repository is set up as a conventional mine, with two shafts, roads and working levels on different depths, and ventilation channels. The

capacity is for the amount of waste of 25,000 MWe installed nuclear power, operated for 40 years, plus the waste of the national hospitals and laboratories over a period of 100 years.

2. The model salt dome is cylindrical, with a diameter of 1500 m and a height of 3050 m; the top is 250 m below the surface.
3. The disposal regions are cylindrical, with a diameter of 1100 m. The HLW disposal region has a height of 100-600 m, depending on the chosen HLW disposal configuration (more than one configuration is considered by the authors); the top of the disposal region is at 600 m depth. The HLW is buried in bore holes, drilled from the mine galleries, in a rectangular pattern with distances up to 75 m. The disposal region of the other radioactive waste has a height of 100 m; the top is at 450 m depth. This waste is buried in a number of vertical cylindrical bunkers.
4. Depending on the HLW disposal configuration mean temperature increases of 40-110 °C will occur. Locally, in the neighbourhood of the HLW-canisters, these temperatures will be exceeded.

Important characteristics of the conventional mine as a disposal option are:

- all the radioactive waste types can be buried in one single repository;
- conventional mining cannot be carried out below depths of more than 1000-1200 m, therefore only the upper parts of salt domes are potential sites for this type of repository;
- the essential layout of a mine (especially the shafts) is very expensive, therefore this option is less attractive in case of relatively small amounts of radioactive waste.

3.3 Bore holes in the salt drilled from the surface

There is a significant difference between bore holes drilled inside a mine and bore holes drilled from the surface:

- Bore holes in a salt mine are usually drilled dry. Dry drilling implies atmospheric pressure in the bore hole. Due to salt creep the diameter of a dry drilled hole will decrease with time, and the closure rate will increase with increasing depth. Therefore there is a limit to the depth of dry drilling of, say, 1500 m.
- Bore holes from the surface are drilled with a drilling fluid permanently in the bore hole. This drilling fluid ensures that the pressure in the

bore hole is much higher than in the corresponding case of a dry hole. With a heavy drilling fluid the difference between the lithostatic pressure and the bottom hole pressure, and, as a result of this, the bore hole closure rate, can be reduced considerably. Consequently, depths that can be reached by means of wet drilling are much larger than for dry drilling: 3000 m or more [2].

Advantages of bore holes in the salt, drilled from the surface, for the disposal of HLW are:

- A mine is not necessary as a base for drilling. Consequently, the disposal costs can be low, especially for relatively small amounts of HLW.
- Because of the large depth that can be achieved not only salt domes (the lower parts included) are potential disposal sites, but also salt pillows and salt layers.

Bore holes drilled from the surface contain a drilling fluid. Dependent on the type of fluid, interaction with the radioactive waste to be buried may take place. Removal of the drilling fluid, after completion of the bore hole, may be necessary.

3.4 Salt cavities

The construction of salt cavities has been described in literature [3,4]. It is a relatively new and not commonly known mining technique. Therefore we treat this technique in some more detail.

Fresh water is pumped down through a bore hole into a salt formation. This water dissolves the salt, and is brought to the surface as brine. Both fresh water and brine flow through the bore hole through separate tubings. As more and more salt dissolves, a hole in the salt is formed, the "salt cavity". The process leads to a fast upward growth caused by the rapid dissolution of the cavity roof, where the salt is permanently exposed to fresh water or to unsaturated brine. This is a result of a density difference: the heavy brine, saturated with roof salt, sinks in the liquid mass and is replaced by the lighter fresh water (or by unsaturated brine). To enforce extension of the cavity in a horizontal direction and to prevent uncontrolled vertical growth a "blanket" - usually oil - is introduced. This blanket prevents contact of the roof salt with the (unsaturated) brine in the cavity.

The construction of a cavity proceeds as follows. Soon after the start of the solution process the blanket oil is pumped into the cavity. The cavity diameter grows while the cavity roof remains at the same depth. This is an extremely slow process with a duration of, say, one year. When the desired diameter has been reached the process of extension of the cavity in a vertical direction can start. The blanket is moved upward (by letting blanket material flow out of the cavity), and the (unsaturated) brine in the cavity dissolves unprotected roof salt. This is a rapid, free-convection controlled, process. By manipulating with the blanket level and the feeding of fresh water a more or less cylindrical salt mass is dissolved. Usually the vertical extension of the cavity is realized in a number of successive phases, until the desired cavity shape has been reached.

Solution mining is carried out for two purposes:

1. Salt production.

   Sodium chloride and the more valuable magnesium and magnesium-potassium salts can be mined in this way. Near Veendam (NE-Netherlands) bischofite and carnallite are mined by solution mining at a depth of about 1500 m [5].

2. Storage.

   In the USA, the Federal Republic of Germany and France many salt cavities have been constructed for storage of oil, natural gas or compressed air. Especially in the USA the number of cavities is very large, about 200 [6]. To the best of our knowledge no cavities for disposal of radioactive waste have been constructed or are under construction.

In solution mining for salt production the cavity remains permanently filled with brine. In solution mining for storage purposes the brine is, after construction of the cavity, driven out by the medium to be stored. The lowest part of the cavity, corresponding with a few per cent cavity volume, remains filled with brine and insolubles.

Salt cavities of a few 100,000 m^3 are not uncommon (e.g. the volumes of three of the four cavities in Huntorf, FRG (storage of natural gas) are of the order of 400,000 m^3 each [7]). Thus a single cavity would be sufficient for the LAW, MAW and HAW of a 3500 MWe nuclear power plant scheme (see chapter 1).

The convergence of the cavity volume depends mainly on the difference between the lithostatic pressure and the cavity pressure. If, after the leaching of the cavity, the brine is replaced by air at atmospheric

pressure, then the convergence will increase rapidly with increasing depth. In this case it may not be practical to operate a cavity for radioactive waste disposal at depth of more than about 1500 m [8]. If, however, the cavity pressure can be maintained at a level lower than, but close to, the lithostatic pressure, then the convergence of the cavity volume will be small. In this case much larger cavity depths are possible. This implies that not only salt domes are potential host formations for a cavity for radioactive waste disposal, but also salt pillows and salt layers. A large cavity pressure can be realized by compressed air or by brine (in this last case the cavity remains filled with brine; the cavity pressure is maintained at a level between hydrostatic and lithostatic).

For radioactive waste disposal both the brine-filled cavity and the cavity filled with compressed air have disadvantages. In the case of the brine-filled cavity there is a risk that the very large amount of brine can get contaminated. In the case of the compressed-air-cavity an adequate and safe procedure for the filling with waste vessels will have to be developed.

Operation of a deep cavity under atmospheric pressure leads to a rapidly decreasing cavity volume. The cavity is available for waste disposal for a period of, say, a few months and this can be considered a serious drawback. The squeezing process, however, may eventually lead to a very efficient natural sealing of the cavity and, consequently, to a satisfactory isolation of the cavity contents from the biosphere. If this isolation is indeed a consequence of the rapid cavity-convergence, then the deep-lying cavity, operated under atmospheric pressure, posesses a property that is extremely advantageous for waste disposal.

In view of the advantages of a cavity for disposal purposes, a thorough study of the disposal possibilities of deep-lying cavities is recommended.

3.5 Comparison of the two disposal options

We will compare the two disposal options by discussing the several characteristics with respect to radioactive waste disposal. Table 3.1 summarizes the most important conclusions.

Maximum depth and potential salt formations

Salt mine. The largest depth possible for a salt mine repository is about 1000 m. Burial of HLW in dry bore holes drilled from the galleries can be

carried out down to 1200-1500 m. Therefore this option is only possible in the upper part of a salt dome.

Bore holes and cavity. Bore holes from the surface can be drilled to depths of more than 3000 m. Consequently, salt domes as well as salt pillows and layers are potential host formations.

Salt cavities with sufficient internal pressure can be operated at depths of 3000 m or more. Thus also here salt domes as well as salt pillows and layers can be used. For a cavity operated at atmospheric pressure the maximal depth is of the order of 1500 m. In this case the possibility of disposal in a salt layer is absent.

Capacity and flexibility

Salt mine. The capacity of a salt mine repository exceeds the requirements of any Dutch nuclear power plant scheme. The capacity is therefore more than sufficient. Also the flexibility is excellent: once the repository is constructed almost any amount of radioactive waste can be buried.

Bore holes and cavity. The capacity of a single bore hole for HLW depends on the bore hole diameter and the available interval in the salt. For a 3500 MWe nuclear power plant scheme a few bore holes will suffice [9]. The number of bore holes can easily be adapted to the desired amount of waste, thus this HLW disposal option is very flexible.

A single large salt cavity can contain the waste of the mentioned nuclear power plant scheme. An alternative is a number of smaller cavities. The flexibility is good. When the need should arise, extra cavities can be constructed.

Waste handling and transport

Salt mine. Before disposal of the HLW the canisters must be transported through the shaft to a working level. This is also the case with the other radioactive waste. In both cases the waste must cover a fairly long distance before arrival at the burial place. Problems may be encountered with regard to limiting the radiation level for the salt-mine personnel.

Bore holes and cavity. For bore holes as well as for a cavity the disposal operation is carried out from the surface. Therefore problems with the radiation level for underground personnel are absent. The problems with transport to the burial place are, in case of HLW disposal, similar to those of a salt mine. For LAW-, MAW- and HAW-disposal in a salt cavity the transport possibilities depend on the cavity operation method. Possibilities are: free fall of the waste (e.g. in a brine filled cavity)

Table 3.1 Properties of the two options for disposal of radioactive waste.

	option 1	option 2	
property	conventional salt mine (salt mine repository)	bore holes from the surface (for the HLW)	salt cavity (for LAW, MAW and HAW)
maximum depth	1000-1500 m	>3000 m	>3000 m
potential salt formations	salt domes	salt domes, salt pillows, salt layers	salt domes, salt pillows, salt layers
capacity and flexibility	all types of waste can be buried; capacity can easily be adapted to the amount of waste	only for HLW; capacity can easily be adapted to the amount of waste	only for LAW, MAW and HAW; one cavity is probably sufficient; if necessary extra cavities can be constructed
waste handling and transport	few transport problems; protection of underground personnel against radiation necessary	few transport problems, no radiation shielding problems	no radiation shielding problems; some transport problems may arise depending on the operation method
inspection	HLW: very limited; other radioactive waste: limited	none	limited
(international) technical experience	extensive (building of conventional salt mines); some experience with radioactive waste disposal	extensive (drilling through salt formations for oil/gas production and cavity construction)	extensive (several hundred salt cavities already exist)
economic aspects	very expensive for relatively small amounts of radioactive waste	costs are more or less proportional to the amount of waste to be buried	costs are more or less proportional to the amount of waste to be buried

or transport by remote control. Especially for a cavity operated under high pressure a complicated transport system may be necessary.

A problem with the LAW, MAW and HAW for both salt mine and cavity is that part of this waste, the waste from dismantling of nuclear reactors (see chapter 1), may include voluminous pieces. The shafts, galleries and bore holes must be large enough to permit the transport. It may even be necessary to reduce the volumes of the mentioned waste pieces.

Inspection

Salt mine. After burial the HLW is sealed off and inspection possibilities are very limited. The other radioactive waste can be inspected until the closure of the corresponding bunker or of the complete salt mine repository.

Bore holes and cavity. After burial (at large depth) of the HLW, inspection is not possible. Inspection possibilities in a cavity are limited, especially in the case the cavity is operated under pressure.

The possibility of inspection is an advantage as well as a disadvantage. The advantage is, obviously, to observe that all has gone well, and - if this is not the case - to improve the situation. The disadvantage is the following: inspection implies (temporary) absence of isolation of the waste from the biosphere, and this isolation is precisely the aim of radioactive waste disposal. The possibility of inspection, even for a limited period, might therefore be considered a drawback.

Experience with the mining techniques

The (international) experience with the considered mining techniques is extensive. Many salt mines for salt production have been constructed, as was already mentioned in paragraph 3.2. Also the experience with salt cavities is extensive, as will be clear from the number of cavities already in use (see paragraph 3.4). Finally there is much experience with the drilling of bore holes through salt formations in connection with oil and gas production and cavity construction. The types of experience mentioned here apply to activities not related to radioactive waste disposal. Some experience with disposal is only available in the case of the salt mine.

Economic aspects

Salt mine. In the construction of a mine the fundamental layout, especially the building of the two shafts, is very expensive. This implies that the disposal costs, per unit radioactive waste, decrease with increasing amounts of waste. According to Verkerk [10] the disposal costs of a salt

repository are 60×10^{-6} Dfl. per kWh. These costs, however, were calculated for the 25,000 MWe repository of Hamstra and Velzeboer [1]. The disposal costs for the waste of a 3500 MWe nuclear power plant scheme would therefore be larger.

Bore holes and cavity. The costs of HLW disposal in bore holes drilled from the surface are about proportional to the amount of HLW, because more HLW-canisters lead to a proportionally larger number of bore holes. Also for a cavity the costs are to some extent proportional to the amount of waste to be buried. Thus for this option the costs are less dependent on the amount of waste. Dietz [11] calculated the disposal costs for a 3500 MWe nuclear power plant scheme: about 33×10^{-6} Dfl. per produced kWh.

The Van Hattem and Blankevoort report [8] gives more recent information about the costs of the two disposal options. For a nuclear power plant scheme of 500 MWe the total costs of the bore holes/cavity option amount to 53 % of the costs of the salt mine option; for a 3500 MWe nuclear power plant scheme the corresponding figure is 73 %. These figures are for disposal in a salt dome and for a dry operated cavity.

3.6 Conclusions

The salt mine option for radioactive waste disposal has received more attention than the bore holes/cavity option, and most of the national and international research activities have been directed at this salt mine option. Nevertheless this option has a number of disadvantages, especially in the Dutch situation:

- the option is expensive, especially in case of relatively small amounts of waste;
- the amount of potential disposal sites is limited, as opposed to the amount of potential disposal sites for the bore holes/cavity option.

The main advantage of the salt mine option is the available experience. In the case of the bore holes/cavity option specific experience with radioactive waste disposal is admittedly less. However, the general experience on bore holes and cavities is equivalent with the general experience on salt mines. Consequently, a difference in experience is present, but this difference is moderate and can be eliminated.

In view of the advantages of the bore holes/cavity option, this option deserves more attention than it has received until now. Especially research

on deep-lying salt cavities, which possess natural sealing properties, is strongly recommended. Due to the short operation period of such cavities one or a few waste disposal cavities will not suffice, a reasonable number will be required. It may even be considered to dispose a limited amount of HLW in each cavity, together with the other radioactive waste (the HLW-amount has to be small to prevent excessive increases in temperature). In this way HLW-disposal in bore holes will only be necessary for a part of the HLW.

List of abbreviations

FRG Federal Republic of Germany
HAW high-active solid waste
HLW high-level nuclear waste
LAW low-active solid waste
MAW medium-active solid waste
MWe megaWatt (electric)

References

1. Hamstra, J. and Velzeboer, P.T.: Design study of a radioactive waste repository to be mined in a medium-size salt dome, Proceedings Fifth Symposium on Salt, Vol. 1, 251, The Northern Ohio Geological Society, Cleveland, 1980.
2. Dietz., D.N. and Van den Broek, W.M.G.T.: Het TH-project "Ondergrondse berging van radio-actief afval in steenzout" van 1976-1984, Report Delft University of Technology, 1985.
3. Dietz, D.N.: Oplosmijnen (lecture course), Delft University of Technology, 1979.
4. Dreyer, W.: Underground storage of oil and gas in salt deposits and other non-hard rocks, Wiley Ltd., Chichester, 1982.
5. Van Eekelen, H.A.M.: Analytical solutions of some cavity creep problems in layered salt formations, Proceedings Sixth Symposium on Salt, Vol. 1, 487, The Salt institute, Alexandria, 1985.
6. Thoms, R.L. and Gehle, R.M.: Survey of existing caverns in U.S. salt domes, Second Conference on the mechanical behavior of salt, Hannover, 1984.
7. Petersen, H.: Betriebliche und wirtschaftliche Erfahrungen bei der Untertagespeicherung von Hochdruckerdgas in Salzkavernen, Erdoel-Erdgas-Zeitschrift, 96 (1980) 226.
8. Locatie-onafhankelijke studie inzake de aanleg, bedrijfsvoering en afsluiting van mogelijke faciliteiten voor de definitieve opberging van radioactief afval in steenzoutformaties in Nederland, Van Hattum en Blankevoort/Koninklijke Volker Stevin, Beverwijk, 1986.
9. Van den Broek, W.M.G.T.: De temperatuurverhoging tengevolge van de opslag van kernsplijtingsafval in steenzout, Report Delft University of Technology, 1979.
10. Verkerk, B.: Contribution to the "Maatschappelijke Discussie Energiebeleid", Bijlage 4 van de Analytische Verslagen van de

Controversezittingen gehouden in het kader van de Informatiefase, Stuurgroep Maatschappelijke Discussie Energiebeleid, The Hague, 1983.
11. Dietz, D.N.: Energie-behoefte bij berging van radio-actief afval; optie met behulp van boorgaten vanaf maaiveld voor berging van het KSA en van een oploskaverne voor het LAVA en MAVA, Bijlage 4 van de Analytische Verslagen van de Controversezittingen gehouden in het kader van de Informatiefase, Stuurgroep Maatschappelijke Discussie Energiebeleid, The Hague, 1983.

Chapter Four

THE INCREASE IN TEMPERATURE FOLLOWING THE DISPOSAL OF HIGH-LEVEL NUCLEAR WASTE IN ROCK SALT

Abstract

Temperatures in and around the disposal sites will rise as a result of the heat generation of the high-level nuclear waste (HLW) buried in the rock salt. This chapter gives a description of the induced temperature distributions, calculated on the basis of constant thermal properties of the salt. The latter is a reasonable assumption. The results are valid at any disposal depth.

The heat-generation rate of the HLW decreases exponentially, with a half-life of about 30 years. With sufficient distance between the HLW-columns this leads to maximum increases in temperature of the order of 30, 50 and 110 °C for HLW-canister diameters of 15, 20 and 30 cm respectively. The maximum increase in temperature can be reduced by allowing the HLW to give off part of its heat during storage at the surface prior to underground disposal. Consequently, with a suitable choice of disposal parameters any requirement can be met.

The temperature gradient around the HLW is at most of the order of 2 °C/cm. This gradient decreases rapidly with increasing distance from the HLW-canister, and also decreases with time.

The increase in temperature is calculated assuming rock salt to consist of pure halite (NaCl). The presence of impurities may lead to a larger increase in temperature. Under the most unfavourable circumstances an extra increase in temperature of about 3 per cent for every per cent impurity may occur.

4.1 Introduction

High-level nuclear waste (HLW) generates heat. Consequently, temperatures will rise following the disposal of HLW in rock salt. Excessive increases in temperature must be prevented since they may lead to the melting of magnesium salts such as bischofite and carnallite (these can be present in the rock salt). Large temperature gradients must be prevented because these may induce the migration of too much brine inclusions toward the HLW (see

Table 4.1 Thermal properties of rock salt (after Van den Broek [11]).

temperature (°C)	specific mass (kg/m³)	specific heat (J/kg.°C)	thermal conductivity (W/m.°C)
40	2158	872	5.21
80	2148	889	4.51
120	2137	905	3.94

chapter 5). To judge the suitability of rock salt as a host medium for HLW, and to determine the best disposal scheme, one must be able to predict the increase in temperature and the temperature gradient.

A number of studies have been published on the temperature distribution that will occur in practical disposal situations [1-5]. Each study gives the temperature distribution for one or for a few specific HLW-disposal patterns. To cover more general aspects, we have carried out studies on the influence of the several parameters determining the temperature distribution: dimensions and spatial distribution of the heat sources, thermal properties of the rock salt, sequence of disposal of the HLW-canisters, and concentrations of impurities in the rock salt. The results of these studies have been collected in two reports (Van den Broek [6,7]). This chapter contains the most important results of both reports.

The temperature calculations were carried out with a computer program originally developed by Ir. P. Sonneveld (Delft University of Technology, Mathematics Faculty). The program is based on an analytical solution of the transient heat conduction equations. The chosen calculation method requires to treat the specific mass, the specific heat, and the thermal conductivity of rock salt as constants. This approximation is not entirely valid, especially as regards the thermal conductivity. However, the resulting deviations are small for properly chosen values for these constants [8,9].

Two other characteristics of the computer program are:

- The program is very well suited for non-simultaneous placement of heat sources.
- The rock salt is assumed to be of infinite dimensions. This restriction interferes only in case very long-term effects are considered.

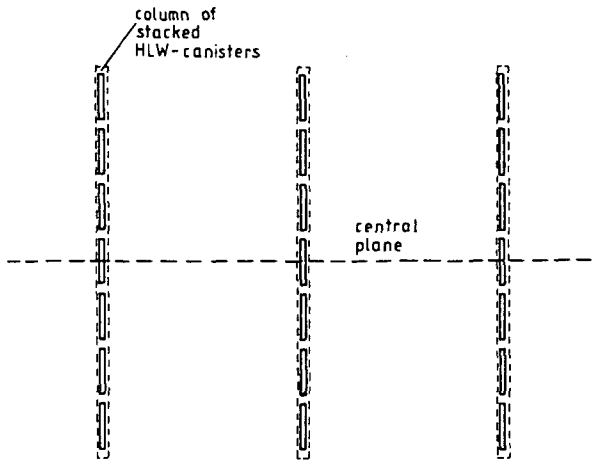

Figure 4.1 Central plane where the increases in temperature have been calculated.

Appendix 4.1 gives the principle of the calculation method. A complete description can be found in the report by Sonneveld [10]. The computer program is listed in one of the already mentioned reports [6].

4.2 Basic parameters for the temperature calculations

The HLW is stored in stacked stainless-steel canisters. Canister diameters of 15, 20, and 30 cm have been considered. The initial heat-generation rate for the 20 cm canister was taken as 300 W/m [5,11]. This yields for the 15 and 30 cm canisters initial heat-generation rates of 169 and 675 W/m respectively, for the same heat-generation rate per volume. The half-life of the exponentially decaying heat-generation rate was taken as 26.7 years (Van den Broek [11]).

For the calculations the thermal properties of rock salt have been chosen at a reference temperature of 80 °C. This somewhat arbitrary choice can be justified as follows. The TPT ("thermal properties temperature", the temperature at which the thermal properties are taken) should reflect the mean temperature of the rock salt in the area of interest. At 1000 m depth the initial temperature level is about 30 °C. Therefore a TPT of 80 °C corresponds at this depth with a mean increase in temperature of the order

of 50 °C. In most of the cases to be presented, the mean increase in temperature is smaller. As the thermal conductivity decreases with increasing temperature [11] (the specific mass and the specific heat are practically independent of temperature [11]), most of the calculated increases in temperature are overestimated.

To get an impression of the influence of the TPT, the results of some calculations are compared with the results of calculations based on TPT's of 40 and 120 °C. The thermal properties of rock salt, used in the calculations, are listed in table 4.1.

The results of the calculations are presented as incremental temperatures relative to the initial temperature, and are applicable for disposal at any depth.

The plane where the increases in temperature have been calculated is at the depth of the middle of the heat source(s). This is illustrated in figure 4.1.

4.3 The increase in temperature in the case of a single heat source

Assessment of the temperature distribution caused by a single heat source is important for two reasons:

1. With the temperature distribution of a single heat source, the solution for more complicated disposal patterns can be constructed by means of superposition.
2. The temperature distribution of a single heat source determines the temperature gradient, up to a few meters distance from a heat source. Knowledge of the temperature gradient is essential in connection with the migration of brine inclusions in rock salt (see chapter 5).

The increase in temperature has been calculated at three different distances from the axis of the heat source, starting with the column/salt-boundary.

Figure 4.2 shows three examples of the increase in temperature for a single heat source, canister diameter 20 cm. The maximum increase in temperature in the rock salt is of the order of 50 °C. This maximum appears at the column/salt-boundary, a few years after disposal. The occurrence of a maximum is caused by the relatively rapid decrease of the heat-generation rate. After a few years this heat-generation rate is much less than the initial one. Then, in the salt near the column/salt-boundary, the loss of

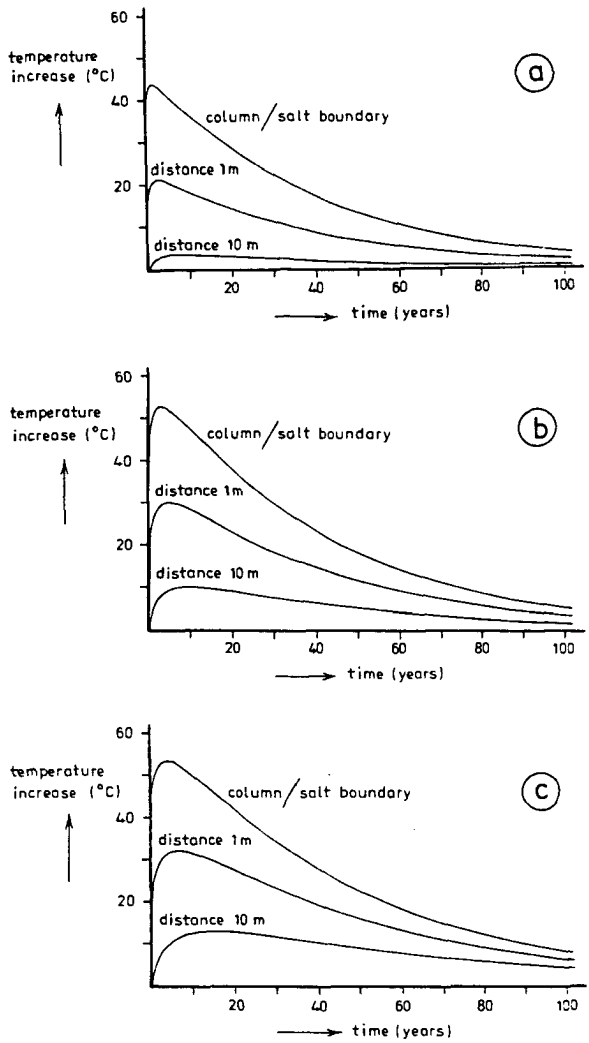

Figure 4.2 The increase in temperature in the case of a single heat source.
Canister diameter: 20 cm.
Column lengths: 10 m (a), 50 m (b) and 1000 m (c).

heat will become larger than the supply of heat, and the temperature will decrease.

For canister diameters of 15 and 30 cm we obtain approximately the same graphs, after multiplying the increase in temperature by a factor of roughly one half (for the 15 cm canister) or two (for the 30 cm canister) [6].

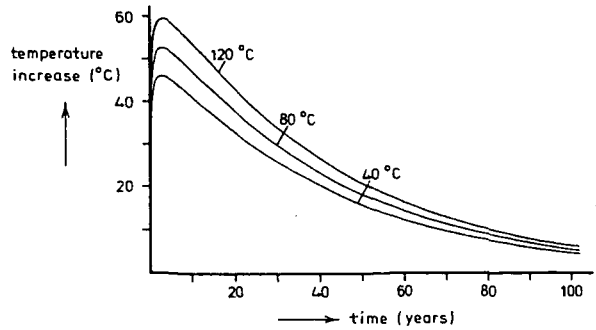

Figure 4.3 Influence of the temperature at which the values of the thermal properties of rock salt are taken, in the case of a single heat source.
Canister diameter: 20 cm.
Column length: 50 m.
The increase in temperature is drawn for the column/salt-boundary.

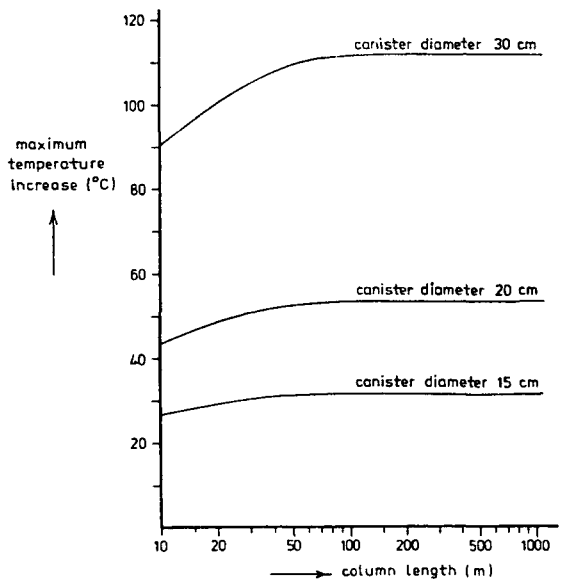

Figure 4.4 Maximum increase in temperature, at the column/salt-boundary, in the case of a single heat source.

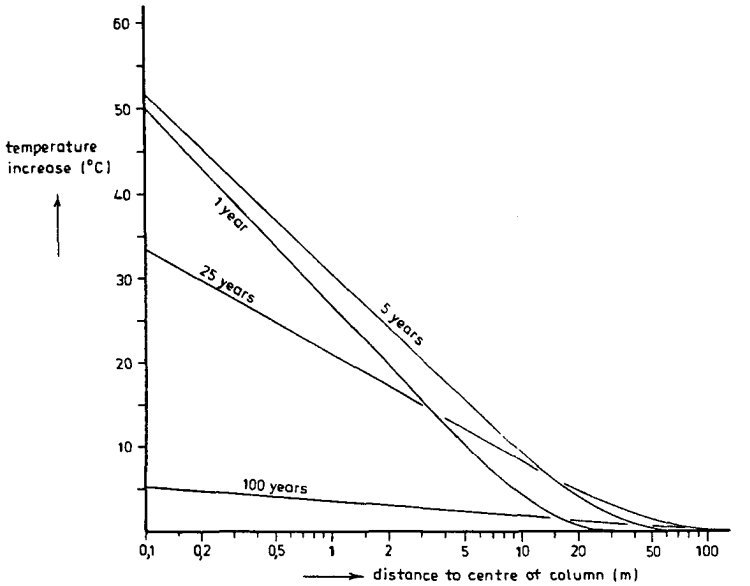

Figure 4.5 Temperature profiles in the case of a single heat source.
Canister diameter: 20 cm.
Column length: 50 m.

Figure 4.3 shows an example of the influence of the TP-temperature. In the case of a single heat source the increase in temperature is, approximately, inversely proportional to the thermal conductivity.

The maximum increase in temperature in the rock salt, appearing at the column/salt-boundary, depends on the length of the column. In figure 4.4 the maximum increase in temperature, as a function of column length, is shown for canister diameters of 15, 20 and 30 cm. For column lengths of about 100 m and more this maximum is almost equal to the maximum for a column of infinite length. The values for the maximum increases in temperature for the last case are listed in table 4.2. These values were obtained for a 1000 m column (this length can be considered infinitely long under the circumstances), for which the maximum between 2 and 7 years was determined.

Figure 4.5 shows an example of the increase in temperature as a function of distance to the column. The increase in temperature is given for four different times; it is, for the larger part, logarithmic with distance to the column.

Table 4.2 Maximum values at the column/salt-boundary for columns of infinite length, in the case of a single heat source.

canister diameter (cm)	maximum increase in temperature (°C)	maximum temperature gradient (°C/cm)
15	32	0.8
20	54	1.1
30	112	1.6

For the temperature gradient, $\partial\theta/\partial r$, the following inequality holds (see appendix 4.2):

$$\left|\frac{\partial\theta}{\partial r}\right| \leq \frac{\phi'_0}{2\pi\lambda_s r} e^{-t/\tau} \qquad (4.1)$$

θ: increase in temperature in the salt;

r: radial coordinate;

ϕ'_0: heat-generation rate, per unit length, at the time of disposal;

λ_s: thermal conductivity of salt;

t: time after disposal;

τ: time constant of the exponentially decaying heat-generation rate (=26.7/(ln 2)= 38.5 years).

The maximum temperature gradient appears at the column/salt-boundary immediately after disposal and is of the order of 1 °C/cm, as can be seen in table 4.2. With increasing distance to the column the temperature gradient decreases rapidly. For 20 cm canisters, for instance, the temperature gradient is less than 0.1 °C/cm for distances to the column axis of more than 1.1 m. The temperature gradient also decreases with time, with the half-life of the heat generation decay of the HLW (see equation 4.1).

4.4 The increase in temperature in the case of an infinite number of heat sources, placed simultaneously

In practice there will be no simultaneous disposal of canisters, nor will there be an infinite number of canisters. Generally speaking, however, the increase in temperature calculated in the case of an infinite number of heat

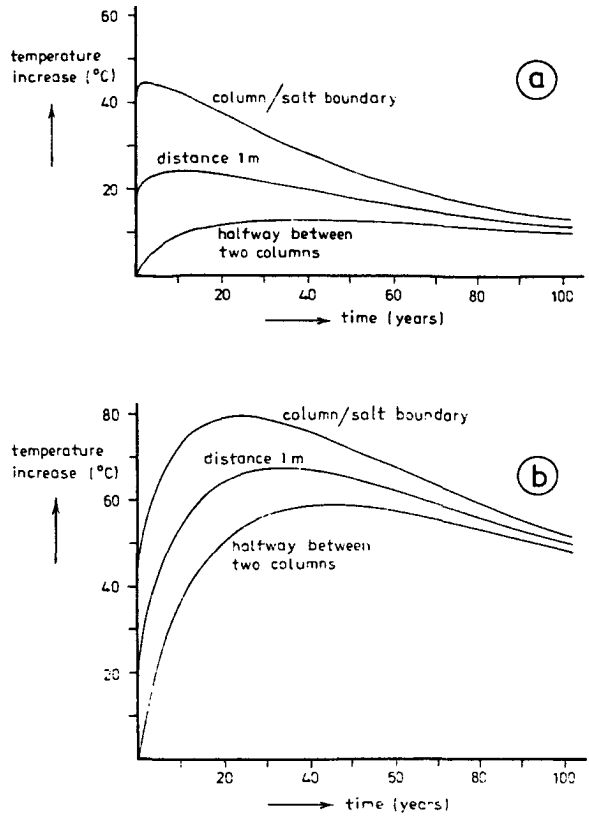

Figure 4.6 The increase in temperature in the case of an infinite number of heat sources, placed simultaneously in a hexagonal pattern.
Canister diameter: 20 cm.
Column lengths: 10 m (a) and 50 m (b).
Distance between the columns: 30 m.

sources, placed simultaneously, gives a good approximation of the increase in temperature that will occur in real disposal situations at the centre of the disposal region.

The calculations have been carried out for a hexagonal disposal pattern.

The increase in temperature has been calculated at three different distances from the axis of a heat source, starting with the column/salt-boundary. The three points all lie on the line connecting two neighbouring heat sources.

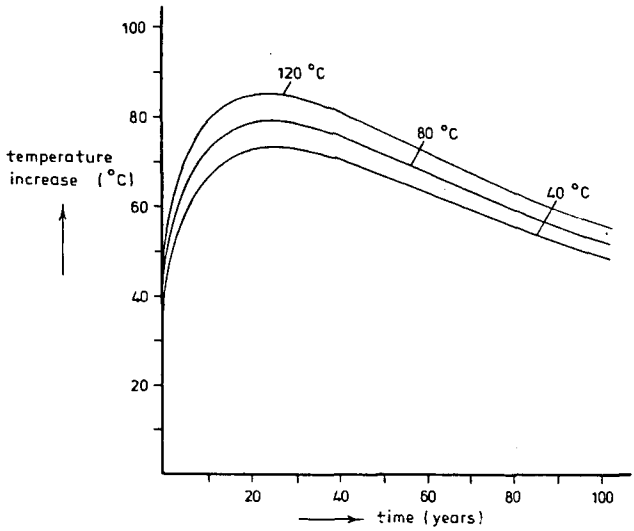

Figure 4.7 Influence of the temperature at which the thermal properties of rock salt are taken, in the case of an infinite number of heat sources, placed simultaneously in a hexagonal pattern.
Canister diameter: 20 cm.
Column length: 50 m.
Distance between the columns: 30 m.
The increase in temperature is drawn for the column/salt-boundary.

Figure 4.6 shows two examples of the increase in temperature in the case of an infinite number of heat sources, placed simultaneously. Results for other values of column length, column distance and canister diameter can be found elsewhere [6]. In the first example (canister diameter 20 cm, column length 10 m, distance between the columns 30 m) the increase in temperature is larger than in the case of a single heat source. For instance, the increase in temperature at the column/salt-boundary after 100 years in this case is about 13 °C, and this was about 4 °C in the case of a single heat source. The maximum increase in temperature in the rock salt, however, is still of the order of 50 °C. In the second example (canister diameter 20 cm, column length 50 m, distance between the columns 30 m) the increase in temperature, and thus the maximum increase in temperature, too, is substantially larger than in the case of a single heat source.

Figure 4.7 shows an example of the influence of the TP-temperature in the case of an infinite number of heat sources, placed simultaneously. It

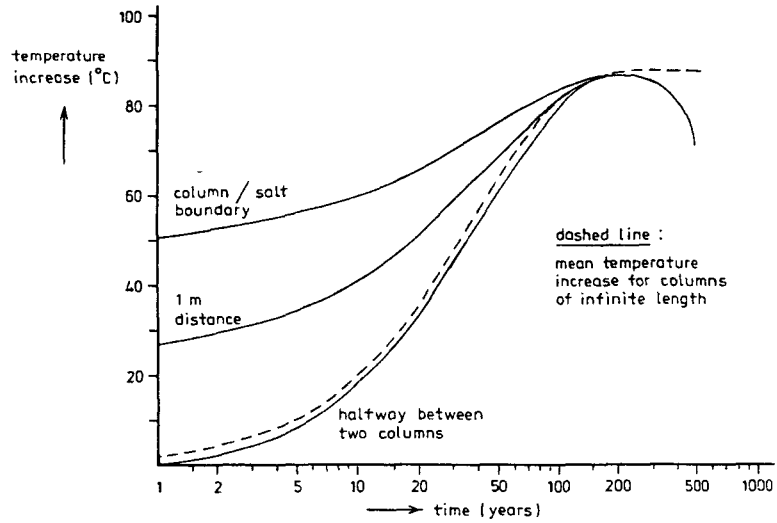

Figure 4.8 The increase in temperature for very long columns, in the case of an infinite number of heat sources, placed simultaneously in a hexagonal pattern.
Canister diameter: 20 cm.
Column length: 1000 m.
Distance between the columns: 50 m.

appears that in this case the influence of the TP-temperature on the calculations is smaller, that is to say the deviation from the 80 °C reference line is somewhat smaller than in the case of a single heat source (figure 4.3). This is caused by the contribution of the surrounding heat sources to the general increase in temperature. This general increase in temperature is much less temperature-dependent than the increase in temperature caused by a single heat source.

Figure 4.8 shows an example of the increase in temperature for very long columns (1000 m). We can derive the following expression for the mean increase in temperature, θ_{mean}, in the case of columns of infinite length (see appendix 4.3):

$$\theta_{mean} = \frac{2\Phi_0'\tau}{\rho_s c_s d^2 \sqrt{3}} (1 - e^{-t/\tau}) \qquad (4.2)$$

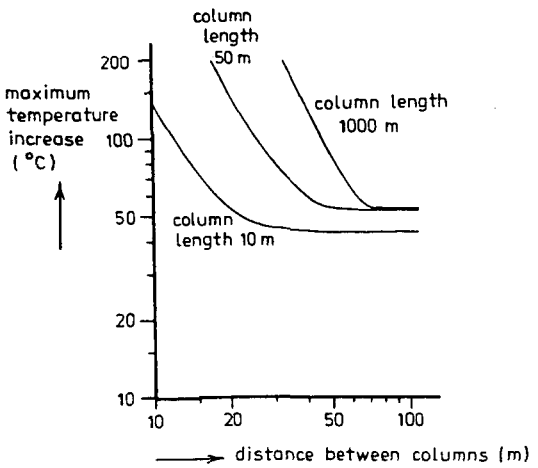

Figure 4.9 Maximum increase in temperature, at the column/salt-boundary, in the case of an infinite number of heat sources, placed simultaneously in a hexagonal pattern.
Canister diameter: 20 cm.

ρ_s: specific mass of salt;
c_s: specific heat of salt;
d: distance between the columns in a hexagonal disposal pattern.

The maximum value of θ_{mean} is reached according to an exponential relation, with the time constant of the decay of the HLW heat generation.

The value of $\theta_{mean,max}$ agrees very well with the maximum increase in temperature for very long columns, as can be seen from the example shown in figure 4.8.

The maximum increase in temperature in the case of an infinite number of heat sources, placed simultaneously, depends on the column length and on the distance between the columns. Figure 4.9 gives this maximum as a function of the distance between the columns for three column lengths, for a canister diameter of 20 cm. For canister diameters of 15 and 30 cm the maximum increase in temperature has to be multiplied by a factor of roughly one half (15 cm canister) or 2 (30 cm canister) [6].

Above a specific column distance the maximum increase in temperature does not change any more. This constant value is identical to the maximum

increase in temperature in the case of a single heat source. Under these circumstances the situation can be described as follows. If the column distance is above a specific value, then the increase in temperature at a point in the neighbourhood of a heat source has already passed its maximum value before the heat of the surrounding heat sources reaches the point considered. For different column lengths this specific column distance has a different value.

The maximum value of the increase in temperature in the case of a single heat source, as presented in table 4.2, is therefore also relevant in the case of an infinite number of heat sources. This maximum increase in temperature gives an indication of the lowest value which this maximum may assume in a real disposal situation. For 20 cm canisters, for instance, the maximum increase in temperature in the rock salt is of the order of 50 °C, if the distance between the columns is large enough. This means that any prescribed limit of increase in temperature of more than 50 °C can be met by a suitable choice of column length and column distance. In fact any temperature limit can be met if the HLW is allowed to release its heat during surface storage for some time prior to disposal in the rock salt. E.g. for 20 cm canisters an increase in temperature limit of 25 °C can be met if the disposal of the waste is postponed for about the half-life of the heat generation decay, about 30 years.

Figure 4.10 shows an example of the increase in temperature as a function of distance to a column. The lines for the single heat source with a constant added (representing the increase in temperature resulting from the presence of the other heat sources) are also drawn. The temperature gradient is the same in both cases, for distances to the column up to about 1/5 of the distance between the columns. Thus in the region where the temperature gradient is largest, this gradient can be estimated in an excellent way using the single heat source concept. The temperature gradient in the case of a single heat source can therefore be applied in the case of an infinite number of heat sources. A short time after the disposal in rock salt (then the temperature gradient is largest) the temperature gradient in the case of 20 cm canisters can be described as follows. At the column/salt-boundary the temperature gradient is 1.1 °C/cm, and this gradient decreases inversely proportional to the distance to the column axis, provided that the distances are small compared to the distance between the columns. The temperature gradient has decreased to 0.1 °C/cm at 1.1 m distance from the column axis,

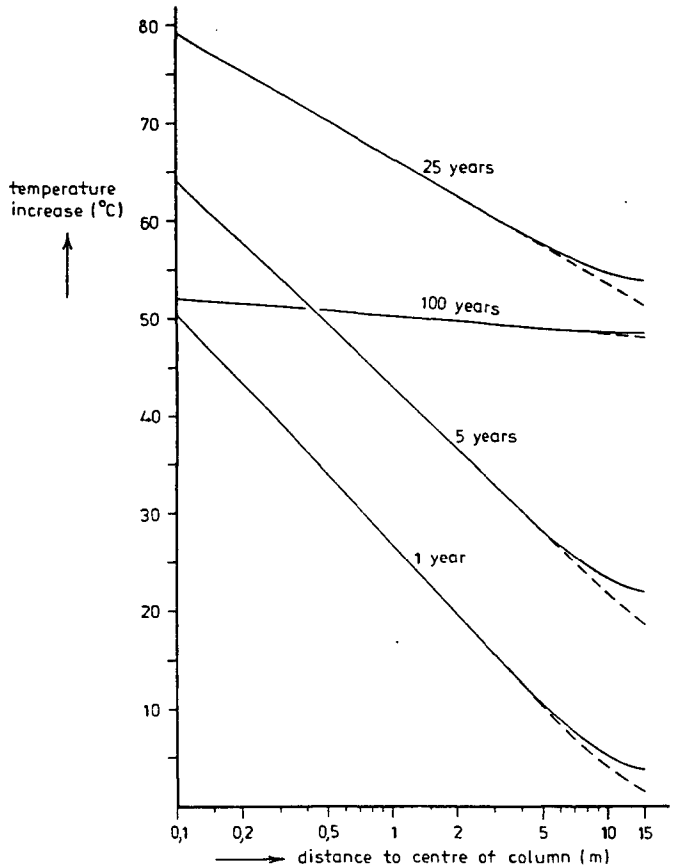

Figure 4.10 Temperature profiles in the case of an infinite number of heat sources, placed simultaneously in a hexagonal pattern.
Canister diameter: 20 cm.
Column length: 50 m.
Distance between the columns: 30 m.
Dashed lines: temperature profiles in the case of a single heat source (to these temperature profiles a constant value has been added, in such a way that the same increase in temperature is obtained at the column/salt-boundary).

and the gradient is less than 0.1 °C/cm for larger distances to the column axis. If the distance between the columns is assumed to be 30 m, then the region where the temperature gradients in the rock salt are less than 0.1 °C/cm is about than 99.5 percent of the disposal area.

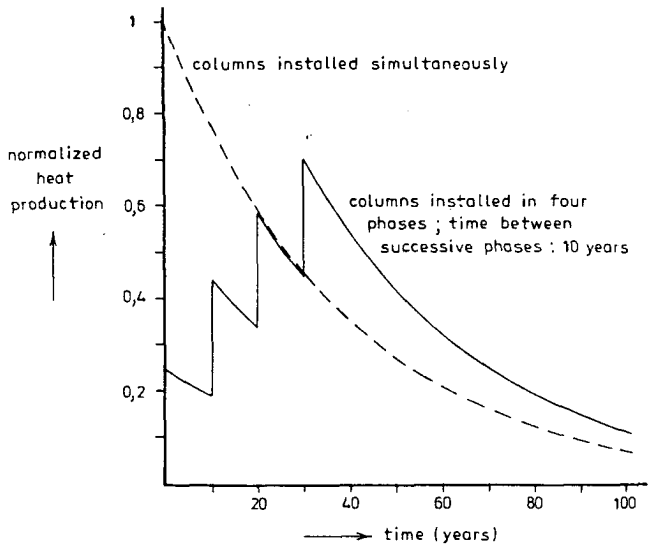

Figure 4.11 The heat production in the case of an infinite number of heat sources, placed simultaneously, compared to the heat production in the case of an infinite number of heat sources, placed in four phases.

4.5 Two examples of non-simultaneous disposal of heat sources

The first example of non-simultaneous disposal describes an infinite number of heat sources, placed in four phases. For the time between successive phases a period of 10 years was chosen, corresponding to an estimated life-time of a nuclear power plant of 40 years [8]. Figure 4.11 shows the heat production and it can be seen that this production is more evenly distributed in time than in the corresponding case of simultaneous placement. Figure 4.12 illustrates the positioning in four phases: four hexagonal patterns are superimposed. After completing the last phase the resulting pattern is also hexagonal, the distance between the columns being reduced with a factor 2.

Figure 4.13 shows the results at the column/salt-boundary for the four phases. The increase in temperature in the corresponding case of simultaneous placement is also drawn. The mean increase in temperature of the four phases combined, i.e. the mean value of the four black lines, gives

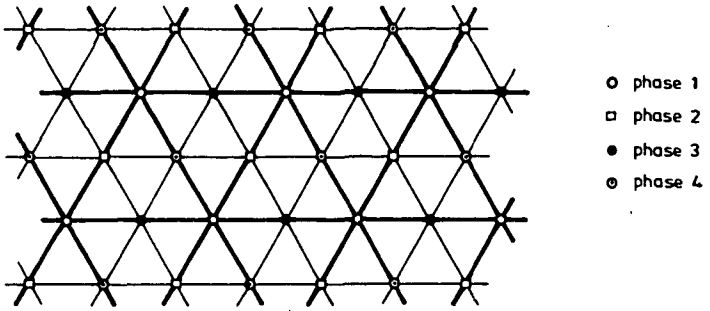

Figure 4.12 Placement of an infinite number of heat sources in four phases, in a hexagonal disposal pattern.

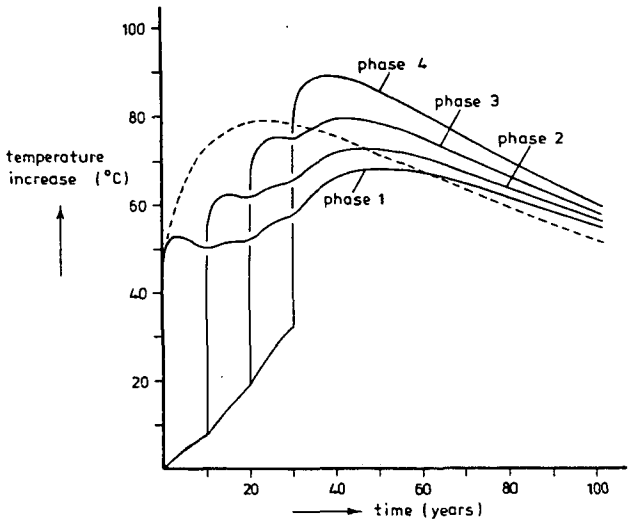

Figure 4.13 The increase in temperature in the case of an infinite number of heat sources, placed in four phases.
Canister diameter: 20 cm.
Column length: 50 m.
Distance between the columns: 30 m.
The increase in temperature is drawn for the column/salt-boundary.
Dashed line: the increase in temperature in the case of simultaneous placement, under the same circumstances.

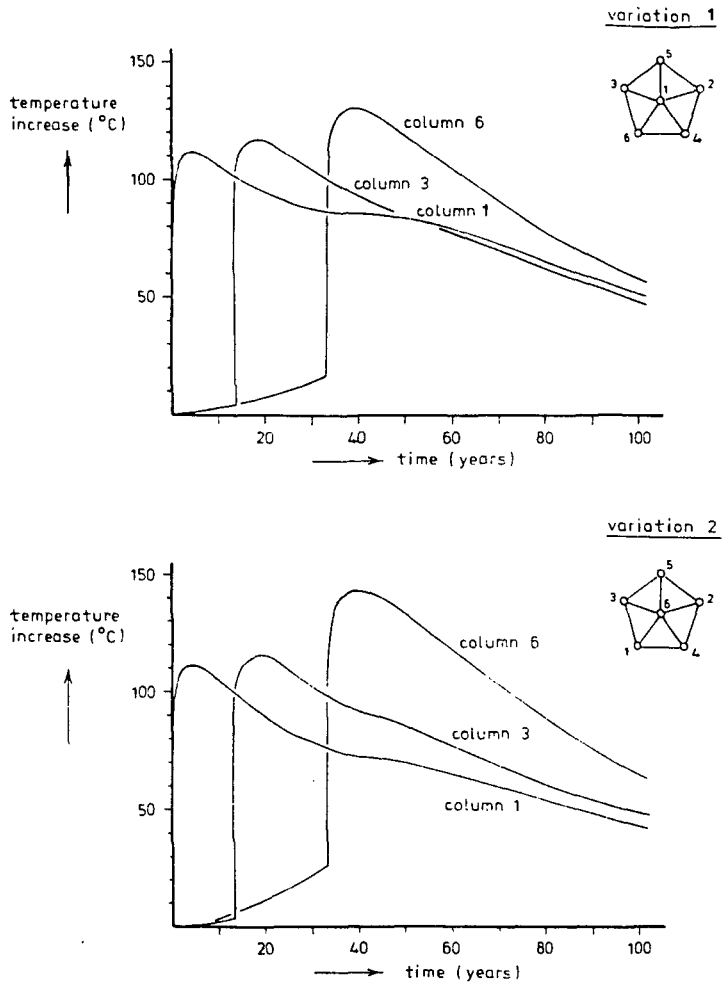

Figure 4.14 The increase in temperature in the case of the deposition of six long columns, regularly placed over a period of 33 years. The columns are placed in a pentagon pattern, in two variations.
Canister diameter: 30 cm.
Column length: 1020 m.
Distance between the outer columns and the column in the centre: 30 m.

a somewhat smaller maximum value than in the case of simultaneous placement. The increase in temperature of phase 4, however, is larger than the increase in temperature in the case of simultaneous placement. So it offers few advantages to position canisters in this way, and, more important, phased placement of canisters may lead, but not necessarily so, to maximum temperatures that are higher than in the case of simultaneous placement.

In the second example of non-simultaneous placement 6 columns of 1020 m length, with a canister diameter of 30 cm, are successively placed over a period of 33 years. The 6 columns contain the amount of HLW produced by nuclear power plants with a total capacity of 3500 MWe, operated for 40 years. Two variations are studied. In the first variation the last column, column 6, is placed on the outside of the pentagon pattern, in the second variation the last column is placed in the centre.

Figure 4.14 gives the increases in temperature at the column/salt-boundary for the columns 1, 3, and 6. For both variations column 6 shows the largest increase in temperature. For variation 2 the increase in temperature is larger than for variation 1. From the temperature point of view it has therefore some advantages to install canisters working from the inside to the outside.

4.6 Influence of the presence of impurities

4.6.1 Introduction

The temperature calculations were based on rock salt consisting of pure halite. The halite concentrations of most rock salt formations, however, lie between 90 and 99 weight % (see chapter 2). In this paragraph we will discuss the consequences of the presence of impurities on the temperature distribution. We will assume total impurity contents of 1, 5, 10, and - as a rather extreme case - 15 %. These percentages are in volume %, a more convenient measure in discussions on temperature effects (differences between percentages by volume and by weight are small [7]). For this discussion we will use literature values of the specific masses, specific heats, and thermal conductivities of the several impurities in rock salt. Unfortunately, literature values of the specific heats of polyhalite, carnallite and kainite could not be found. For these substances we have developed an estimation procedure, presented in appendix 4.4, based on the

Table 4.3 Thermal properties of materials that can be present in rock salt.

material	specific mass, ρ, at room temperature (kg/m^3)	specific heat, c (J/kg.°C)	thermal conductivity, λ (W/m.°C)	specific heat per unit volume ($10^6 J/m^3.°C$)	thermal diffusivity, $\lambda/\rho c$ ($10^{-6} m^2/s$)
halite	2163 [11]	864 (20 °C) [11]	5.63 (20 °C) [11]	1.87	3.01
calcite	2710 [12]	813 (21 °C) [15]	2.19 (30 °C) [16]	2.20	0.99
dolomite	2872 [12]	824 (23 °C) [15]	5.0 (10 °C) [17]	2.37	2.11
gypsum	2320 [12]	1109 (36 °C) [15]	1.1 (50 °C) [17]	2.57	0.43
anhydrite	2960 [12]	728 (20 °C) [15]	5.3 (35 °C) [17]	2.15	2.46
polyhalite	2775 [13]	900 DPL	2 [7]	2.50	0.80
kieserite	2445 [12]	1000 (9 °C) [15]	2 (60 °C) [7]	2.45	0.82
bischofite	1569 [12]	1582 (44 °C) [15]	1 [18]	2.48	0.40
sylvite	1984 [12]	691 (20 °C) [15]	5.2 (20 °C) [17]	1.37	3.79
carnallite	1610 [12]	1200 DPL	0.8 (60 °C) [7]	1.93	0.41
kainite	2131 [12]	1070 DPL	0.9 (60 °C) [7]	2.28	0.39
hematite	5240 [12]	648 (20 °C) [15]	1.26 (15 °C) [16]	3.40	0.37
quartz	2635-2660 [12]	730 (20 °C) [16]	5.1-6.0 (25 °C) [17]	1.92-1.94	2.63-3.12
clay	2550-3200 [14]	1100-1350 (20 °C) [15]	1.1-3.7 [17,19]	2.86-3.78	0.29-1.29

DPL: calculated according to the Dulong and Petit Law - see appendix 4.4.

Dulong and Petit (DPL) Law. Table 4.3 gives the collected literature values and the DPL specific heats.

The influence of the non-halite salts upon the temperature distribution is twofold:

a. Specific heat.

The specific heat per unit volume is a measure of the heat that can be absorbed by the rock mass. The larger the specific heat, the smaller the corresponding increase in temperature. Table 4.3 shows that only sylvite has a smaller specific heat than halite. Thus in rock salt with impurities the increase in temperature will be smaller than in pure halite, as long as sylvite is not predominantly involved. With sylvite as the only impurity the increase in temperature will be marginally larger (4.0 % for a rock salt consisting of 85 volume % halite and 15 volume % sylvite [7]).

b. Thermal conductivity.

For the mean thermal conductivity, λ_{mean}, of a combination of two materials with different thermal conductivities the following relation holds [20]:

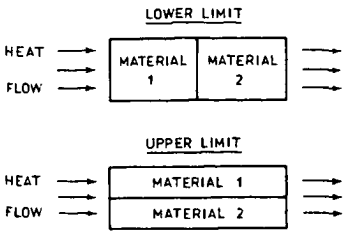

Figure 4.15 Thermal conductivity of a combination of two materials: situations corresponding with the upper and lower limit for the mean thermal conductivity.

$$\frac{1}{\frac{x_1}{\lambda_1} + \frac{x_2}{\lambda_2}} \leq \lambda_{mean} \leq x_1\lambda_1 + x_2\lambda_2 \qquad (4.3)$$

x_1: volume fraction of material 1;
x_2: volume fraction of material 2;
λ_1: thermal conductivity of material 1;
λ_2: thermal conductivity of material 2.

Upper and lower limits correspond to the two cases sketched in figure 4.15.

According to table 4.3 the thermal conductivities of the impurities are of the order of 5 W/m.°C (anhydrite, sylvite, dolomite, quartz) or 1-2 W/m.°C (other impurities). Consider the very unfavourable case of rock salt, consisting of (i) halite with a thermal conductivity of 5 W/m.°C and (ii) impurities with a thermal conductivity of 1 W/m.°C. The upper and lower limits for the thermal conductivity of this rock salt can be calculated with equation (4.3). The results are listed in table 4.4.

We see that the presence of impurities with a low thermal conductivity can have a substantial influence on the mean thermal conductivity. In the considered case 15 % impurities may cause a decrease of the thermal conductivity of rock salt of about 40 %.

4.6.2 Long-term effect

The heat-generation rate of the HLW decreases exponentially, with a half-life of some 30 years (see paragraph 4.2). For periods of the order of 100

Table 4.4 Upper and lower limits for the mean thermal conductivity of rock salt consisting of (i) halite with a thermal conductivity of 5 W/m.°C and (ii) impurities with a thermal conductivity of 1 W/m.°C.

composition		thermal conductivity	
halite (vol. %)	impurities (vol. %)	lower limit (W/m.°C)	upper limit (W/m.°C)
99	1	4.81	4.96
95	5	4.17	4.80
90	10	3.57	4.60
85	15	3.13	4.40

years or more, when the HLW has given off most of its heat, this heat has been absorbed in the rock salt mass in and around the disposal region. Temperature variations over short distances have practically disappeared.

As we are considering long-term effects, only heat flow in a vertical direction, out of the disposal region, is of importance. Impurities in rock-salt formations will generally be present in the form of horizontal layers. Consequently, the directions of heat flow and layer structure will generally be perpendicular to one another. Therefore the mean thermal conductivity can be close to the lower limit. In salt domes the layer structure can be vertical - see figure 4.16 - which is more favourable. In good approximation the long-term increase in temperature is inversely proportional to the square root of the thermal conductivity [6]. Thus a lower thermal conductivity leads to a larger increase in temperature. In the most unfavourable case, horizontal layer structure and impurities with low thermal conductivities, this will lead to extra increases in temperature of 2, 10, 18 and 26 % for total impurity concentrations of 1, 5, 10 and 15 % respectively.

4.6.3 Short-term effect

The temperature distribution in a rock-salt formation can be described as the superposition of the temperature distribution of a single nearby HLW-column and a general increase in temperature, caused by the other HLW-columns. The general increase in temperature will be affected by the

presence of impurities in approximately the same way as was described for the long-term effect.

The temperature distribution around a single HLW-column is dominated by the thermal conductivity. In good approximation the increase in temperature in this case is inversely proportional to the thermal conductivity. A calculation for thermal conductivities of 1 and 5 W/m.°C (constant specific heat per unit volume) confirmed this.

An impurity content of A % implies a mean concentration of impurities of A % in a certain volume. If this volume is very large (e.g. the region where the HLW will be buried), then the concentration of impurities on a smaller scale will peek out above the mean concentration of impurities in a number of regions. Consider a most unfavourable situation:

- some HLW-columns are buried in a region with a concentration of impurities of, say, 1.5 times the mean concentration of impurities,
- the impurities have a very low thermal conductivity of, say, 1 W/m.°C,

then the upper and lower limits for the thermal conductivity are correspondingly lower than the values of table 4.4. For instance, the values for a concentration of impurities of 15 % ($3.13 < \lambda_s < 4.40$ W/m.°C) are now locally valid within a formation with a mean concentration of impurities of 10 %. Thus local variations in the impurity content can lead to lower thermal conductivities. In a real disposal situation, however, the thermal conductivity will always be near the upper limit as defined in equation (4.3); only for a cylindersymmetrical layer structure† around the HLW-column the thermal conductivity would be equal to the lower limit, and the possibility of such a disposal situation can be ruled out. Consequently, even under the most unfavourable conditions the thermal conductivity will not be lower than the lower limits of table 4.4. Thus the extra increase in temperature, due to the presence of a single HLW-column, will be at most 4, 20, 40 and 60 % for impurity concentrations of 1, 5, 10 and 15 % respectively.

The extra increase in temperature for short periods of time will be somewhat smaller than the corresponding value mentioned above. The total

† For a cylindrical heat source the heat flow is radially outward. The layer structure equivalent with the lower limit for the mean thermal conductivity is cylindersymmetrical (heat flow and layer structure perpendicular to one another - see figure 4.15).

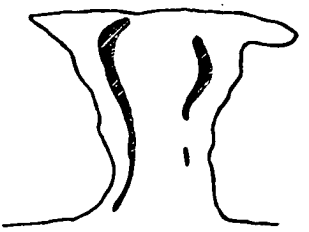

Figure 4.16 Possible distribution of potassium-magnesium salts in a salt dome.
Source: Dietz and Van den Broek [21].

increase in temperature is the sum of the single HLW-column increase in temperature and the general increase in temperature, and this latter quantity is less sensitive to variations of the thermal conductivity.

4.6.4 Implications for radioactive waste disposal

The calculation of the increase in temperature will generally be based on the assumption that rock salt consists of pure halite. As we have seen, this assumption can lead to an underestimation of the temperatures that will occur in a real disposal situation. Two strategies can be followed to ensure that certain temperature limits will not be exceeded:

1. A safety margin.
   If the information about the rock salt is scarce, than a safety margin has to be applied: the temperature calculations have to yield results that are below the temperature limits. The magnitude of the safety margin depends on the extra increase in temperature that may occur. This extra increase in temperature is a function of the impurity content (therefore this parameter of the rock salt formation has to be known). We have seen in the preceding paragraph that under the most unfavourable conditions the extra increase in temperature will be somewhat less than the extra increase in temperature for a single nearby HLW-column. Consequently, the safety margins in terms of increases in temperature are about 3, 15, 30 and 50 % for impurity concentrations of 1, 5, 10 and 15 % respectively.
2. Detailed geological information.
   If there is very detailed information about the disposal region, then the extra increase in temperature can be estimated. This extra increase in temperature will generally be smaller than the value corresponding to the

safety margin mentioned above. An extra increase in temperature can be practically absent if the impurities in the rock salt are materials with a high thermal conductivity (dolomite, anhydrite, sylvite, quartz). With detailed geological information the disposal pattern can be designed more critically: because the temperatures can be estimated more accurately, the safety margin can be smaller. Also there is the option to place no HLW-columns, or less columns, in those parts of the disposal region where the thermal conductivity is low.

4.7 Conclusions

The most important conclusion is, that the increase in temperature does not present a fundamental problem for disposal of HLW in rock salt. In practice any requirement can be met by a suitable arrangement of disposal colums and by allowing the waste to cool down for a sufficiently long period before disposal.

Specific conclusions are:

- Without a cool-down period the disposal of HLW will result in maximum increases in temperature of at least 30, 50 or 110 °C for canister diameters of 15, 20 and 30 cm respectively. This maximum can be larger, especially when relatively small spacing distances between the columns are chosen. Distances of some tens of meters will generally be necessary to prevent excessive temperatures to occur.
- Without a cool-down period the disposal of HLW will result in a maximum value for the temperature gradient in the rock salt that is at most of the order of 2 °C/cm. However, it is only in a very small part, about 1 % or less, of the disposal area, that the temperature gradients will exceed at all a value of 0.1 °C/cm.
- Non-simultaneous deposition of columns can lead to a larger maximum increase in temperature than simultaneous placement.
- The impurity content of the rock salt can have a substantial influence on the increase in temperature. Specifically impurities with a low thermal conductivity may occur, augmenting the increase in temperature.
- Under the most unfavourable conditions - impurities with thermal conductivities 5 times as small as the conductivity of halite and an unfavourable distribution of the impurities - an extra increase in temperature of about 3 % can occur for every per cent impurity.

- The design of a disposal configuration should take into account the influence of the impurities on the temperature distribution. If sufficient information regarding the nature of the impurities is absent, then a general safety margin should be applied.

List of symbols

c specific heat
c_s specific heat of salt
c_M molar specific heat
d distance between the columns in a hexagonal disposal pattern
ei symbol for the exponential integral
f number of degrees of freedom
F distance- and time-dependent function for the description of the point source temperature distribution
g $\underline{r}$-dependent part of the heat source density
H heat capacity per heat source and per unit length
M molecular weight
n first argument of the F-function
p second argument of the F-function
q heat source density
Q amount of heat given off per heat source and per unit length
r radial coordinate
$\underline{r}$ distance to point heat source
$\underline{r}'$ distance integration parameter
R universal gas constant
s integration parameter
t time after disposal/start of the heat generation
t' time integration parameter
V integration volume
x_1 volume fraction of material 1
x_2 volume fraction of material 2
x' x-coordinate of $\underline{r}'$
y' y-coordinate of $\underline{r}'$
z' z-coordinate of $\underline{r}'$
θ increase in temperature in the salt

θ_{mean} mean increase in temperature in the case of columns of infinite length

$\theta_{mean,max}$ maximum mean increase in temperature in the case of columns of infinite length

θ_p point source temperature distribution

κ thermal diffusivity

λ thermal conductivity

λ_{mean} mean thermal conductivity of a combination of two materials

λ_s thermal conductivity of salt

λ_1 thermal conductivity of material 1

λ_2 thermal conductivity of material 2

ρ specific mass

ρ_s specific mass of salt

τ time constant of the exponentially decaying heat-generation rate

ϕ' constant heat-generation rate per unit length

ϕ_p point source heat-generation rate

ϕ'_0 heat-generation rate, per unit length, at the time of disposal

List of abbreviations

DPL Dulong and Petit Law

HLW high-level nuclear waste

TPT thermal properties temperature

MWe megaWatt (electric)

References

1. Schmidt, H.: Numerische Langzeitberechnung instationärer Temperaturfelder mit diskreter Quellenverteilung unter Berücksichtigung temperatur- und ortsabhängiger Stoffwerte, Thesis, Technische Hochschule Aachen, 1971.
2. Cheverton, R.D. and Turner, W.D.: Thermal analysis of the national radioactive waste repository; progress through June 1971, Report Oak Ridge National Laboratory, ORNL-4789, 1971.
3. Cheverton, R.D. and Turner, W.D.: Thermal analysis of the national radioactive waste repository; progress through March 1972, Report Oak Ridge National Laboratory, ORNL-4789, 1972.
4. Ploumen, P. and Strickmann, G.: Berechnung der zeitlichen und räumlichen Temperaturverteilung bei der säkularen Lagerung hochradioaktiver Abfälle in Salzstöcken, Report Technische Hochschule Aachen (on behalf of the Ministry of the Interior of the Federal Republic of Germany), 1977.
5. Hamstra, J. and Kevenaar, J.W.A.M.: Temperature calculations on different configurations for disposal of a high-level reprocessing waste

in a salt dome model, Report Netherlands Energy Research Foundation, ECN-42, Petten, 1978.
6. Van den Broek, W.M.G.T.: De temperatuurverhoging tengevolge van de opslag van kernsplijtingsafval in steenzout, Report Delft University of Technology, 1979.
7. Van den Broek, W.M.G.T.: Impurities in rock salt; consequences for the increases in temperature at the disposal of high-level nuclear waste, Report Delft University of Technology, 1982.
8. Kevenaar, J.W.A.M., Ploumen, P., Janssen, L.G.J. and Winske, P.: Comparison of temperature calculations for an arbitrary high-level waste disposal configuration in salt formations, Report Netherlands Energy Research Foundation, ECN-63, Petten, 1979.
9. Van den Broek, W.M.G.T.: Disposal of high-level nuclear waste in rock salt; a comparison of temperature increases calculated at ECN-Petten, RWTH-Aachen, and THD-Delft, Report Delft University of Technology, 1982.
10. Sonneveld, P.: Een semi-analytische methode voor het berekenen van de temperatuurverdeling tengevolge van een exponentieel met de tijd afnemende warmtebron, Report Delft University of Technology (Mathematics Faculty), 1982.
11. Van den Broek, W.M.G.T.: Fysische constanten van kernsplijtingsafval ten behoeve van temperatuurberekeningen, Report Delft University of Technology, 1978.
12. Weast, R.C. (editor): Handbook of Chemistry and Physics (62nd edition), CRC Press, Boca Raton, 1981.
13. Lotze, F.: Steinsalz und Kalisalze, I. Teil (Zweite Auflage), Borntraeger, Berlin, 1957.
14. Physical properties data for rock salt, NBS Monograph 167, U.S. Department of Commerce, Washington, D.C., 1981.
15. Landolt-Börnstein, Zahlenwerte und Funktionen, 4.Teil, Bandteil a, Springer Verlag, Berlin, 1967.
16. Intern. Crit. Tables, Vol. V, McGraw-Hill, New York, 1929.
17. Landolt-Börnstein, Zahlenwerte und Funktionen, 4.Teil, Bandteil b, Springer Verlag, Berlin, 1972.
18. Hartemink, W. and Teeuw, D. (Kon./Shell Exploratie en Produktie Laboratorium, Rijswijk, The Netherlands), personal communication, May 1985.
19. Behrens, J., Roters, B. and Villinger, H.: In situ determination of the thermal conductivity in cased drill holes, Proceedings Advances in European Geothermal Research, Commission of the European Communities, Strasbourg, 1980.
20. Schneider, K-J.: Die Wärmeleitfähigkeit körniger Stoffe und ihre Beeinflussung durch freie Konvektion, Thesis, Technische Hochschule Karlsruhe, 1963.
21. Dietz, D.N. and Van den Broek, W.M.G.T.: Berging van radio-actief afval in steenzout, PT/Procestechniek, 37 (1982), No. 3, 95.
22. Carslaw, H.S., and Jaeger, J.C.: Conduction of heat in solids (second edition), Oxford University Press, London, 1959.
23. Zemansky, M.W.: Heat and thermodynamics (fourth edition), McGraw-Hill, New York, 1957.
24. Kittel, C.: Introduction to solid state physics (fifth edition), John Wiley & Sons, New York, 1976.

Appendix 4.1

Principle of the calculation method of the increases in temperature

The basis of the calculation method by Sonneveld [10] is the increase in temperature, θ_p, in a homogeneous, isotropic, infinite solid as a result of a point heat source with a time dependent strength, $\phi_p(t)$ [22]:

$$\theta_p(\underline{r},t) = \int_0^t \frac{\phi_p(t')}{8(\pi\kappa)^{3/2}\rho c} \frac{e^{-|r|^2/\{4\kappa(t-t')\}}}{(t-t')^{3/2}} dt' \qquad (4.4)$$

$\underline{r}$: radial distance to the point source;
t: time since the start of the heat generation;
t': time integration parameter;
κ: thermal diffusivity of the solid;
ρ: specific mass of the solid;
c: specific heat of the solid.

At time t=0 a heat source density $q(\underline{r},t)$ is placed in the solid:

$$q(\underline{r},t) = g(\underline{r}).\phi_p(t) \qquad (4.5)$$

This results in a increase in temperature $\theta(\underline{r},t)$:

$$\theta(\underline{r},t) = \iiint_V \theta_p(\underline{r}-\underline{r}',t)g(\underline{r}')dx'dy'dz' \qquad (4.6)$$

$\underline{r}'$: distance integration parameter;
x': x-coordinate of $\underline{r}'$;
y': y-coordinate of $\underline{r}'$;
z': z-coordinate of $\underline{r}'$;
V: integration volume.

The heat source strength decreases exponentially with time:

$$\phi_p(t) = \phi_p(0).e^{-t/\tau} \qquad (4.7)$$

With equation (4.7), equation (4.4) can be converted to [10]:

$$\theta_p(\underline{r},t) = \frac{\phi_p(0)}{8(\pi\kappa)^{3/2}\rho c\sqrt{t}} F(\frac{t}{\tau}, \frac{|\underline{r}|^2}{4\kappa t}) \qquad (4.8)$$

with F defined as:

$$F(n,p) = \int_0^1 \frac{e^{-n(1-s)-p/s}}{s^{3/2}}\, ds \qquad (4.9)$$

n: first argument of the F-function;

p: second argument of the F-function;

s: integration parameter.

For the calculation of F after a given time two rapid methods exist:

1. For small and medium p-values F can be calculated with the help of development of power series.
2. For medium and large p-values an asymptotic approximation for F can be used, based on a "Stieltjes-representation". This leads to a fast converging "continued fraction" development.

The two methods for the calculation of F cover the complete range of p-values. Thus F, and consequently θ_p, can be rapidly calculated for any value of p. With F known, the increase in temperature $\theta(\underline{r},t)$ for a line source of finite length can subsequently be calculated (the single heat source problem).

For an infinite number of heat sources the increases in temperature of the neighbouring sources are added to the temperature of the "central" heat source. The number of neighbouring sources being taken into account, depends on the respective increases in temperature: is the increase in temperature from a source below a certain limit (say, 0.0001 °C), then this source and the sources farther away are not taken into account. The number of heat sources contributing to the calculated increase in temperature is therefore not constant, but increases with time.

For a limited number of heat sources the same adding procedure was applied. Because of the relatively small number of heat sources, however, it was not necessary to test the level of the different increases in temperature. Thus in this case all heat sources were permanently taken into account.

The details of the calculation method can be found in the report by Sonneveld [10]; the computer program is listed in the report by Van den Broek [6].

Appendix 4.2

The upper limit for the temperature gradient

According to Carslaw and Jaeger [22] the temperature distribution of a line source of infinite length, in a homogeneous infinite solid, and generating heat at a constant rate, is described by the line-source solution:

$$\theta = \frac{\phi'}{4\pi\lambda} \, ei\left(\frac{\rho c r^2}{4\lambda t}\right) \tag{4.10}$$

θ: increase in temperature;

ϕ': constant heat-generation rate, per unit length;

λ: thermal conductivity;

ei: symbol for the exponential integral.

For $(\rho c r^2/4\lambda t) < 0.01$ this expression can be approximated by a logarithmic function [22]:

$$\theta = \frac{\phi'}{4\pi\lambda} \left(-0.5772.... + \ln \frac{4\lambda t}{\rho c r^2}\right) \tag{4.11}$$

Differentiating this equation with respect to r yields:

$$\frac{\partial \theta}{\partial r} = - \frac{\phi'}{2\pi\lambda r} \tag{4.12}$$

Or, in absolute terms,

$$\left|\frac{\partial \theta}{\partial r}\right| = \frac{\phi'}{2\pi\lambda r} \tag{4.13}$$

which is independent of time.

However, in disposal of radioactive waste in rock salt we are dealing with a heat source that decreases exponentially with time (half-life of about 30 years - see paragraph 4.2). Consequently, also the temperature

Table 4.5 The temperature gradient in rock salt for a single heat source of infinite length: comparison of values calculated with a computer program and values predicted by equation (4.14).
Source of computer data: Van den Broek [6], table 17 (column length: 1000 m; this length can be considered as "infinitely long" for the times and distances considered here).
Heat-generation rate and assumed thermal properties: ϕ'=300 W/m; ρ=2148 kg/m³; c=889 J/kg.°C; λ=4.51 W/m.°C.

time (years)	computer calculations			equation (4.14)		difference in temper. gradients (%)
	interval of distance to heat source (m)	temper. difference (°C)	temper. gradient (°C/cm)	distance to heat source (m)	temper. gradient (°C/cm)	
1	0.1-0.15	4.18	0.8360	0.125	0.8252	-1.3
5	0.1-0.15	3.77	0.7540	0.125	0.7438	-1.4
25	0.1-0.15	2.24	0.4480	0.125	0.4426	-1.2
100	0.1-0.15	0.32	0.0640	0.125	0.0632	-1.2
1	2-3	4.10	0.04100	2.5	0.04126	+0.6
5	2-3	3.76	0.03760	2.5	0.03719	-1.1
25	2-3	2.25	0.02250	2.5	0.02213	-1.6
100	2-3	0.32	0.00320	2.5	0.00316	-1.2

gradient will not be constant, but will decrease with time. A first estimate for the temperature gradient in rock salt is therefore:

$$\left|\frac{\partial\theta}{\partial r}\right| = \frac{\phi'}{2\pi\lambda r} e^{-t/\tau} \qquad (4.14)$$

an exponential decay with the same time constant as the heat generation decay. This equation agrees very well with computer calculations of temperature gradients for a single heat source. This is demonstrated in table 4.5. The differences between the calculated temperature gradients and those predicted by equation (4.14) are all less than 2 %.

Thus, in case the temperature is described by a logarithmic function, equation (4.14) describes very well the temperature gradient for a single heat source of infinite length. This is also the upper limit for the temperature gradient. This can be seen as follows:

1. The temperature gradient in the case of a heat source of finite length is smaller than, or, at most, equal to the temperature gradient in the case of a heat source of infinite length.

2. In the region where the exponential integral cannot be approximated by the logarithmic function, the temperature gradient is overestimated. This is demonstrated in a qualitative way in figure 4.5: in the region where the straight line (the logarithmic function) does not hold, the temperature gradient is smaller than in the case of extrapolation of the logarithmic function.
3. The presence of other heat sources has practically no effect on the temperature gradients, except in the region between the heat sources. There the temperature gradients become smaller (see figure 4.10).

Appendix 4.3

Mean increase in temperature in the case of an infinite number of heat sources of infinite length, placed simultaneously

We consider an infinite number of heat sources of infinite length. This implies that (i) we are dealing with a two-dimensional problem, and (ii) we can limit the calculations to one heat source.

For a hexagonal disposal pattern one heat source corresponds with a cross-section of $0.5\ d^2\sqrt{3}$. Thus the heat capacity, H, per heat source and per unit length is $0.5\ \rho_s c_s d^2\sqrt{3}$.

The heat-generation rate, per heat source and per unit length, is $\phi' e^{-t/\tau}$. Thus the amount of heat, Q, per heat source and per unit length, given off to the rock salt at time t, is:

$$Q = \int_0^t \phi'_0 e^{-t'/\tau} dt' = \phi'_0 \tau (1-e^{-t/\tau}) \qquad (4.15)$$

Consequently, the mean increase in temperature, θ_{mean}, at time t is:

$$\theta_{mean} = \frac{Q}{H} = \frac{2\phi'\tau}{\rho_s c_s d^2\sqrt{3}} (1-e^{-t/\tau}) \qquad (4.16)$$

For very long times, when the HLW has given off all of its heat, we find:

$$\theta_{mean,max} = \frac{2\phi'\tau}{\rho_s c_s d^2\sqrt{3}} \qquad (4.17)$$

Appendix 4.4

Theoretical estimates of the specific heats of carnallite, kainite and polyhalite

According to the Dulong and Petit Law [23] the molar specific heat, at constant volume, of solids like metals is equal to 3R (R: universal gas constant). For more complex solids like salts the specific heat is equal to 3R.f, where f is the number of degrees of freedom [24]. This number of degrees of freedom is usually rather equal to the number of atoms in one molecule (for example: the f-value of $BaCl_2$ is approximately 3). An atom group behaves ambiguously in this respect. For the SO_4-group the number of degrees of freedom turns out to be neither 5 (number of atoms in the group) nor 1 (the group seen as a single unit), but a number in between. In the same way the number of degrees of freedom for the crystal water group lies between 1 and 3.

In order to estimate the number of degrees of freedom, at normal temperatures, corresponding with the SO_4-group and that corresponding with the H_2O-group we have collected the specific heats† of a number of salts from Landolt-Börnstein [15]. The temperatures for which these specific heats are valid lie between 0 and 61 °C. For these salts the numbers of degrees of freedom were calculated, based on the assumption that the Dulong and Petit Law holds:

$$c_M = M.c = 3R.f \qquad (4.18)$$

or

$$f = \frac{M.c}{3R} \qquad (4.19)$$

c_M: molar specific heat;

M: molecular weight.

† These specific heats are specific heats at constant pressure, while the Dulong and Petit Law holds for the specific heats at constant volume. At room temperature, however, the difference between both specific heats for a solid is very small [23]. We will disregard this difference and speak simply of "the" specific heat.

Table 4.6. Specific heats of a number of selected salts, after Landolt-Börnstein [15], and the calculated number of degrees of freedom, f, according to the Dulong and Petit Law.

salt	specific heat (J/kg.°C)	molecular weight	number of degrees of freedom, f	calculated f(SO_4)	calculated f(H_2O)
$BaCl_2$	357	208.25	2.98		
$BaCl_2.2H_2O$	586	244.28	5.74		1.38
$CaCl_2$	686	110.99	3.05		
$CaCl_2.6H_2O$	1339	219.08	11.76		1.45
$CaSO_4$	740	136.14	4.04	3.04	
$CaSO_4.2H_2O$	1109	172.17	7.66		1.81
$FeSO_4$	699	169.95	4.76	3.76	
$FeSO_4.4H_2O$	1189	224.01	10.68		1.48
$FeSO_4.7H_2O$	1360	278.05	15.16		1.49
$CuSO_4$	695	159.60	4.45	3.45	
$CuSO_4.H_2O$	760	177.62	5.41		0.96
$CuSO_4.3H_2O$	954	213.64	8.17		1.24
$CuSO_4.5H_2O$	1130	249.68	11.31		1.37
$MgCl_2$	812	95.22	3.10		
$MgCl_2.6H_2O$	1582	203.31	12.90		1.63
$MgSO_4$	929	120.37	4.48	3.48	
$MgSO_4.H_2O$	1000	138.39	5.55		1.07
$MgSO_4.6H_2O$	1461	228.46	13.38		1.48
$MgSO_4.7H_2O$	1511	246.48	14.93		1.49
$ZnSO_4$	728	161.43	4.71	3.71	
$ZnSO_4.H_2O$	812	179.45	5.84		1.13
$ZnSO_4.6H_2O$	1251	269.52	13.52		1.47
$ZnSO_4.7H_2O$	1348	287.54	15.54		1.55

Average value for f(SO_4): 3.49.
Average value for f(H_2O): 1.40.

The results for the different salts are collected in table 4.6. The data on $BaCl_2$, $CaCl_2$ and $MgCl_2$ demonstrate that each metal atom or halogen atom corresponds fairly closely to one degree of freedom. The number of degrees of freedom corresponding with the SO_4-group was calculated from the salts without crystal water, assuming the number of degrees of freedom for the metal was 1.

Example

$f(MgSO_4)$ = 4.48;

$f(SO_4)$ = $f(MgSO_4)$ - 1 = 3.48.

The number of degrees of freedom corresponding with the H_2O-group was calculated through combining the result for a salt with crystal water with the result for the corresponding salt without crystal water.

Example

$f(CaCl_2.6H_2O)$ = 11.76;

$f(CaCl_2)$ = 3.05;

$f(H_2O)$ = (11.76-3.05)/6 = 1.45.

In this way 5 values for $f(SO_4)$ and 15 values for $f(H_2O)$ were found. The arithmetical averages for both numbers of degrees of freedom were:

average value $f(SO_4)$: 3.49;

average value $f(H_2O)$: 1.40.

With these values for $f(SO_4)$ and $f(H_2O)$ the specific heats of carnallite, kainite and polyhalite can be estimated. Rearranging equation (4.19) yields:

$$c = \frac{3R.f}{M} \qquad (4.20)$$

For R the value of 8.314×10^3 J/kmol.°C was used (this value was also used for the calculation of the f-values of table 4.6). The resulting dimension of c is then J/kg.°C.

Carnallite ($KCl.MgCl_2.6H_2O$):

f = 5 + 6×1.40 = 13.40;

M = 277.86;

c = 1202.8 J/kg.°C, rounded off 1200 J/kg.°C.

Kainite ($KCl.MgSO_4.3H_2O$):

f = 3 + 3.49 + 3×1.40 = 10.69;

M = 248.98;

c = 1070.9 J/kg.°C, rounded off 1070 J/kg.°C.

Polyhalite ($K_2SO_4.MgSO_4.2CaSO_4.2H_2O$):

f = 5 + 4×3.49 + 2×1.40 = 21.76;

M = 602.95;

c = 900.1 J/kg.°C, rounded off 900 J/kg.°C.

Chapter Five

THERMAL MIGRATION OF BRINE INCLUSIONS IN SODIUM CHLORIDE SINGLE CRYSTALS

Abstract

Temperature gradients in rock salt can lead to migration of brine inclusions in the direction of the heat generating high-level nuclear waste (HLW). This phenomenon is caused by the temperature dependency of the salt solubility and by thermodiffusion.

About 100 migration experiments in sodium chloride single crystals have been carried out. The propagation velocities of artificial brine inclusions, at varying temperatures and temperature gradients, were measured with the help of a microscope. These velocities are temperature dependent: 20 °C temperature increase leads to a velocity increase of about 2. The propagation velocities are higher at higher temperature gradients. There are strong indications that for very small temperature gradients, of the order of 0.5 °C/cm or less, brine inclusions do not migrate at all. A comparison of the experimental data of this study with literature data on rock salt indicates, that brine inclusions do not migrate more rapidly in rock salt than in sodium chloride single crystals.

Based on very conservative assumptions a calculation shows that ultimately, per meter HLW-canister, an amount of about 2 liter brine may be attracted by the HLW-heat. In a practical disposal situation this amount will almost certainly be much less.

5.1 Introduction

In general rock-salt formations contain brine inclusions. These inclusions are remnants of the salt solution from which the rock salt has crystallized. On average the brine inclusions make up for a few tenths of a per cent of the salt volume; the dimensions of the inclusions are of the order of tenths of millimeters [1,2,3].

Disposal of high-level nuclear waste, HLW, in rock salt causes temperature gradients in the salt (see chapter 4). Holdoway [4] and Bradshaw and Sanchez [5] have demonstrated that brine inclusions in rock salt can migrate towards a heat source. This phenomenon is caused by the temperature

dependency of the salt solubility and by thermodiffusion. Consequently, some brine may accumulate around HLW-canisters, which may corrode the steel canister walls. In order to judge the safety of underground disposal of radioactive waste, it is necessary to know the amount of brine that can be expected to assemble around a HLW-canister.

Cline and Anthony [1,6-10] and Geguzin et al. [11] have studied brine droplet migration in potassium chloride single crystals. So did Olander et al. [12] both in potassium chloride and in sodium chloride single crystals. Holdoway [4] (under in-situ circumstances) and Bradshaw and Sanchez [5] (in the laboratory) have carried out experiments on brine migration in rock salt. In all these investigations temperature levels as well as temperature gradients had been chosen on the high side, viz. up to some 200 °C and 30 °C/cm respectively. Such conditions are not representative for those prevailing around HLW-columns. Since data on brine migration in sodium chloride or in rock salt under more moderate circumstances are not available, the present study on brine migration has been undertaken to provide some relevant data.

5.2 Theory

5.2.1 Propagation velocity of a brine inclusion

Consider a salt mass containing a brine inclusion, which consists of a saturated solution of the salt in water. A temperature gradient is being imposed on the salt mass. We can distinguish a "cold" side of the inclusion with a temperature T_1 and a "hot" side with a temperature T_2. Because the solubility increases with temperature, the salt concentration is higher at the hot side than at the cold side. Consequently, salt will be transported by diffusion from the hot side to the cold side. At the cold side this salt is precipitated, at the hot side fresh salt is dissolved. The net result is migration of the inclusion towards the region with the highest temperature.

Figure 5.1 gives, schematically, the temperatures and salt concentrations in a brine inclusion when a temperature gradient is present. The temperature gradient in the brine is steeper than the overall gradient in the salt mass, as the thermal conductivity of the salt is much larger than that of the brine. At the cold side the brine is supersaturated and at the hot side it is undersaturated. The degrees of supersaturation and undersaturation determine the rates of dissolution and precipitation of the salt.

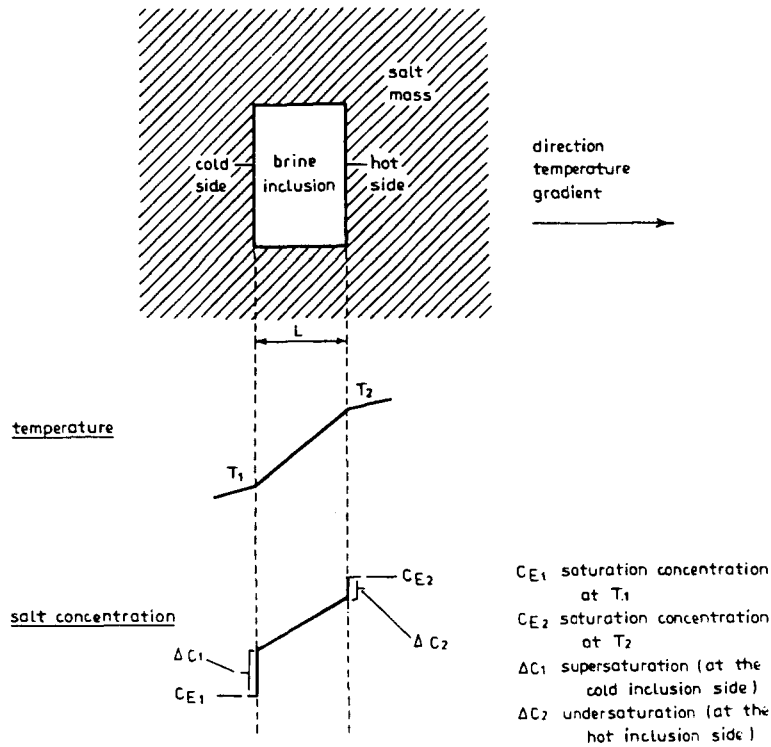

Figure 5.1 Schematic representation of temperatures and salt concentrations in a brine inclusion in the presence of a temperature gradient.

Suppose L is the dimension of the inclusion in the direction of the temperature gradient. The concentration gradient in the body of the brine then is:

$$\frac{\Delta c}{L} = \frac{(c_{E2}-c_{E1}) - (\Delta c_1+\Delta c_2)}{L} \qquad (5.1)$$

Δc: concentration step across the brine inclusion, excluding the walls;
c_{E1}: equilibrium concentration of salt in water at T_1;
c_{E2}: equilibrium concentration of salt in water at T_2;
Δc_1: supersaturation at the cold side of the brine inclusion;
Δc_2: undersaturation at the hot side of the brine inclusion.

Rearranging equation (5.1) yields:

$$\frac{\Delta c}{L} = \frac{c_{E2}-c_{E1}}{\Delta T}\cdot\frac{\Delta T}{L} - \frac{\Delta c_1+\Delta c_2}{L} \qquad (5.2)$$

ΔT: temperature difference between the hot and cold sides of the brine inclusion.

Due to the small inclusion's dimensions generally encountered (L is of the order of 10 μm), ΔT is of the order of a tenth of a centigrade or less. The derivative of the equilibrium concentration with temperature varies little with temperature [13]. Consequently, $(c_{E2}-c_{E1})/\Delta T$ can be replaced by:

$$\frac{c_{E2}-c_{E1}}{\Delta T} = \frac{dc_E}{dT} \qquad (5.3)$$

c_E: thermodynamic equilibrium concentration of salt in water at the prevailing pressure and temperature;

T: temperature.

Define:

$$G_1 = \frac{\Delta T}{L} \qquad (5.4)$$

G_1: temperature gradient in the brine inclusion.

Equation (5.2) can then be written as:

$$\frac{\Delta c}{L} = \frac{dc_E}{dT}\cdot G_1 - \frac{\Delta c_1+\Delta c_2}{L} \qquad (5.5)$$

Mass transport takes place primarily through diffusion. Free-convection velocities are relatively small, as is demonstrated in Appendix 5.1. Moreover, convection leads to a more uniform concentration, and this gives rise in this case to reduction of the rate of propagation of the inclusion, as is also shown in appendix 5.1. Thus, if we assume free convection to be absent, we aim at an upper limit of the propagation velocity.

According to Fick's Law the concentration gradient corresponds with a diffusional salt mass flow per unit area, ϕ''_D:

$$\phi''_D = - D \{\frac{dc_E}{dT}.G_1 - \frac{\Delta c_1+\Delta c_2}{L}\} \qquad (5.6)$$

D: diffusion coefficient of salt in water.

(Fick's Law is only valid for dilute solutions. For a saturated sodium chloride solution D should be replaced by 0.97 D [14]. We will disregard this difference.)

Through the temperature dependency of the saturation concentration the temperature gradient induces a mass flow. However, also the temperature gradient itself causes a mass flow. This effect is called thermodiffusion or Soret-effect. The expression for the thermodiffusional salt mass flow, ϕ''_T, is [8,12]:

$$\phi''_T = - D\sigma c G_1 \qquad (5.7)$$

c: salt concentration in the brine inclusion;

σ: Soret-coefficient of salt in water.

The difference between the salt concentration c and the corresponding saturation concentration c_E will be very small. In equation (5.7) c can therefore be replaced by c_E. The flow according to Fick's Law combined with the thermodiffusional flow yields the total salt mass flow, ϕ''_{total}:

$$\phi''_{total} = \phi''_D + \phi''_T = - D \{(\frac{dc_E}{dT}+\sigma c_E)G_1 - \frac{\Delta c_1+\Delta c_2}{L}\} \qquad (5.8)$$

The relation between the total salt mass flow, ϕ''_{total}, and the propagation velocity of the brine inclusion, v, is:

$$\phi''_{total} = - v.\rho_s \qquad (5.9)$$

ρ_s: specific mass of solid salt.

This leads to the following expression for the propagation velocity:

$$v = \frac{D}{\rho_s} \{(\frac{dc_E}{dT}+\sigma c_E)G_1 - \frac{\Delta c_1+\Delta c_2}{L}\} \qquad (5.10)$$

The temperature gradient in the liquid, G_l, is dependent on the temperature gradient in the solid far away from the inclusion (the overall temperature gradient, G_s) and on the shape of the inclusion. It is more convenient to incorporate G_s in equation (5.8) than G_l. We define:

$$\alpha = \frac{G_l}{G_s} \tag{5.11}$$

α is dependent on the inclusion shape and on the ratio of the thermal conductivities in solid salt and brine. Appendix 5.2 presents the values that α can assume in practice. For the calculation of these values the inclusion shape was approximated by an ellipsoid.

Equation (5.8) can now be written as:

$$v = \frac{D}{\rho_s} \{(\frac{dc_E}{dT}+\sigma c_E)\alpha G_s - \frac{\Delta c_1+\Delta c_2}{L}\} \tag{5.12}$$

5.2.2 Processes in the migrating brine inclusion

When a brine inclusion is migrating in the direction of a main crystallographic axis, it adopts the shape of a rectangular block, with equal width, W, and height, H, both larger than the length, L, the dimension in the direction of the temperature gradient ($L \leq W=H$) (Anthony and Cline [7,8], Olander et al. [12], this study). Another phenomenon is that crystal boundaries can trap migrating brine inclusions, as was shown by Cline and Anthony [7]. They created an artificial crystal boundary by sintering two potassium chloride single crystals for a day at 20 bar and 740 °C. Then they generated artificial brine inclusions with a method such as we used in our experiments (see paragraph 5.3). The migration behaviour of a specific inclusion (L=15 μm, W=H=22 μm) near the artificial boundary was studied. Only at a temperature gradient G_s of 3 °C/cm or larger could the brine inclusion be made to pass the crystal boundary. For smaller gradients the inclusion was trapped at the boundary. According to Cline and Anthony this phenomenon is caused by boundary tension.

A qualitative explanation of the last process may be the following. With the migrating brine inclusion the crystallographic orientation of the first single crystal is introduced in the second single crystal. This leads to an increase of the boundary area between both crystals, and this requires energy. This energy can only be provided if the driving force for migration,

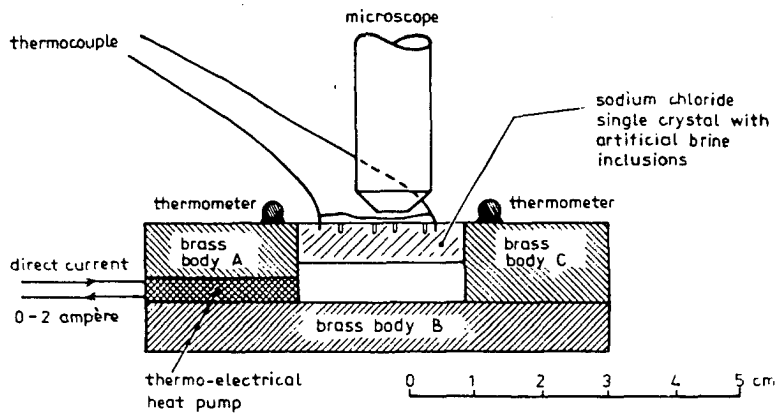

Figure 5.2 Experimental set-up for the measurement of propagation velocities of brine inclusions.

i.e. the temperature gradient, is sufficiently large. A critical temperature gradient for passing a crystal boundary may therefore be expected.

5.3 Experiments

5.3.1 Experimental set-up

Figure 5.2 gives the experimental set-up. Direct current is sent through a thermo-electrical heat pump, type Melcor CP 1.4-71.10. (A thermo-electrical heat pump is based on the Peltier-effect [15]; in an array of thermocouples connected in series, a direct current causes temperature increase and decrease respectively in successive thermocouple junctions.) One side of the heat pump warms up, the other side cools down. The pump is fixed between the brass bodies A and B. The heat circuit is closed by brass body C and the salt body. The interfaces of the salt body and the brass bodies A, B and C are slightly greased to improve the heat contact. The direct current through the heat pump is adjusted between 0-2 A, and in this way any temperature gradient between 0-20 °C/cm can be imposed on the salt. The base temperature of the salt can be varied between 20-90 °C. A low base temperature can be achieved by water-cooling of brass body B, a higher base temperature by electrical heating of this body. The maximum temperature allowed for our type heat pump is about 100 °C, and this limits the salt base temperature.

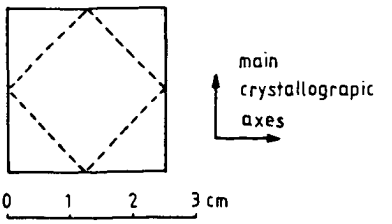

Figure 5.3 Orientation of a 18×18×10 mm³ sodium chloride single crystal (dashed lines), made from a 25×25×10 mm³ crystal (seen from above). The main crystallographic axes in the original crystal are parallel to the edges of this crystal, and make angles of 45° with the horizontal edges of the smaller crystal.

The salt body consists of a sodium chloride single crystal, or, in one experiment, a potassium chloride single crystal, from Highways International, Baarn. Several crystal sizes were used:

- 25×25×10 mm^3, the original size of a sodium chloride single crystal;
- 25×12×10 mm^3, made by cleaving an original sodium chloride single crystal in two halves (this size was used in most experiments);
- 25×15×10 mm^3, the original size of a potassium chloride single crystal;
- 18×18×10 mm^3, made from an original sodium chloride single crystal as sketched in figure 5.3.

In each single crystal 4-8 holes were drilled, 1.5-2 mm deep, with a diameter of 0.6 mm. These holes were filled with distilled water, using a syringe. Then they were sealed by a thin, greased, transparant plastic sheet. The holes formed the original artificial brine inclusions, or, as we will call them from now on: "primary brine inclusions".

Near each end of the single crystal a hole was drilled with a diameter of about 1.5 mm, and about 1.5 mm deep. In these holes the junctions of a chromel-alumel thermocouple were inserted. Thermal contact was established by a small amount of grease. During the experiment the voltage between the junctions was permanently recorded, yielding the temperature gradient.

On the brass bodies A and C mercury thermometers were placed, some 5 mm from the single crystal. Also here grease ensured thermal contact. It was assumed that the temperature in the centre of the single crystal was equal to the average value of the temperatures of the mercury thermometers. With

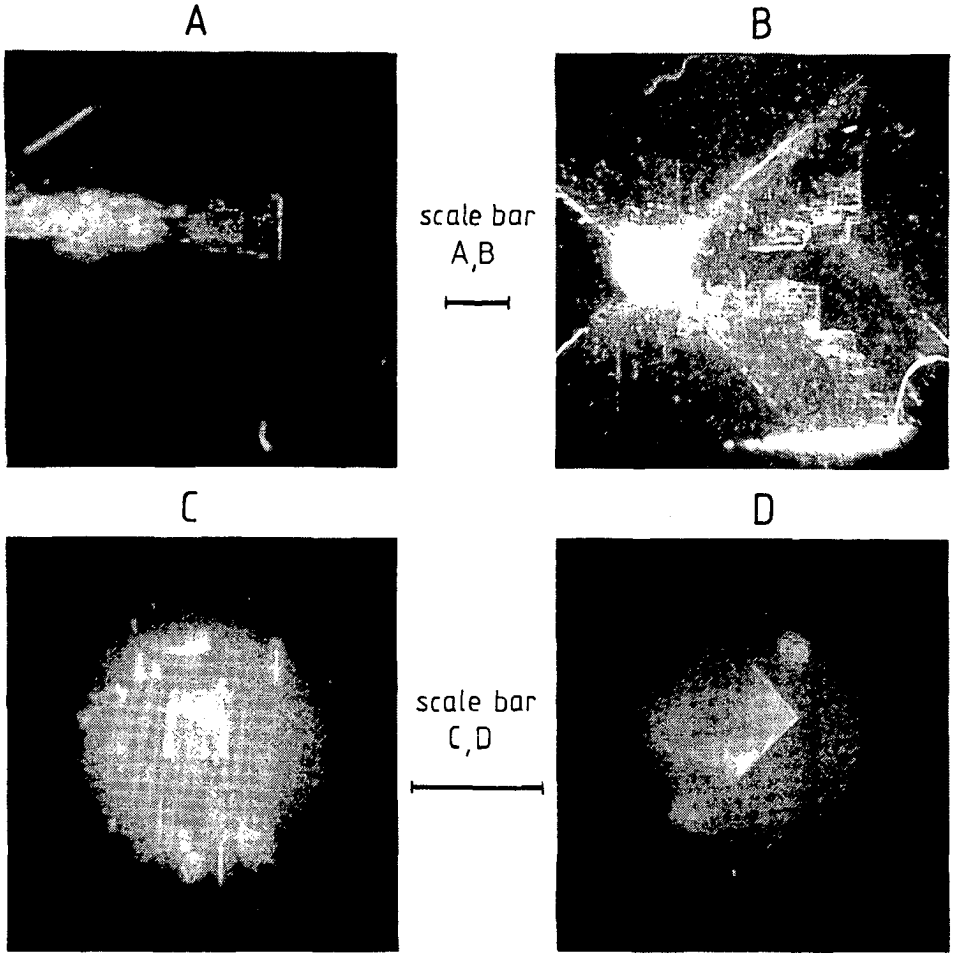

Figure 5.4 Photographs of brine inclusions in a sodium chloride single crystal.

A. Generation of secondary brine inclusions from a primary inclusion (a 0.6 mm bore hole).
B. Generation of secondary brine inclusions from cracks near the primary inclusion.
C. Individual secondary brine inclusions.
D. Chevron-shaped secondary brine inclusion (angle of 45° between the temperature gradient and a main crystallographic axis).

Direction of migration: from left to right.
Scale bar: 1 mm.

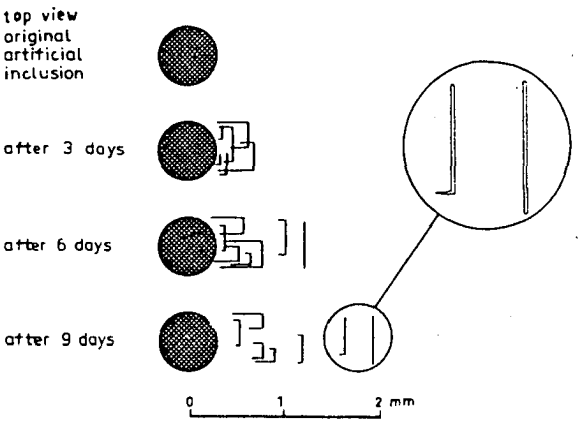

Figure 5.5 Scheme of the development of secondary brine inclusions from a primary inclusion in a sodium chloride single crystal at a temperature gradient of about 10 °C/cm.

the temperature gradient known, this provided the temperature in each primary brine inclusion.

The temperature difference was spread over the total length of the crystal, i.e. 25 mm, except for the last crystal, which had a length of only 18 mm. The directions of the edges of the salt body were identical with those of the main crystallographic axes, with the exception of the last crystal. Here the two horizontal crystallographic axes made angles of about 45° with the horizontal edges (see figure 5.3).

Most experiments started with a temperature gradient of 10-12 °C/cm and a base temperature of about 40 °C ("standard conditions") maintained for about a week. In this week a number of small brine inclusions detached themselves from the primary brine inclusions, i.e. the 0.6 mm bore holes filled with water. We will indicate these small brine inclusions as "secondary brine inclusions". In some cases the drilling had caused cracks around the 0.6 mm holes. Also from these cracks secondary brine inclusions were generated. Figures 5.4A and 5.4B show photographs of the generation of secondary brine inclusions, figure 5.5 gives a scheme of this generation.

5.3.2 Experimental results

After the generation of a large number of secondary brine inclusions under standard conditions, these inclusions were subjected to varying

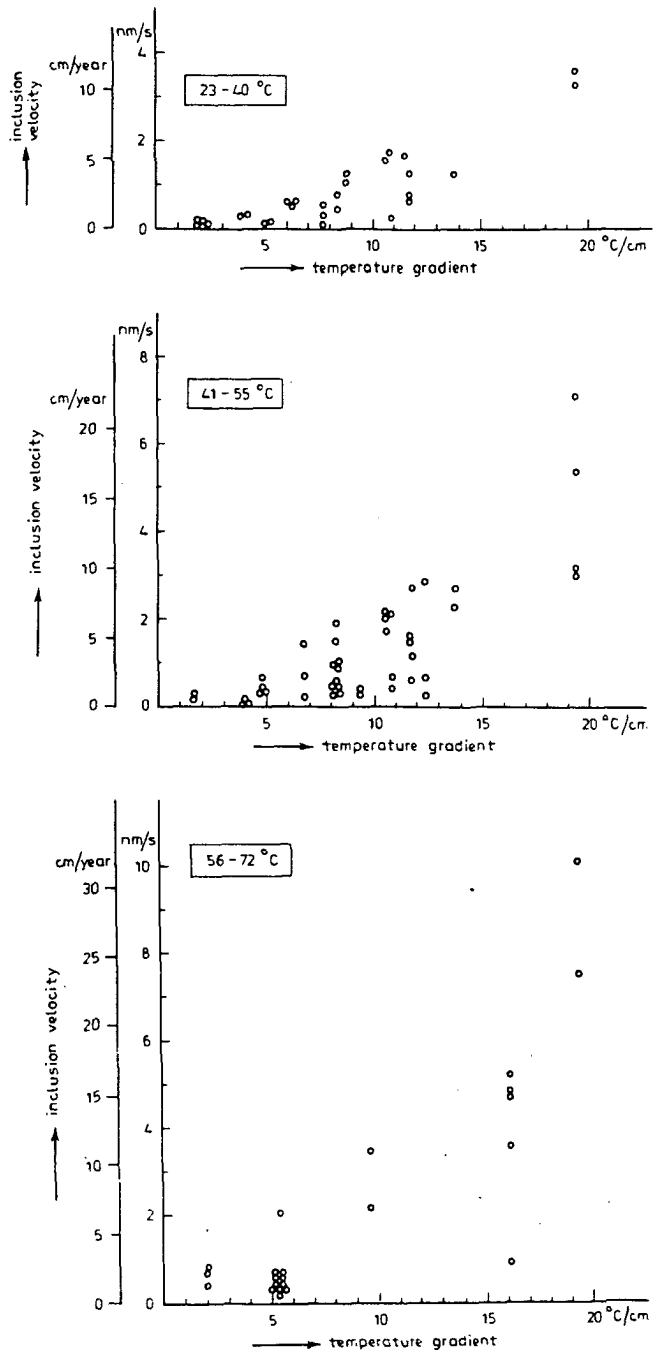

Figure 5.6 Propagation velocities of brine inclusions in sodium chloride single crystals as a function of the temperature gradient.

Table 5.1 Measured brine inclusion velocities in sodium chloride single crystals.

number exper.	brine inclus. code	temper. grad. (°C/cm)	temp. (°C)	brine inclus. veloc. (nm/s)	duration exper. (days)	number exper.	brine inclus. code	temper. grad. (°C/cm)	temp. (°C)	brine inclus. veloc. (nm/s)	duration exper. (days)
1	2.1	19.4	67	7.50	4	49	9B.3	12.4	43	0.67	17
2	2.2	19.4	64	10.10	4	50	9B.3	6.7	49	0.68	6
3	2.3	19.4	54	7.10	4	51	9C.6	10.7	38	1.74	17
4	2.4	19.4	54	5.40	4	52	9D.2a	16.1	72	5.21	5
5	2.5	19.4	44	3.00	4	53	9D.2b	16.1	72	4.85	5
6	2.6	19.4	45	3.20	4	54	9D.2c	16.1	72	4.69	5
7	2.7	19.4	36	3.30	4	55	9D.2d	16.1	72	3.57	5
8	2.8	19.4	36	3.60	4	56	9D.6	16.1	56	0.92	5
9	3A.1	6.2	28	0.65	38	57	9E.1	4.0	52	0.06	21
10	3A.3	6.2	28	0.62	38	58	9E.4a	4.0	49	0.09	21
11	3A.4	6.2	30	0.55	38	59	9E.4b	4.0	49	0.13	21
12	3B.1	5.1	34	0.11	38	60	10A.1a	8.2	44	0.99	17
13	3B.2	5.1	32	0.15	38	61	10A.1a	5.4	64	0.41	11
14	3C.1	7.7	30	0.55	38	62	10A.1b	8.2	44	0.47	17
15	3C.3	7.7	28	0.11	38	63	10A.1b	5.4	64	0.23	11
16	3C.4	7.7	29	0.34	38	64	10A.1c	8.2	44	0.26	17
17	4A.4	11.5	37	1.68	20	65	10A.1c	5.4	64	0.53	11
18	4B.2	9.6	66	3.47	7	66	10A.1d	8.2	44	0.36	17
19	4B.3	9.6	60	2.15	7	67	10A.1d	5.4	64	0.59	11
20	5C.1	8.7	36	1.25	16	68	10A.1e	5.4	64	0.59	11
21	5C.5	8.7	35	1.05	16	69	10A.1f	5.4	64	0.53	11
22	6B.1a	13.7	47	2.28	9	70	10A.2a	8.2	43	1.92	17
23	6B.1b	13.7	47	2.73	9	71	10A.2a	5.4	64	2.08	11
24	6B.2	13.7	40	1.26	9	72	10A.2b	8.2	43	1.50	17
25	7B.6	11.7	42	1.50	11	73	10A.2b	5.4	64	0.65	11
26	7B.6	1.6	46	0.27	15	74	10A.2c	8.2	43	1.04	17
27	7B.7	11.7	38	1.26	11	75	10A.3a	8.2	41	0.88	17
28	7B.7	1.6	45	0.19	15	76	10A.3a	5.4	62	0.49	11
29	7B.8	11.7	37	0.79	11	77	10A.3b	8.2	41	0.47	17
30	7C.2	4.0	29	0.28	62	78	10A.3b	5.4	62	0.61	11
31	7C.8	4.0	24	0.31	62	79	10A.3c	8.2	41	0.58	17
32	8B.2a	11.8	50	1.16	9	80	10A.3c	5.4	62	0.38	11
33	8B.2b	11.8	50	2.75	9	81	10B.3a	8.3	40	0.77	12
34	8E.3	11.7	50	1.57	9	82	10B.3b	8.3	40	0.45	12
35	8E.3	4.8	52	0.69	8	83	10C.1a	9.3	45	0.41	12
36	8E.4	11.7	46	0.63	9	84	10C.1b	9.3	45	0.37	12
37	8E.4	4.8	50	0.29	8	85	11A.3	2.1	25	0.06	60
38	8E.6a	11.7	40	0.70	9	86	11A.4	2.1	24	0.13	60
39	8E.6a	4.8	48	0.33	8	87	11A.5	2.1	23	0.11	60
40	8E.6b	4.8	48	0.44	8	88	11B.3	1.9	24	0.18	60
41	9A.1	10.8	52	0.68	17	89	11B.4	1.9	24	0.12	60
42	9A.3	10.8	47	0.44	17	90	11C.2a	10.5	45	2.17	4
43	9A.4	10.8	45	2.12	17	91	11C.2a	2.0	66	0.73	16
44	9A.7	10.8	38	0.25	17	92	11C.2b	10.5	45	1.74	4
45	9B.1	12.4	49	0.25	17	93	11C.3	10.5	42	2.03	4
46	9B.1	6.7	53	0.24	6	94	11C.3	2.0	66	0.80	16
47	9B.2	12.4	47	2.89	17	95	11C.6	10.5	35	1.59	4
48	9B.2	6.7	52	1.45	6	96	11C.6	2.0	64	0.42	16

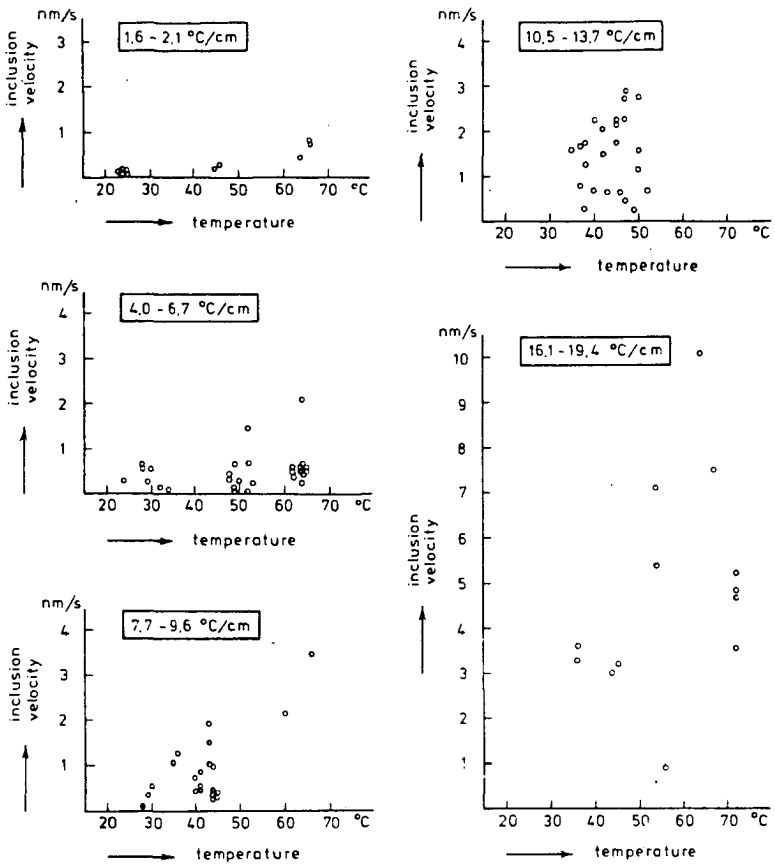

Figure 5.7 Propagation velocities of brine inclusions in sodium chloride single crystals as a function of the temperature.

temperature gradients and base temperatures. The temperature-gradient and base-temperature ranges were 0.8-19.4 °C/cm and 23-72 °C respectively. The propagation velocities of a large number of inclusions were measured by following the positions of the inclusions microscopically using the micrometer in the ocular. The results are presented in a number of graphs. Figure 5.6 presents the propagation velocities as a function of the temperature gradient for three temperature ranges. Figure 5.7 gives these velocities as a function of temperature for five temperature-gradient ranges. Table 5.1 gives the numerical data.

As can be seen in figure 5.7, the propagation velocities increase with increasing temperature. For every temperature-gradient range we selected two propagation velocities: the largest velocity at a low temperature and the largest velocity at a high temperature (experiment pairs 88-94, 9-71, 20-18, 95-47 and 8-2 respectively). With the assumption of an exponential relationship the average increase in temperature for a doubling of the velocity was calculated as 19 °C.

For a specific set of experiments (with sodium chloride crystal 10A) the dimensions of 11 secondary brine inclusions were measured with a microscope. The long edge varied between 150 and 1300 μm, the short edge between 8 and 16 μm. The average values were 400 and 14 μm respectively. Figure 5.4C gives a photograph of some secondary brine inclusions. It was observed that sometimes the inclusions were not perfectly rectangular, but that a trailing effect occurred: at the extremities of the inclusions some brine lags behind.

For the crystal with the main crystallographic axis at an angle of 45° with the temperature gradient, chevron shaped inclusions were observed, as can be seen in figure 5.4D. These inclusions consist of two rectangular slabs, each parallel to a main crystallographic axis, and thus making an angle of 90° with one another.

Other results and observations are:

a. In one case brine migration in a potassium chloride single crystal was investigated. Here the propagation velocities were much larger than for sodium chloride. Accurate velocity measurements were not carried out, but from photographs these velocities can be estimated as 4-16 nm/s (temperature about 40 °C, temperature gradient 11.2 °C/cm).
b. In quite a number of cases generation of secondary brine inclusions did not occur. This may have been caused by the presence of some grease from the covering plastic sheet in the inclusions.
c. In some cases secondary brine inclusions remained immobile after a certain period of migration, under unchanged circumstances. The opposite effect, a more or less sudden velocity increase, was also observed for one inclusion.
d. A decrease of the temperature gradient always resulted in a decrease of the propagation velocity, in some cases to zero velocity. These measuring points, and the zero velocities, are not included in the results as presented in figures 5.6 and 5.7 and in table 5.1.

e. In two cases (crystals 11A and 11C) the primary brine inclusions were immediately subjected to a very small temperature gradient of about 0.8 °C/cm (temperature about 20 °C), thus the standard 10-12 °C/cm temperature-gradient step was omitted. After 10 days of observation no movement had been detected. The temperature and temperature gradient were then increased and this led to the results of experiments 85-87 and 90-96 of table 5.1.

f. In many cases also migration to the cold side was observed. This is a well-known effect for inclusions where liquid and gas are present [1]. In the inclusion water evaporates at the hot side and condenses at the cold side. Consequently, the salt concentration increases at the hot side (this leads to precipitation) and decreases at the cold side (this leads to dissolution), i.e. the inclusion migrates away from the heat source. In our experiments the gas is air entrapped between the plastic sheet and the water of the primary brine inclusion.

g. The velocity of the chevron shaped brine inclusion (see figure 5.4D) is not included in table 5.1. The numerical value was 1.03 nm/s (temperature 44 °C; temperature gradient 13.8 °C/cm), a very "normal" value compared to the results for migration parallel to a main crystallographic axis.

h. In two cases the inserted water contained dye (methylene blue and erytrocine, respectively). This gave some additional visual information about the migration process.

i. Blank experiments (with and without dye) were carried out at room temperature and at a higher temperature. Alterations inside the primary inclusions could not be detected.

5.4 Discussion

5.4.1 Theoretical model

Suppose the crystal growth and crystal dissolution processes are very rapid compared with the diffusion processes. This implies $(\Delta c_1+\Delta c_2)=0$ in equation (5.12). This equation reduces then to:

$$v = \frac{D}{\rho_s}.\left(\frac{dc_E}{dT} + \sigma c_E\right).\alpha G_s \qquad (5.13)$$

Assume a temperature of 30 °C, a temperature gradient of 10 °C/cm and an inclusion-dimension-ratio W/L of 400/14=28.6 (see paragraph 5.3.2). Then the value of α is about 7 (see appendix 5.2: tables 5.2 and 5.3). We calculate v with the following physical properties for sodium chloride at 30 °C:

$D = 2.31 \times 10^{-9}$ m^2/s [16];

$\rho_s = 36.75$ kMol/m^3 [17];

$dc_E/dT = 4.0 \times 10^{-3}$ kMol/m^3.°C [13];

$\sigma = 1.91 \times 10^{-3}$ °C^{-1} [18];

$c_E = 6.165$ kMol/m^3 [13];

The resulting propagation velocity is 6.94 nm/s.

The largest measured velocity for a temperature of 30 °C and a temperature gradient of 10 °C/cm is about 2 nm/s (see figure 5.6). Thus the assumption of rapid dissolution and precipitation leads to much larger propagation velocities than the observed ones.

Also Olander et al. [12] and Cline and Anthony [9] have calculated the propagation velocities of the inclusions in case diffusion (normal plus thermal) is the dominant process, thus assuming infinitely rapid dissolution and precipitation. Just as in our case these velocities were much larger than their measured velocities. Consequently, there is a rapid transport from hot side to cold side, and it must be concluded that this diffusion process is not dominant. It was already noted that the influence of free convection is limited. The processes at the salt/brine-interfaces must therefore be dominant: the resistances to salt dissolution and precipitation will largely determine the propagation velocity.

Furthermore it must be mentioned that the presented theoretical model has some shortcomings:

- In order to describe the temperature gradient inside an inclusion it was assumed that the inclusion shape could be approximated by an ellipsoid (see appendix 5.2). The main reason for this simplification was, that this procedure yields a homogeneous temperature gradient. For a rectangular inclusion this is no longer true. The inhomogeneity of the temperature distribution in a rectangular inclusion can be demonstrated by calculations on a two-dimensional model. Figure 5.8 gives the result in a specific case. The temperature distribution in the centre is fairly homogeneous. At the sides the temperature gradient is lower than in the centre, but from the sides to the corners the gradient increases. Qualitatively these effects will also be present in three dimensions. By

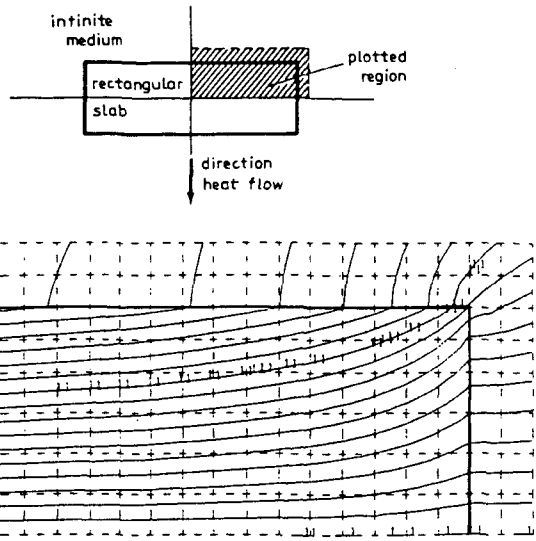

Figure 5.8 Isotherms in the two-dimensional case of heat flow perpendicular to a rectangular slab in an infinite medium (calculated by C.J. de Pater with the computer program MARC).
Ratio thermal conductivities medium/slab: 10.

assuming an ellipsoidal inclusion shape a reasonable estimate of the central temperature gradient can be obtained. The temperature gradient at the inclusion side, however, will generally be overestimated.

- In reality the inclusions adopt a rectangular shape, thus show a strong preference for flat surfaces. This phenomenon is connected with the crystal structure of the salt: a flat surface is energetically more advantageous than a surface of arbitrary shape. In the theoretical model this effect is not incorporated.

5.4.2 Experiments

No definite proof can be presented for the existence of a minimum temperature gradient necessary for migration. However, there are strong indications that this minimum temperature gradient does exist:

- The graphs presented in figure 5.6 suggest this existence. Straight lines through the largest velocities at about 20 °C/cm and at about 2 °C/cm yield the following gradients for zero velocity:

  0.9 °C/cm for the temperature range 23-40 °C;

1.0 °C/cm for the temperature range 41-55 °C;

0.6 °C/cm for the temperature range 56-72 °C.

- When the temperature gradient was suddenly decreased to a relatively low level, the velocities of some small inclusions decreased to zero.
- At our experiments with temperature gradients below 1 °C/cm (room temperature) no movement whatsoever could be detected.
- Cline and Anthony [9] measured a minimum temperature gradient for migration of 1 °C/cm for a specific inclusion in a potassium chloride single crystal.
- Under natural underground circumstances, in rock salt, brine inclusions are permantly subjected to the geothermal gradient of about 0.03 °C/m. An estimate based on extrapolation of the experimental data found in our study yields a migration of tens of meters over a period of 200 million years, approximately the age of the Zechstein salt. This analysis is presented in appendix 5.3. Migration under these circumstances implies the presence of a number of completely dry rock salt regions. Completely dry salt has (to the author's knowledge) never been mentioned in the literature; thus migration under the influence of the natural geothermal gradient seems very unlikely. It would, however, be interesting to investigate suitable rock-salt samples (from beneath formations containing little or no water) for a definite proof of the absence of natural thermal migration.

Our experiments on potassium chloride were carried out as a reference for the experiments on sodium chloride. The measured propagation velocities were in the same range as those of Anthony and Cline [7,8]. Also the development of chevron shaped inclusions is a phenomenon already observed for potassium chloride [9].

The large spread of the propagation velocities of the brine inclusions makes it difficult to draw conclusions on, for example, the existence of a minimum temperature gradient for migration; at a certain temperature and temperature gradient only a maximum measured velocity can be presented. This spread is not caused by experimental errors, but is inherent to processes connected with crystal growth and crystal dissolution; it was also observed in similar experiments on brine migration [5,8,12]. According to Olander et al. [12] an explanation must be sought in the presence of dislocations. Inclusion dimensions are so small that, in single crystals, the inclusions are intersected by only a few dislocations. The presence of a dislocation

leads to more rapid dissolution and precipitation. Consequently, rapidly migrating inclusions are intersected by a relatively large number of dislocations, while slowly moving or immobile inclusions are intersected by few dislocations (or none at all).

5.5 Brine migration in rock salt

Rock salt is a conglomerate of small, impure, sodium chloride single crystals. The crystal boundaries may form natural barriers for migrating brine inclusions. On the other hand the possibility exists that the boundary surfaces form an alternative path for a migrating brine inclusion. The influence of impurities is an uncertain factor. We compare our experimental results on sodium chloride single crystals with some literature data on rock salt.

In-situ experiments with radioactive waste in rock salt showed that brine inclusions do migrate (Holdoway [4]). Unfortunately Holdoway does not give propagation velocities. Nevertheless we will try to derive some information about these velocities. Holdoway's experiment took about 19 months. Temperature and temperature gradient were about 150 °C and 2-5 °C/cm respectively. The increase in propagation velocity with temperature can be roughly put at a factor 2 for every 20 °C temperature increase (see paragraph 5.3.2). Thus the velocities at 150 °C can be estimated at about 16 times those of the central graph of figure 5.6 (41-55 °C). In the temperature-gradient region 2-5 °C/cm the maximum velocities for 150 °C would then be 16×(1-3 cm/year) ≈ 15-50 cm/year, or 25-80 cm per 19 months. Holdoway does not mention inclusion trails over such distances, thus it is probable that experiments with sodium chloride single crystals give rise to larger propagation velocities than experiments with the natural material, rock salt. This supposition is confirmed by the data of Bradshaw and Sanchez on rock salt [5]. They measured propagation velocities of about 1-5 cm/year at 150 °C, normalized at a temperature gradient of 1 °C/cm. This implies a velocity range of 2-25 cm/year for the temperature-gradient range 2-5 °C/cm, thus smaller values for the propagation velocities than our extrapolated data. From the comparison of migration data on sodium chloride single crystals and those on rock salt it appears therefore that the propagation velocities of brine inclusions in natural rock salt are smaller than or at

most of the same order of magnitude as the velocities in sodium chloride single crystals.

Apart from temperature gradients, disposal of radioactive waste will cause pressure gradients. Brine inclusions can also migrate under the influence of a pressure gradient [19]. Extremely large pressure gradients will be necessary to produce inclusion velocities of a magnitude comparable to those presented in this study. Pressure-gradient-induced brine migration in rock salt is therefore a negligible effect and need not be taken into account.

5.6 Estimate of the maximum influx of brine in a specific disposal situation

To estimate the maximum influx of brine in a specific disposal situation we base ourselves on the following assumptions:

a. The propagation velocities vary linearly with the temperature gradient.
b. The proportionality constant between velocity and gradient can be derived from the largest measured propagation velocity (10.10 nm/s for a temperature gradient of 19.4 °C/cm; experiment 2, see table 5.1).
c. The HLW-canister diameter is 20 cm.
d. The half-life of the heat generation is 26.7 years (see chapter 4).

These assumptions are for the main part conservative: (i) the largest measured propagation velocity determines the outcome of the calculation, (ii) the negative effect of grain boundaries on the velocity is not taken into account and (iii) also the possible existence of a minimum temperature gradient for migration is not taken into account. Two factors can lead, however, to an underestimation of the brine influx: (i) disposal temperatures may be (temporarily) higher than the temperatures imposed on the salt in this migration study and (ii) the HLW-canister may be larger than 20 cm (this leads to larger temperature gradients). An uncertain factor is, that the calculation presented here is based on experimental data measured in pure sodium chloride; in practice rock salt will be present. In the preceding paragraph we have seen, however, that propagation velocities in rock salt are not larger than those in sodium chloride single crystals. The use of data obtained with single crystals is therefore justified.

The temperature gradient G_s varies with the distance, r, to the axis of the HLW-canister and with the time after disposal, t (see chapter 4), and can be approximated by:

$$G_s(r,t) = G_s(r_0,0)\,\frac{r_0}{r}\,e^{-t/\tau} \qquad (5.14)$$

r_0: radius of the HLW-canister;

τ: time constant of the exponentially decaying heat generation of the HLW (=26.7/(ln 2) years).

The propagation velocity is assumed to be linear with the temperature gradient, consequently:

$$v = B.G_s(r_0,0).r_0\,\frac{e^{-t/\tau}}{r} \qquad (5.15)$$

B: proportionality constant, numerical value 5.21×10^{-12} $m^2/s.°C$ according to assumption b.

We define:

$$E = B.G_s(r_0,0).r_0 \qquad (5.16)$$

For a 20 cm HLW-canister $G_s(r_0,0)$ is 1.1 °C/cm, thus the numerical value of E is 1.15×10^{-10} m^2/s.

(The temperature gradients decrease slowly with time. For the largest temperature gradients, those near the HLW-canister, it takes about 300 years to decrease to the level of the natural geological gradient. The period corresponding with the possible HLW-heat-induced brine migration can therefore be defined as 0-300 years after the disposal of the HLW.)

Combination of equations (5.15) and (5.16) gives:

$$v = \frac{E}{r}\,e^{-t/\tau} \qquad (5.17)$$

In an infinitely small time-period dt an inclusion migrates over a distance dr:

$$dr = -\,v.dt \qquad (5.18)$$

Combination with equation (5.17) yields:

$$dr = -\frac{E}{r} e^{-t/\tau} dt \qquad (5.19)$$

Or:

$$r.dr = -E.e^{-t/\tau} dt \qquad (5.20)$$

This differential equation can be easily solved. The result is, for the boundaries t=0 and t=∞:

$$r^2_{(t=0)} - r^2_{(t=\infty)} = 2\,E\tau = 0.2794\ m^2 \qquad (5.21)$$

Suppose $r_{(t=\infty)}=r_0$, i.e. after an infinite period of time the inclusion has just reached the HLW-canister. Then $r_{(t=0)}$ can be calculated as 0.54 m. Thus, for the assumptions mentioned, an inclusion can only reach the HLW-canister in a finite time if its original position is 0.44 m or less from the canister wall.

The salt with a distance of 0.44 m or less from the canister wall corresponds with a volume of 0.88 m^3 per meter HLW-canister. Assume a moderate brine concentration of 0.2 to 0.25 volume % [2]. Then the total influx of brine after an infinite period of time amounts to about 2 liter per meter HLW-canister. The influx rate of the brine decays exponentially, at the same rate as the heat generation of the HLW.

The estimate for the amount of brine which can maximally be attracted by the heat source will be considerably lower in case the temperature and/or the temperature gradient are much smaller than those assumed in the calculation. Smaller temperatures and temperature gradients can be achieved by allowing the waste to give off its heat for an extra period of time prior to disposal.

5.7 Conclusions

1. A theoretical model for the migration of brine inclusions is developed. This model incorporates molecular diffusion and thermodiffusion and takes into account the occurrence of the salt dissolution and precipitation processes.
2. The combined salt dissolution and precipitation process is the rate-determining process for the propagation velocity of a brine inclusion.

3. The propagation velocity depends on the temperature and on the temperature gradient. The velocities are roughly doubled for every 20 °C increase in temperature. The relationship with the temperature gradient is approximately linear for the larger gradients (above 5 °C/cm). For small gradients the ratio velocity/gradient decreases. There are strong indications that for temperature gradients of the order of 0.5 °C/cm or less inclusions do not migrate at all.
4. Comparison of our data on sodium chloride single crystals with literature data on natural rock salt shows, that propagation velocities in natural rock salt are smaller than or at most of the same order of magnitude as the velocities measured in sodium chloride single crystals.
5. Based on very conservative assumptions a calculation reveals that ultimately, per meter HLW-canister, an amount of about 2 liter of the brine may be attracted by the HLW-heat. In a practical disposal situation this amount will probably be much less.
6. As migration of brine towards canisters may result in a substantial accumulation of brine at the canister walls, these walls should be able to withstand brine corrosion.
7. Investigation of suitable natural rock-salt samples may provide evidence that thermal migration under very low thermal gradients (of the order of the natural geological gradient) does not occur.

List of symbols

b ratio (long axis ellipsoid)/(short axis ellipsoid)
B proportionality constant in equation (5.15)
c salt concentration in the brine inclusion
c_E thermodynamic equilibrium concentration of salt in water at the prevailing pressure and temperature
c_{E1} equilibrium concentration of salt in water at T_1
c_{E2} equilibrium concentration of salt in water at T_2
d diameter of a spherical particle rising in a viscous liquid
D diffusion coefficient of salt in water
E proportionality constant defined by equation (5.16)
g acceleration of gravity
G_l temperature gradient in the brine inclusion
G_s overall temperature gradient in the solid salt

H height of the brine inclusion

L dimension of the brine inclusion in the direction of the temperature gradient

r distance to the axis of the HLW-canister

r_0 radius of the HLW-canister

t time after disposal of the HLW

T temperature

T_1 temperature at the cold side of the brine inclusion

T_2 temperature at the hot side of the brine inclusion

v propagation velocity of the brine inclusion

v_{down} downward velocity of a brine inclusion under natural geological circumstances

v_{up} rise velocity of a brine inclusion under natural geological circumstances

v_x horizontal velocity of the salt in the brine

v_z free-convection velocity

$v_{z,max}$ maximum free-convection velocity

$v_{z,aver}$ average free-convection velocity

W width of the brine inclusion

x horizontal coordinate

α ratio (temperature gradient in the brine inclusion)/(overall temperature gradient in the solid salt)

β cubic expansion coefficient of brine

Δc concentration step across the brine inclusion, excluding the walls

Δc_1 supersaturation at the cold side of the brine inclusion

Δc_2 undersaturation at the hot side of the brine inclusion

ΔT temperature difference between the hot and cold sides of the brine inclusion

$\Delta \rho$ density difference between a viscous liquid and a spherical particle rising in the liquid

λ_1 thermal conductivity of brine

λ_s thermal conductivity of solid salt

μ_1 dynamic viscosity of the liquid wherein a spherical particle is rising

μ dynamic viscosity of brine

ρ_1 average specific mass of brine

ρ_s specific mass of solid salt

τ time constant of the exponentially decaying heat generation of the HLW

ϕ''_D diffusional salt mass flow per unit area

ϕ''_T thermodiffusional salt mass flow per unit area

ϕ''_{total} total salt mass flow per unit area

σ Soret-coefficient of salt in water

List of abbreviations

HLW high-level nuclear waste

References

1. Anthony, T.R. and Cline, H.E.: Thermomigration of liquid droplets in salt, Proceedings Fourth Symposium on Salt, Vol. 1, 313, The Northern Ohio Geological Society, Cleveland, 1974.
2. Verkerk, B.: Glas in zout, beschouwing van enkele facetten van het opbergen van kernsplijtingsafval in een zoutformatie, Energiespectrum, 1 (1977) 348.
3. Jenks, G.H.: Radiolysis and hydrolysis in salt-mine-brines, Report Oak Ridge National Laboratory, ORNL-TM-3717, 1972.
4. Holdoway, K.A.: Behavior of fluid inclusions in salt during heating and irradiation, Proceedings Fourth Symposium on Salt, Vol. 1, 303, The Northern Ohio Geological Society, Cleveland, 1974.
5. Bradshaw, R.L. and Sanchez, F.: Brine cavity migration studies (Health physics division annual progress report), Report Oak Ridge National Laboratory, ORNL-4316, 1968.
6. Cline, H.E. and Anthony, T.R.: The shape relaxation of liquid droplets in solids, Acta Metall., 19 (1971) 175.
7. Cline, H.E. and Anthony, T.R.: The thermomigration of liquid droplets through grain boundaries in solids, Acta Metall., 19 (1971) 491.
8. Anthony, T.R. and Cline, H.E.: Thermal migration of liquid droplets through solids, J. Appl. Phys., 42 (1971) 3380.
9. Cline, H.E. and Anthony, T.R.: Effects of the magnitude and crystallographic direction of a thermal gradient on droplet migration in solids, J. Appl. Phys., 43 (1972) 10.
10. Cline, H.E. and Anthony, T.R.: The migration of liquid droplets in solids, J. Crystal Growth, 13/14 (1973) 790.
11. Geguzin, Y.E., Dzyuba, A.S. and Kruzhanov, V.S.: Response to a temperature gradient from liquid inclusions in a crystal, Sov. Phys. Crystallogr., 20 (1975) 234.
12. Olander, D.R., Machiels, A.J., Balooch, M. and Yagnik, S.K.: Thermal gradient migration of brine inclusions in synthetic alkali halide single crystals, J. Appl. Phys., 53 (1982) 669.
13. Intern. Crit. Tables, Vol. IV, McGraw-Hill, New York, 1928.
14. Van den Broek, W.M.G.T.: Beweging van vloeistofinsluitsels in steenzout onder invloed van een temperatuurgradiënt (optimale vloeistofsnelheid), Internal report Delft University of Technology (Faculty of Mining and Petroleum Engineering), 1983.
15. Zemansky, M.W.: Heat and thermodynamics (fourth edition), McGraw-Hill, New York, 1957.
16. Intern. Crit. Tables, Vol. V, McGraw-Hill, New York, 1929.
17. Weast, R.C. (editor): Handbook of Chemistry and Physics (62nd edition), CRC Press, Boca Raton, 1981.

18. Alexander, K.F.: Zur Theorie der Thermodiffusion in Flussigkeiten III, Zeitschr. Phys. Chem., 203 (1954) 213.
19. Anthony, T.R. and Cline, H.E.: The kinetics of droplet migration in solids in an accelerational field, Phil. Mag., 22 (1970) 893.
20. Bird, R.B., Stewart, W.E. and Lightfoot, E.N.: Transport phenomena, John Wiley & Sons, New York, 1960.
21. Intern. Crit. Tables, Vol. II, McGraw-Hill, New York, 1927.
22. Van den Broek, W.M.G.T.: Fysische constanten van steenzout en kernsplijtingsafval ten behoeve van temperatuurberekeneingen, Report Delft University of Technology, 1978.
23. Carslaw, H.S. and Jaeger, J.C.: Conduction of heat in solids (second edition), Oxford University Press, London, 1959.
24. Van den Broek, W.M.G.T.: Some theoretical aspects of de-oiling of water by plate separation, Delft Progr. Rep., 13 (1988/1989) 87.
25. Bérest, P. and Nguyen Minh, D.: Deep underground storage cavities in rock salt; interpretation of in situ data from French and foreign sites, Proceedings First Conference on the Mechanical Behavior of Salt, Trans Tech Publications, Clausthal, 1984.

Appendix 5.1

Free convection in a secondary brine inclusion

For the analysis of free convection in a secondary brine inclusion we simplify the inclusion geometry to two vertical planes with a distance equal to the distance between the hot and cold sides of a brine inclusion, L. The temperature difference between the planes is assumed to be ΔT, equal to the temperature difference between the hot and cold sides of the brine inclusion. First we will analyse free convection as a result of the temperature dependency of the specific mass of a salt solution. According to Bird et al. [20], the free-convection velocity, v_z, in a homogeneous liquid - thus also in brine with a constant concentration - is:

$$v_z = \frac{\rho_1 \beta g L^2 \Delta T}{6\mu} \left\{ \frac{x^3}{L^3} - \frac{x}{4L} \right\} \qquad (5.22)$$

ρ_1: average specific mass of brine;
β: cubic expansion coefficient of brine;
g: acceleration of gravity;
μ: dynamic viscosity of brine;
x: horizontal coordinate (x=0 halfway between the vertical planes).

At the hot side the velocity is upward, at the cold side the velocity is downward. The velocity is zero for x=-L/2, x=0 and x=L/2. The maximum

velocities, $v_{z,max}$, in the hot and cold regions are equal (but with opposite signs), and appear for $x=(L\sqrt{3})/6$ and $x=-(L\sqrt{3})/6$. Also the average velocities, $v_{z,aver}$ for both regions are equal (but with opposite signs). $v_{z,max}$ and $v_{z,aver}$ can be calculated as:

$$v_{z,max} = \frac{\rho_l \beta g L^2 \Delta T \sqrt{3}}{216\mu} \tag{5.23}$$

$$v_{z,aver} = \frac{\rho_l \beta g L^2 \Delta T}{192\mu} \tag{5.24}$$

We will calculate the average free-convection velocity in a specific case for two temperatures, 30 °C and 60 °C.

Assume an overall temperature gradient in the brine of 10 °C/cm and inclusion dimensions of $14\times400\times400$ μm^3 (average dimensions of a secondary brine inclusion, see paragraph 5.3.2). The ratio width/length of the inclusion is 28.6, and this yields ratios $\alpha=G_l/G_s$ of about 7 (30 °C) and 6 (60 °C) (see tables 5.2 and 5.3). The temperature gradients in the brine are then about 70 °C/cm (30 °C) and 60 °C/cm (60 °C). The values for ΔT are 0.098 °C (30 °C) and 0.084 °C (60 °C). Values from standard data books [17,21] for the expansion coefficient are 3.0×10^{-4} $°C^{-1}$ (30 °C) and 5.2×10^{-4} $°C^{-1}$ (60 °C), and for the dynamic viscosity of a saturated salt solution 2.2×10^{-3} Ns/m^2 (30 °C) and 0.80×10^{-3} Ns/m^2 (60 °C). With $\rho_l=1200$ kg/m^3 and $g=9.8$ m/s^2 we find for the average free-convection velocity:

$$30\ °C:\ v_{z,aver} = 2.2\times10^{-10}\ m/s = 0.22\ nm/s \tag{5.25}$$

$$60\ °C:\ v_{z,aver} = 7.7\times10^{-10}\ m/s = 0.77\ nm/s \tag{5.26}$$

The analysed case is for free convection as a result of the temperature dependency of the specific mass, for a constant salt concentration. The salt concentration in a brine inclusion, however, is <u>not</u> constant; due to thermodiffusion the concentration at the cold side is higher than at the hot side. A higher concentration corresponds with a higher specific mass. The effect of temperature on the specific mass is similar: also here the highest specific mass is at the cold side. Thus in practice free convection occurs (i) as a result of the temperature dependency of the specific mass and (ii) as a result of the concentration dependency of the specific mass. For the

already discussed specific-mass effect the free-convection velocity is proportional to $\beta.\Delta T$, with β of the order 4×10^{-4} °C^{-1}. For the concentration effect the corresponding proportionality factor is:

$$\frac{1}{\rho_l}.\frac{d\rho_l}{dc}.\sigma c_E.\Delta T \qquad (5.27)$$

A calculation based on values from standard data books yields about 3×10^{-4} °C^{-1} for the factor preceding ΔT in equation (5.26). The specific-mass effect and the concentration effect are therefore of the same order of magnitude. This will lead to average free-convection velocities of about 2 times the velocities given above: about 0.4 nm/s at 30 °C and about 1.5 nm/s at 60 °C.

The largest measured inclusion velocities at 30 °C and at 60 °C, for an overall temperature gradient in the solid of 10 °C/cm, are about 2 nm/s and 4 nm/s, respectively. However, these are not the velocities of the salt in the inclusion. The inclusion velocity, v, is defined by equation (5.9). The horizontal velocity of the salt in the brine, v_x, is:

$$\phi''_{total} = v_x.c_E \qquad (5.28)$$

Combination of this equation with equation (5.9) yields:

$$\left|\frac{v_x}{v}\right| = \frac{\rho_s}{c_E} \qquad (5.29)$$

For sodium chloride the ratio ρ_s/c_E is about 6. Consequently, the salt velocity in the inclusion is about 6 times as rapid as the inclusion velocity. For 30 °C and 60 °C the maximum horizontal salt velocities in the brine are therefore 12 and 24 nm/s. Thus for rapidly migrating brine inclusions the free-convection velocity is much smaller than the velocity of salt transported from the hot to the cold inclusion side. There is, however, a large spread in inclusion velocities (see figure 5.6). For slowly migrating brine inclusions the free-convection velocity can be of the same order of magnitude as the salt velocity v_x. Then free convection may play an important role: it can lead to a reasonably constant salt concentration. This leads to smaller under- and supersaturation levels, minimizing the concentration effect, and therefore to smaller propagation velocities.

Consequently, free convection in a migrating brine inclusion leads to a reduction of the inclusion velocity.

The free-convection velocities were calculated for a temperature gradient of 10 °C/cm. A calculation for, say, 1 °C/cm would result in free-convection velocities of 0.1 times the calculated velocities. However, the inclusion velocities are less than 0.1 times the velocities at 10 °C/cm. We conclude that for temperature gradients of 1 °C/cm or less free convection is more important than for temperature gradients of the order of 10 °C/cm. Also for very small temperature gradients free convection has a negative effect on the propagation velocities of the brine inclusions.

Appendix 5.2
Temperature gradient in the brine inclusion

The thermal conductivity of sodium chloride is, dependent on the temperature, 7-12 times the thermal conductivity of a saturated solution of sodium chloride in water. See table 5.2. Because of this difference in thermal conductivity the overall temperature gradient in the solid salt, G_s, induces a larger temperature gradient in the brine, G_l. The ratio $\alpha = G_l/G_s$ is dependent on the inclusion shape and on the ratio of the thermal conductivities of the solid salt and the brine.

The temperature distribution inside a rectangular block is not uniform (this was discussed in paragraph 5.4.1), but the temperature distribution inside an ellipsoid is. An additional advantage of this distribution is, that it can be calculated analytically, and this does not apply to a rectangular block. For the approximate calculation of the temperature gradient in the brine it is therefore convenient to assume an ellipsoidal shape (see figure 5.9). Carslaw and Jaeger [23] give the ratio α for an inclusion with the form of an oblate ellipsoid (two equally long axes, one short axis):

$$\alpha = \frac{G_l}{G_s} = \{1 - \frac{b^2}{(b^2-1)^{3/2}}(\sqrt{b^2-1} - \arctan\sqrt{b^2-1})(1 - \frac{\lambda_l}{\lambda_s})\}^{-1} \qquad (5.30)$$

b: ratio (long axis of the ellipsoid)/(short axis of the ellipsoid);

λ_l: thermal conductivity of brine;

λ_s: thermal conductivity of solid salt.

Table 5.2 Thermal conductivities of rock salt and solid sodium chloride, λ_s, and of a saturated solution of sodium chloride in water, λ_l.

temperature (°C)	λ_s (W/m.°C) [22]		λ_l (W/m.°C) [16]	λ_s/λ_l	
	rock salt	NaCl single crystal		rock salt	NaCl single crystal
20	5.63	6.38	0.543	10.37	11.75
40	5.21	5.90	0.570	9.14	10.35
60	4.84	5.48	0.600	8.07	9.13
80	4.51	5.11	0.604	7.47	8.46
100	4.21	4.77	0.608	6.92	7.85

Table 5.3 The ratio α, (temperature gradient in the brine)/(overall temperature gradient in the solid salt), for an oblate ellipsoid, as a function of the thermal conductivity ratio λ_s/λ_l, with b the ratio (long axis ellipsoid)/(short axis ellipsoid).

b	λ_s/λ_l						
	6	7	8	9	10	11	12
1	1.38	1.40	1.41	1.42	1.43	1.43	1.44
1.5	1.59	1.62	1.64	1.66	1.67	1.68	1.69
2	1.78	1.82	1.86	1.88	1.90	1.92	1.94
3	2.13	2.20	2.25	2.30	2.34	2.37	2.39
5	2.67	2.80	2.91	3.00	3.08	3.15	3.20
7	3.08	3.28	3.44	3.58	3.70	3.80	3.89
10	3.54	3.81	4.05	4.26	4.44	4.60	4.74
15	4.05	4.43	4.78	5.08	5.35	5.60	5.82
20	4.38	4.85	5.27	5.66	6.01	6.33	6.62
30	4.80	5.38	5.92	6.42	6.89	7.32	7.73
50	5.20	5.91	6.59	7.23	7.84	8.42	8.98
70	5.40	6.18	6.93	7.65	8.34	9.01	9.66
100	5.57	6.40	7.22	8.01	8.78	9.52	10.25
150	5.70	6.59	7.46	8.31	9.15	9.97	10.77
200	5.77	6.69	7.59	8.47	9.34	10.20	11.05
300	5.85	6.79	7.72	8.64	9.55	10.46	11.35
500	5.91	6.87	7.83	8.78	9.73	10.67	11.60
700	5.93	6.91	7.88	8.84	9.80	10.76	11.71
1000	5.95	6.93	7.91	8.89	9.86	10.83	11.80
∞	6.00	7.00	8.00	9.00	10.00	11.00	12.00

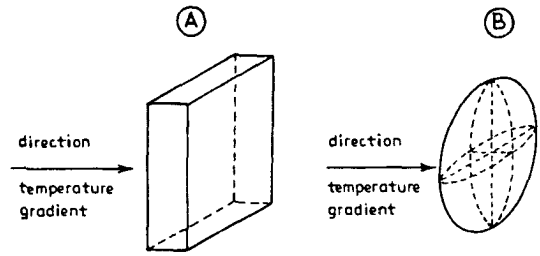

Figure 5.9 Replacement of a rectangular block (A), the real shape of a brine inclusion, for an oblate ellipsoid (B), the assumed shape of a brine inclusion, for the calculation of the temperature gradient in the brine.

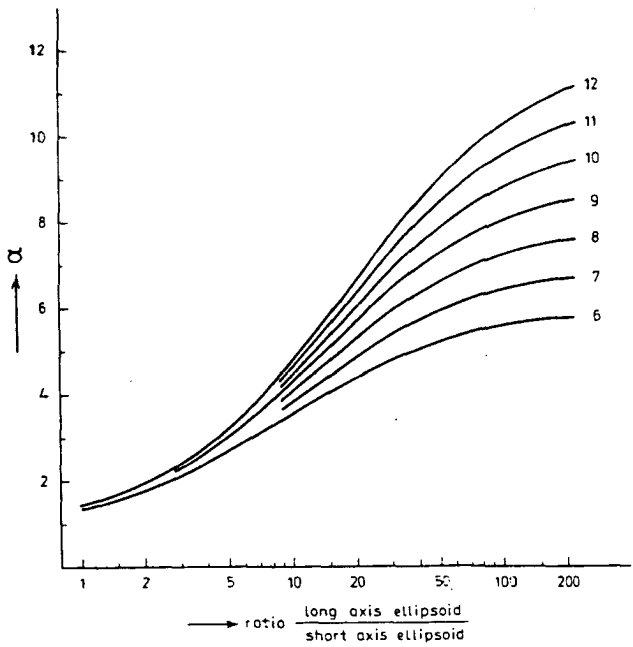

Figure 5.10 The ratio α, (temperature gradient in the brine)/(temperature gradient in the solid), for an oblate ellipsoid, for thermal conductivity ratios, λ_s/λ_l, of 6-12.

Calculation results for relevant values of λ_s/λ_l and b are presented in figure 5.10. Table 5.3 gives the corresponding data.

Appendix 5.3
Migration of a brine inclusion under geological circumstances

We consider two mechanisms for the migration of a brine inclusion under geological circumstances:

- the density difference between salt and brine, possibly leading to an upward movement of the brine inclusion;
- the natural geothermal gradient of 0.02-0.03 °C/m, possibly leading to a downward movement of the brine inclusion.

Upward movement

The (stationary) rise velocity, v_{up}, of a spherical particle in a liquid as a result of the density difference, $\Delta\rho$, between liquid and particle, is [24]:

$$v_{up} = \frac{\Delta\rho.g.d^2}{18\,\mu_l} \qquad (5.31)$$

d: diameter of the spherical particle;

μ_l: dynamic viscosity of the liquid.

Solid salt can be considered as an extremely viscous liquid. The dynamic viscosity is of the order of 1000 MPa.year, about 4×10^{16} Ns/m^2 [25]. If we take a rather large characteristic inclusion dimension of 1 mm and assume that equation (5.31) gives an estimate of the upward velocity, also in the case of a non-spherical particle, then we find (with $\Delta\rho$=1000 kg/m^3 and g=9.8 m/s^2) a v_{up} of about 2×10^{-20} m/s.

Downward movement

For an estimate of the downward movement we use a simplified form of equation (5.12). On the one hand we do not take into account the thermodiffusion effect: this leads to an underestimation of the propagation velocity. On the other hand we do not take into account the resistances to salt dissolution and precipitation: this leads to an overestimation of the propagation velocity. For the simplified equation we find:

$$v_{down} = \frac{D}{\rho_s} \cdot \frac{dc_E}{dT} \cdot \alpha G_s \qquad (5.32)$$

For extremely small temperature gradients an inclusion has a shape close to that of a cube [6], thus it is realistic to assume a small value of 1.5 for α. With values for D, ρ_s and Dc_E/dT as given in paragraph 5.4.1, and with a value for G_s of 0.025 °C/m, we find a downward propagation velocity of 9×10^{-15} m/s $\approx$ 10^{-14} m/s.

Evaluation

Rock salt from the Zechstein period is more than 200 million years old. The distance corresponding with the upward velocity is about 0.1 mm. This effect is therefore totally negligible. The distance corresponding with the downward velocity amounts to about 60 m. Due to the simplified calculation procedure this figure may be under- or overestimated. It is, however, justified to conclude that the theory presented in this chapter, extrapolated to extremely small temperature gradients, predicts a downward migration of brine inclusions over 200 million years of tens of meters under influence of the natural geothermal gradient.

Chapter Six

SEPARATION OF HIGH-LEVEL NUCLEAR WASTE INTO TWO WASTE CATEGORIES

Abstract

High-level nuclear waste (HLW) contains two groups of radioactive nuclides with very different characteristics: (i) the "heat generators" which produce heat during several hundred years and (ii) the long-living radioactive nuclides, especially the "transuranes", which remain radioactive for a much longer period, but with practically no heat production. Each group has different disposal requirements. Separation of the HLW into two waste categories, viz. a heat-generators category and a transuranes category, may lead to a simpler, safer and more efficient disposal of the waste.

An analysis of the consequences of separation of HLW into two waste categories is presented. This analysis is based on relative toxic risks: both radiotoxicity and chemical toxicity are taken into account. Four separation schemes have been considered. As for chemical separation a favourable separation scheme proved to be the scheme where the transuranes category contains the actinides and the (non-radioactive) lanthanides, and the heat-generators category the rest of the HLW.

6.1 Introduction

The several types of radioactive waste differ in volume, heat generation, type and intensity of radiation, and time span within which the waste remains radioactive. The waste that poses the greatest difficulties for disposal in a geological formation is the high-level nuclear waste, HLW. These difficulties arise from large heat generation on the one hand and from long-term persistent radioactivity on the other hand.

1. Heat generation

   The HLW generates heat and this leads to increase in temperature in the geological formation. The heat evolution decreases with a half-life of about 30 years, and will practically be expired in about 200 years. The

increases in temperature will correspondingly die out within about 1000 years (see chapter 4 and Van den Broek [1]).

2. Long-term radioactivity

HLW contains radioactive nuclides[†] with extremely long half-lifes: of the order of 10^6 years or more. Isolation of the HLW from the biosphere must therefore be guaranteed for a very long period.

Those nuclides which are mainly heat generators, decay to stable elements in a few hundred years. Consequently, for these nuclides a relatively short isolation time would suffice if they were not mixed up in the HLW with the long-living radioactive nuclides. This prompted us to investigate the merits of separation of HLW into two waste categories, viz. one category containing the heat-generating nuclides (the "heat-generators category") and the other containing the long-living radioactive nuclides, mainly transuranes[††] (the "transuranes category").

Separation of HLW into two waste categories offers the following advantages:

a. The isolation time required for the heat-generators category is relatively short. It is therefore much easier to show that this isolation time can be guaranteed.
b. The isolation time for the transuranes category is very long. The volume of waste that requires a long isolation time, however, is now smaller.
c. Heat-generation effects need not be taken into account for the transuranes category.

The object of this preliminary study is to investigate whether these advantages are sufficiently large to outweigh the disadvantages of separation, for a limited number of separation schemes. The disadvantages concern mainly the effects on the nuclear fuel cycle (i.e. the complete cycle of the management and processing of the nuclear fuel and nuclear waste).

[†] A nuclide is a species characterized by the atom number, defining the chemical element, and the number of protons plus neutrons in the nucleus, defining the particular isotope.

[††] A transurane is an element with an atom number of 93 or more: Np, Pu, Am, Cm, ...

To analyse the concept of separation of the HLW into two waste categories we have to take three aspects into account. The first aspect is the toxicity aspect: we must be able to quantify the toxicity of the two waste categories in order to judge the effect of the separation. This implies radiotoxicity as well as the combination of radiotoxicity and chemical toxicity. The second aspect is the volume aspect: it may turn out that the separation leads to a larger bulk volume of HLW. The last aspect is the separation-technology aspect: some difficulties with respect to the chemical separation are presented and are subsequently taken into account in the final analysis.

6.2 Definition of the different relative toxic risks

Separation of the high-level nuclear waste leads to spreading of the toxicity over the two HLW-categories. In order to analyse the consequences of splitting up the HLW, one needs to have yard-sticks for the toxicities of both radioactive and non-radioactive materials. The toxicities will be expressed as relative toxic risks, as follows:

1. Relative Radiotoxic Risk (RRR).
   A measure for the toxicity of an amount of radioactive material is the relative radiotoxic risk, RRR [2,3]. This is defined as the volume of water needed to take up the given amount of radioactive material, so as to meet the maximum allowable concentration in drinking-water, MAC (example: for an amount of radioactive material of A grammes with a MAC of B g/m^3 the RRR is A/B m^3). For a mixture of different radioactive materials the total RRR is defined as the sum of the respective RRR's [2].
2. Relative Chemical-toxic Risk (RCR).
   In order to compare radiotoxicity with chemical toxicity we introduce here, analogous to the RRR for radiotoxicity, the relative chemical-toxic risk, RCR, for a non-radioactive compound. This is the volume of diluting water that, for the given amount of non-radioactive material, corresponds with the maximum allowable concentration in drinking-water. Just as for the RRR we define: for a mixture of different (non-radioactive) materials the total RCR is the sum of the respective RCR's.

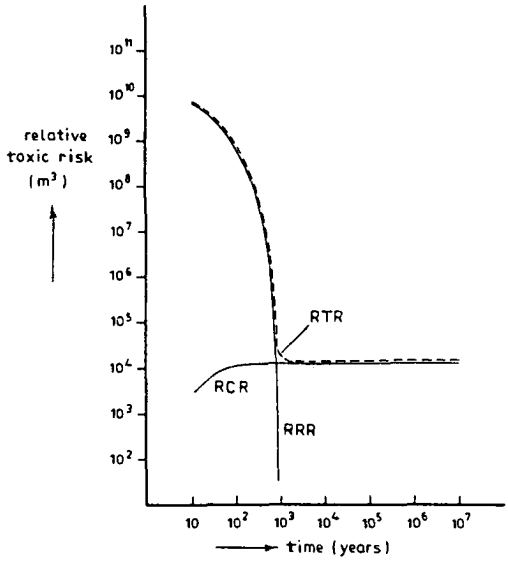

Figure 6.1 The three relative toxic risks for the system Cs-137/Ba-137.
RRR: the relative radiotoxic risk of the radioactive nuclide Cs-137.
RCR: the relative chemical-toxic risk of the stable nuclide Ba-137, the decay product of Cs-137.
RTR: the relative total-toxic risk, the sum of RRR and RCR.
The relative toxic risks are given per 1000 kg reactor fuel.

3. Relative Total-toxic Risk (RTR).

In figure 6.1 the RRR of the radioactive nuclide Cs-137 is drawn. The RRR decreases rapidly and is negligibly small after about 1000 years. The decay of Cs-137 yields a stable nuclide: Ba-137. Barium has a toxic effect on the heart, the nervous system and the blood vessels [4]; the allowable concentration in drinking-water is limited to 100 mg/m^3 [5]. The RCR of the produced barium is also drawn in figure 6.1. To describe the toxicity of the system Cs-137/Ba-137 a logical step is to add up the RRR and the RCR. We denote this sum as the relative total-toxic risk, RTR. This RTR of the system is also drawn in figure 6.1. The numerical values of RRR, RCR and RTR are presented in table 6.1.

An extension of the RTR concept is to use it not only for a decaying nuclide, but also for an arbitrary mixture of radioactive and non-radioactive materials. This leads to the following definition of the

Table 6.1 The relative toxic risks for the system Cs-137/Ba-137.
The relative toxic risks are given per 1000 kg reactor fuel.
Sources for the RRR's: Hamstra [2] and Hamstra and Van der Feer [3].
For the RCR calculation procedure see appendix 6.2.

risk type	relative toxic risks (m^3) at different points in time						
	(10 y)	(10^2 y)	(10^3 y)	(10^4 y)	(10^5 y)	(10^6 y)	(10^7 y)
RRR	6.41×10^3	8.01×10^8	0.7	-	-	-	-
RCR	2.64×10^3	1.15×10^4	1.28×10^4	1.28×10^4	1.28×10^4	1.28×10^4	1.28×10^4
RTR	6.41×10^3	8.01×10^8	1.28×10^4	1.28×10^4	1.28×10^4	1.28×10^4	1.28×10^4

"total" relative total-toxic risk: the total RTR of a mixture of radioactive and non-radioactive materials is the sum of the respective RRR's (of the radioactive materials) and the respective RCR's (of the non-radioactive materials and of the non-radioactive decay products of radioactive materials).

The several relative toxic risk denominations have their drawbacks as yard-sticks for the toxicity evolving from an amount of material. In a practical situation the hazard posed by a toxic component is not only dependent on its maximum allowable concentration in drinking-water, but also on its solubility in water and on its adsorption characteristics. These effects are not taken into account. Therefore the effective toxicities of the different nuclides, elements, compounds or groups may be underestimated or overestimated relative to one another.

A second point of discussion is the procedure for adding-up the relative toxic risks of nuclides, elements, or compounds, in order to calculate the relative toxic risk of, for example, a group. Summation of relative toxic risks in the case of radioactive nuclides is a logical step, because, in a way, it is a method to keep the maximum radiation level constant. This argument cannot be applied in the case of chemical toxicity. Strictly speaking, summation of relative chemical-toxic risks would only be permitted if the respective elements or compounds have identical toxic effects. This will be sometimes the case, for example for heavy metals [6], but it will not be true in general. Furthermore it is possible that the toxicity of a combination of materials is larger than the sum of the separate toxicities, in other words: the total toxicity is being enhanced as a result of a

Table 6.2 The relative radiotoxic risks, RRR's, of the different radioactive nuclides and groups of HLW.
The RRR's are given per 1000 kg reactor fuel.
Sources: Hamstra [2] and Hamstra and Van der Feer [3].
(Ra-225, Ra-226, Th-230, Ac-225, U-233, U-234 and U-238 of group c are decay products).

group/ nuclide	half-time (y)	RRR (m^3) at different points in time						
		(10 y)	(10^2 y)	(10^3 y)	(10^4 y)	(10^5 y)	(10^6 y)	(10^7 y)
a Sr-90	28.1	1.51×10^{13}	1.64×10^{9}	0.4	-	-	-	-
a Cs-137	30.0	6.41×10^{9}	8.01×10^{6}	0.7	-	-	-	-
total group a		2.15×10^{13}	2.44×10^{9}	1.1	-	-	-	-
b U-234	2.47×10^{5}	2.86×10^{3}	2.86×10^{3}	2.85×10^{3}	2.78×10^{3}	2.16×10^{3}	173	-
b U-238	4.51×10^{9}	750	750	750	750	750	750	749
total group b		3.61×10^{3}	3.61×10^{3}	3.60×10^{3}	3.53×10^{3}	2.91×10^{3}	923	749
c Am-241	433	4.89×10^{8}	4.23×10^{8}	1.00×10^{8}	55	-	-	-
c Am-243	7950	4.83×10^{7}	4.80×10^{7}	4.43×10^{7}	2.02×10^{7}	7.91×10^{3}	-	-
c Cm-244	18.1	1.23×10^{3}	3.92×10^{7}	-	-	-	-	-
c Np-237	2.14×10^{6}	2.03×10^{6}	2.06×10^{6}	2.21×10^{6}	2.26×10^{6}	2.19×10^{6}	1.64×10^{6}	8.88×10^{4}
c Pu-238	86.4	1.02×10^{8}	4.95×10^{7}	3.62×10^{4}	-	-	-	-
c Pu-239	2.44×10^{4}	1.66×10^{6}	1.70×10^{6}	2.06×10^{6}	3.99×10^{6}	5.74×10^{5}	-	-
c Pu-240	6600	4.48×10^{6}	8.95×10^{6}	8.28×10^{6}	3.22×10^{6}	252	-	-
c Pu-242	3.80×10^{5}	1.00×10^{6}	1.00×10^{6}	9.98×10^{7}	9.82×10^{3}	8.33×10^{3}	1.61×10^{3}	-
c Ra-225	0.0405	0.3	3	33	3.00×10^{3}	6.50×10^{4}	1.61×10^{5}	8.33×10^{3}
c Ra-226	1600	0.9	9	90	4.35×10^{3}	3.56×10^{4}	8.55×10^{3}	3.45×10^{3}
c Th-229	7340	4	40	400	3.80×10^{4}	7.80×10^{5}	1.93×10^{6}	1.00×10^{5}
c Th-230	7.50×10^{4}	15	41	300	3.00×10^{3}	1.80×10^{4}	4.50×10^{3}	1.50×10^{3}
c Ac-225	0.0274	0.1	1	10	1.00×10^{3}	2.30×10^{4}	5.80×10^{4}	3.00×10^{3}
c U-233	1.62×10^{5}	6	57	571	5.71×10^{3}	4.57×10^{4}	1.03×10^{5}	5.71×10^{3}
c U-234	2.47×10^{5}	-	6.17×10^{3}	1.20×10^{4}	1.17×10^{4}	9.06×10^{3}	725	-
c U-238	4.51×10^{9}	-	-	-	-	-	0.2	0.3
total group c		1.88×10^{3}	5.72×10^{4}	1.57×10^{5}	2.97×10^{7}	3.76×10^{6}	3.91×10^{6}	2.11×10^{5}
d J-129	1.70×10^{7}	1.36×10^{4}	1.36×10^{4}	1.36×10^{4}	1.36×10^{4}	1.35×10^{4}	1.30×10^{4}	9.03×10^{3}
d Cs-135	2.00×10^{6}	4.00×10^{3}	4.00×10^{3}	4.00×10^{3}	3.99×10^{3}	3.86×10^{3}	2.83×10^{3}	125
d Zr-93	1.50×10^{6}	4.00×10^{3}	4.00×10^{3}	4.00×10^{3}	3.98×10^{3}	3.82×10^{3}	2.52×10^{3}	39
d Tc-99	2.10×10^{5}	4.70×10^{4}	4.70×10^{4}	4.68×10^{4}	4.55×10^{4}	3.38×10^{4}	1.73×10^{3}	-
total group d		6.86×10^{4}	6.86×10^{4}	6.84×10^{4}	6.71×10^{4}	5.50×10^{4}	2.01×10^{4}	9.19×10^{3}
total groups (a + b + + c + d)		2.34×10^{13}	3.01×10^{9}	1.57×10^{5}	2.98×10^{7}	3.82×10^{6}	3.93×10^{6}	2.21×10^{5}

certain combination of materials. There are, however, two reasons for using the adding procedure for the toxic risks also in the case of chemical toxicity:

a. Very often relative toxic risks of different orders of magnitude are added-up. This implies that the largest relative toxic risk determines

the ultimate result, as the smaller relative toxic risks can be neglected. Thus a more sophisticated treatment would, in most cases, not lead to data substantially differing from the data presented here.

b. The addition procedure is simple and leads to an identical treatment of radiotoxicity, chemical toxicity and combined radio-chemical toxicity. For a preliminary, qualitative, analysis on separation of HLW such a simplified procedure is a logical choice. For a more detailed analysis a better system for the description of the different toxicities may well be necessary.

In view of the above we judged the adding procedure to be adequate also in the case of chemical toxicity.

6.3 Radiotoxicity of high-level nuclear waste

6.3.1 Data for the calculations of the relative radiotoxic risks

The data on radiotoxicity useful for our analysis are found in a paper by Hamstra and Van der Feer [3]. In this paper the authors have revised earlier data by Hamstra on the relative radiotoxic risk of HLW [2]. The revision was necessary because of the new standards set by the International Commission on Radiological Protection (ICRP) for the limits of bodily intake of radioactive nuclides [7,8]. The new standards are given as annual limits of intake, ALI's, while the earlier standards were in terms of maximum allowable concentrations, MAC's, in drinking-water [9,10].

The change of standards from MAC's to ALI's led Hamstra and Van der Feer to the introduction of a new, dimensionless, radiotoxic unit, the potential risk index [3]. For our analysis, however, the relative radiotoxic risk, RRR, was preferred as a unit for radiotoxicity, because in this way radiotoxicity and chemical toxicity can be treated in a comparable way, and can be added-up to describe the total toxicity.

MAC's (and thus RRR's) can be calculated from ALI's assuming a yearly intake by the "standard" human being of 0.8 m^3 of drinking water [3]. The RRR's of all nuclides and of the groups of nuclides are presented in table 6.2. Appendix 6.1 gives the details of how the RRR's were calculated.

All RRR's were calculated per 1000 kg reactor fuel, assuming a burn-up of the nuclear reactor, i.e. an amount of produced thermal energy, of 33,000 MW.day for this amount of fuel [2]. This corresponds with an electrical energy amount of about 11,000 MWe.day. Thus 1000 kg of reactor fuel is about

Table 6.3 The composition of a 50 l standard HLW-canister (containing the waste of 538 kg fuel).
Source: Hamstra [2].
Source for the non-radioactive materials: ORNL-report 4451 [12].

	group/description	weight (%)	weight (kg)
	radioactive HLW-components:		
a	heat generators	3.5	
b	uranium isotopes	11.6	
c	transuranes	2.4	
d	other radioactive nuclides	4.3	
	total	21.8	
	non-radioactive HLW-components:		
e	lanthanides	13.5	
	other non-radioactive materials	64.7	
	total	78.2	
	total waste materials	100.0	22
	other HLW-canister components:		
f	glass matrix		118
g	stainless-steel cylinder		25
	total weight		165

the 1/900-th part of the fuel consumed in a 1000 MWe nuclear reactor, 40 years in operation, operation factor 70 %. Consequently, for a 3500 MWe nuclear power plant scheme about 3000 ton reactor fuel is required; the corresponding amount of HLW is about 400 m^3, or 1200 ton (see chapter 1).

6.3.2 Classification of high-level nuclear waste

The radioactive nuclides of HLW can be classified as follows:

- group a: the "heat generators" Sr-90 and Cs-137 (moderately short-living);
- group b: the "uranium isotopes" U-235 and U-238 (abundance in natural uranium: 0.720 % and 99.275 %, respectively [11]);
- group c: the "transuranes" and their daughter products, containing the most important long-living radioactive nuclides;

- group d: the "other radioactive nuclides" J-129, Cs-135, Zr-93 and Tc-99.

Apart from these four groups of radioactive nuclides the HLW also comprises non-radioactive materials (and, in final form, glass matrix and stainless steel). Thus three additional groups can be distinguished:

- group e: the "non-radioactive materials" (mostly metal oxides);
- group f: the "glass matrix" used to solidify the HLW;
- group g: the "stainless-steel cylinders" (the vitrified HLW is contained in stainless steel - see chapter 1).

Of course the last three groups do not play a role in the analysis in terms of RRR's. They will be incorporated in the analysis in terms of RTR's later on.

Hamstra [2] gives the weight distribution of the different HLW-groups in a typical HLW-canister, ten years after the fuel elements were removed from the nuclear reactor. Table 6.3 gives the percentages.

6.3.3 The relative radiotoxic risks of the different HLW-nuclides and HLW-groups

Figure 6.2a gives the relative radiotoxic risks of the nuclides of HLW-group c, the transuranes and their daughter products (the daughter products show an increasing RRR at first); figure 6.2b presents the relative radiotoxic risks of the nuclides of HLW-groups a (heat generators), b (uranium isotopes) and d (other radioactive nuclides).

Figure 6.3 gives the total of the relative radiotoxic risks of the four different groups. During the first few hundred years the heat generators (group a) are the most radiotoxic nuclides. The RRR of this group decreases very rapidly. After about 500 years the total radiotoxicity of the HLW is practically equal to the radiotoxicity of the transuranes (group c). The radiotoxicity of the other radioactive nuclides (group d) is much smaller than that of the transuranes (by a factor of about 30,000, decreasing to about 20). The radiotoxicity of the uranium isotopes (group b) is again smaller by a factor of about 20.

6.3.4 Separation into two waste categories

The groups with the radioactive nuclides can be combined in various ways into two HLW-categories. This is schematically shown in table 6.4. The essence of the separation - see paragraph 6.1 - is the separation between

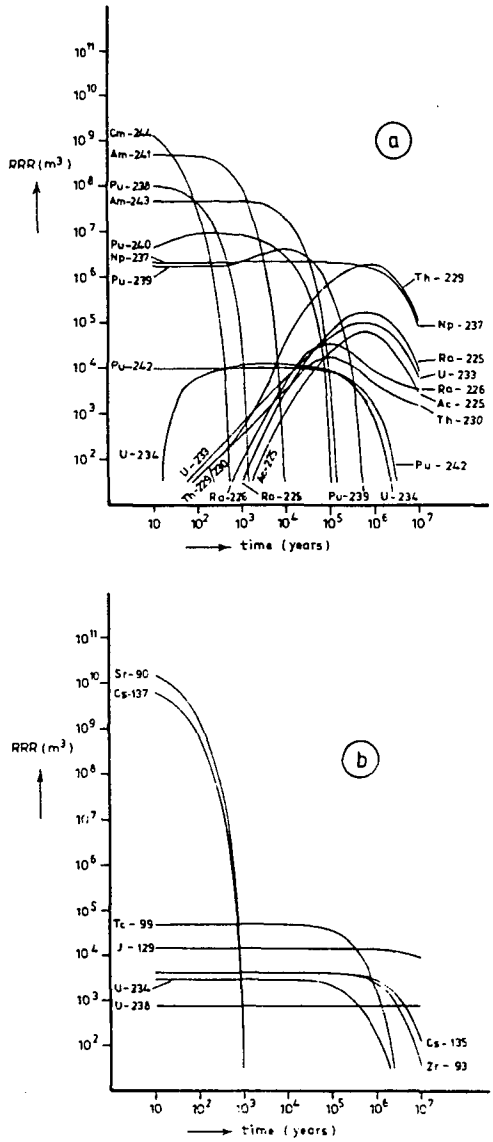

Figure 6.2 The relative radiotoxic risks, RRR's, of the different nuclides of the four groups of radioactive nuclides present in high-level nuclear waste:
(a) the RRR's of the transuranes and their daughter products;
(b) the RRR's of the heat generators (Sr-90 and Cs-137), of the uranium isotopes (U-234 and U-238) and of the other radioactive nuclides (J-129, Cs-135, Zr-93 and Tc-99).
The RRR's are given per 1000 kg reactor fuel.

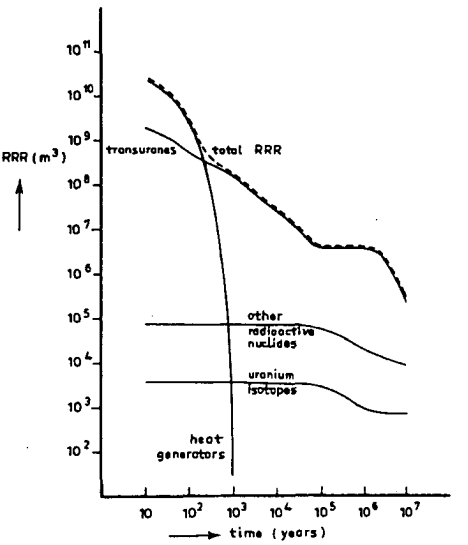

Figure 6.3 The relative radiotoxic risks, RRR's, of the four different groups of radioactive nuclides present in high-level nuclear waste.
The RRR's are given per 1000 kg reactor fuel.

heat generators and long-living radioactive nuclides. This leads to a classification as in separation scheme A, presented in table 6.4, where the heat-generators category contains only the heat generators (plus glass matrix and stainless-steel cylinders) and the transuranes category the rest of the HLW (plus glass matrix and stainless-steel cylinders). Table 6.4 shows next to separation scheme A, the other three separation schemes considered in this analysis.

From the radiotoxic point of view scheme A is the most logical separation scheme. In practice, however, other options may be considered as dictated by e.g. chemical separation means and favoured weight balance. Therefore some flexibility in category classification is needed. This flexibility can be introduced through a slight alteration of our basic point of separation of heat generators and long-living radioactive nuclides. This modified separation principle is that the transuranes category must at least contain the transuranes and their daughter products. Consequently, the transuranes category need not contain all the long-living radioactive nuclides, just the by far most radiotoxic group, the transuranes themselves.

Table 6.4 The four considered schemes for separation of HLW into two waste categories.
The category's weight percentages are given with respect to total HLW.

separation scheme	heat-generators category		transuranes category	
	composition	weight %	composition	weight %
A	heat generators glass matrix stainless-steel cylinders	3.5	transuranes uranium isotopes other radioactive nuclides non-radioactive materials glass matrix stainless-steel cylinders	96.5
B	heat generators other radioactive nuclides non-radioactive materials (except the lanthanides) glass matrix stainless-steel cylinders	72.5	transuranes uranium isotopes non-radioactive materials (lanthanides) glass matrix stainless-steel cylinders	27.5
C	heat generators other radioactive nuclides non-radioactive materials glass matrix stainless-steel cylinders	86.0	transuranes uranium isotopes glass matrix stainless-steel cylinders	14.0
D	heat generators uranium isotopes other radioactive nuclides non-radioactive materials glass matrix stainless-steel cylinders	97.6	transuranes glass matrix stainless-steel cylinders	2.4

Table 6.5 The relative radiotoxic risks, RRR's, for separation schemes A and D.
The RRR's are given per 1000 kg reactor fuel.

separation scheme/category	RRR (m^3) at different points in time						
	(10 y)	(10^2 y)	(10^3 y)	(10^4 y)	(10^5 y)	(10^6 y)	(10^7 y)
separation scheme A:							
- heat-generators category (group a)	2.15×10^{10}	2.44×10^{9}	1.1	-	-	-	-
- transuranes category (groups b + c + d)	1.88×10^{9}	5.72×10^{8}	1.57×10^{8}	2.98×10^{7}	3.82×10^{6}	3.93×10^{6}	2.21×10^{5}
separation scheme D:							
- heat-generators category (groups a + b + d)	2.15×10^{10}	2.44×10^{9}	7.20×10^{4}	7.06×10^{4}	5.79×10^{4}	2.10×10^{4}	9.94×10^{3}
- transuranes category (group c)	1.88×10^{9}	5.72×10^{8}	1.57×10^{8}	2.97×10^{7}	3.76×10^{6}	3.91×10^{6}	2.11×10^{5}

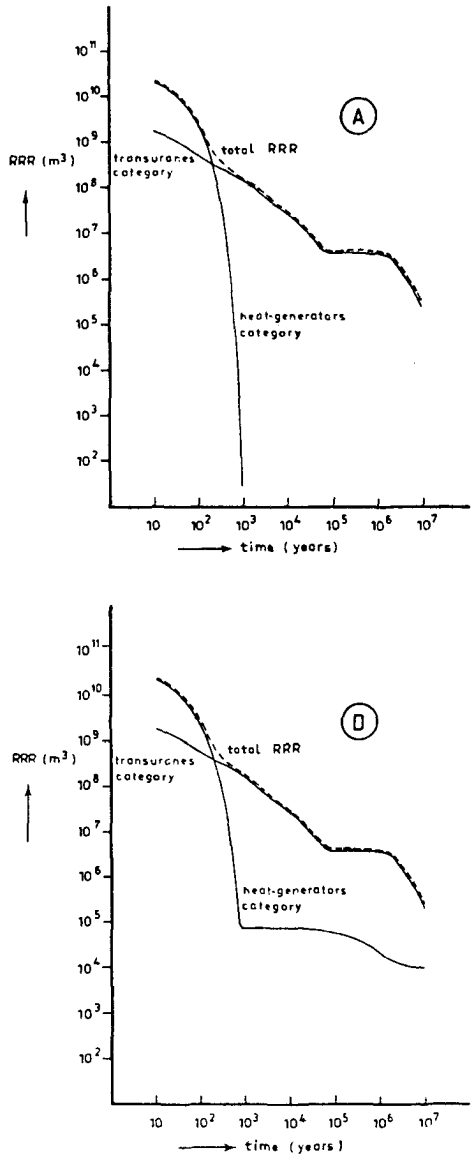

Figure 6.4 The relative radiotoxic risks, RRR's, of both HLW-categories for the extreme separation schemes A and D (for the category classifications of the schemes see table 6.4).
The RRR's are given per 1000 kg reactor fuel.

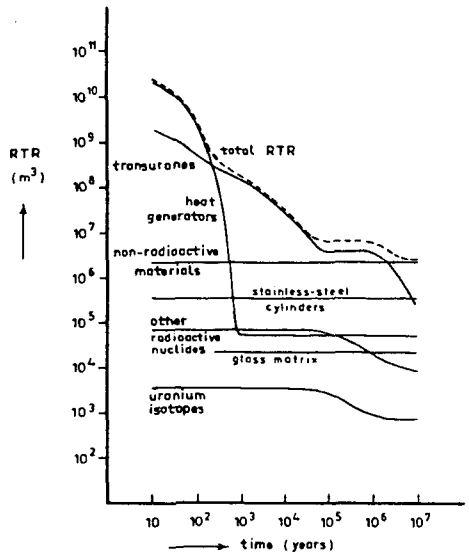

Figure 6.5 The relative total-toxic risks, RTR's, of the seven radioactive and non-radioactive groups present in high-level nuclear waste. The RTR's are given per 1000 kg reactor fuel.

As a result of this principle all possible separation schemes lie between two extremes. The first extreme is separation scheme A mentioned above. The other extreme is separation scheme D, where the transuranes category contains only the transuranes (plus glass matrix and stainless-steel cylinders) and the heat-generators category the rest of the HLW (plus glass matrix and stainless-steel cylinders); see table 6.4. Figure 6.4 gives the RRR's of the two categories for both extreme schemes; table 6.5 gives the corresponding numerical values. Separation schemes B and C, intermediate schemes between the two extreme schemes A and D, will be introduced later on.

6.4 Total toxicity of high-level nuclear waste

6.4.1 Relative total-toxic risks of the HLW-groups

Introduction of the chemical toxicity leads to extension of the number of HLW-groups that must be taken into account (a-d versus a-g). Appendix 6.2 gives the calculation procedure for the relative chemical-toxic risks, RCR's.

Table 6.6 The relative total-toxic risks, RTR's, for the different HLW-groups.
The RTR's are given per 1000 kg reactor fuel.

group	RTR (m^3) at different points in time						
	(10 y)	(10^2 y)	(10^3 y)	(10^4 y)	(10^5 y)	(10^6 y)	(10^7 y)
a heat generators	2.15×10^{18}	2.44×10^{9}	5.55×10^{4}	5.55×10^{4}	5.55×10^{4}	5.55×10^{4}	5.55×10^{4}
b uranium isotopes	3.61×10^{3}	3.61×10^{3}	3.60×10^{3}	3.53×10^{3}	2.91×10^{3}	923	749
c transuranes	1.88×10^{9}	5.72×10^{8}	1.57×10^{8}	2.97×10^{7}	3.76×10^{6}	3.91×10^{6}	2.11×10^{5}
d other radioactive nuclides	6.86×10^{4}	6.86×10^{4}	6.84×10^{4}	6.71×10^{4}	5.50×10^{4}	2.01×10^{4}	9.19×10^{3}
e non-radioactive materials	2.29×10^{6}	2.29×10^{6}	2.29×10^{6}	2.29×10^{6}	2.29×10^{6}	2.29×10^{6}	2.29×10^{6}
f glass matrix	2.20×10^{4}	2.20×10^{4}	2.20×10^{4}	2.20×10^{4}	2.20×10^{4}	2.20×10^{4}	2.20×10^{4}
g stainless-steel cylinders	3.57×10^{5}	3.57×10^{5}	3.57×10^{5}	3.57×10^{5}	3.57×10^{5}	3.57×10^{5}	3.57×10^{5}
total RTR	2.34×10^{18}	3.01×10^{9}	1.60×10^{8}	3.25×10^{7}	6.54×10^{6}	6.66×10^{6}	2.95×10^{6}

As we have seen for the system Cs-137/Ba-137 the decay of a radioactive nuclide can yield a stable, but chemically toxic nuclide. After a few hundred years the relative total-toxic risk, RTR, of the heat generators is dominated by the RCR. For the other radioactive groups the amount of stable decay products is relatively small. Even if these non-radioactive products would have a very high chemical toxicity, the total RCR would still be considerably smaller than the RRR of the parent groups. Therefore we neglect the RCR's of the groups b, c and d: the relative total-toxic risk, RTR, is equal to the RRR for these groups.

Figure 6.5 presents the RTR's of the seven HLW-groups. Table 6.6 gives the numerical values. Also in terms of RTR's the transuranes remain the most toxic group for periods of considerably more than a few thousand years. For times larger than a few hundred years the non-radioactive materials form the second most toxic group. From about 10^5 years on, the RTR of the transuranes is of the same order of magnitude as the RTR of the non-radioactive materials.

6.4.2 Toxicity of the two waste categories

In figure 6.4 the toxicities of the two extreme separation schemes A and D were presented in terms of RRR's. The consequences for these separation schemes in terms of relative total-toxic risks, RTR's, are presented in figure 6.6 (numerical values in table 6.7). Comparison of the corresponding

figures shows that also in the last case, scheme A is superior to scheme D: after about 1000 years the toxicity of the heat-generators category for scheme A is lower than for scheme D. If the chemical toxicity is taken into account, however, the differences between the two schemes are much less.

6.5 Volume of HLW and amount of HLW-canisters

The heat generators form 3.5 weight % of the unsolidified HLW. With respect to unseparated HLW, the heat-generators and transuranes categories for separation scheme A would form 3.5 and 96.5 weight %, respectively, of the total amount of waste canisters. The small amount of the heat-generators category canisters, however, would pose disposal problems because the heat generation of these canisters is concentrated by a factor 30 as compared to the heat generation of unseparated HLW. For all separation schemes it was therefore assumed that the heat-generators concentration in the "heat-generators" canisters is the same as in the case of canisters with unseparated HLW, thus a constant initial heat generation per unit volume. Evidently this assumption leads to more HLW-canisters: in the extreme case of separation scheme A one canister of unseparated HLW corresponds with one canister of the heat-generators category and 0.965 canister of the transuranes category (total: 1.965 canisters). For separation scheme D one canister of unseparated HLW corresponds with one canister of the heat-generators category and 0.024 canister of the transuranes category (total: 1.024 canisters).

6.6 Chemical separation aspects

6.6.1 Separation techniques

The idea of separation of HLW into different waste streams is not new. An almost complete annihilation of long-term radioactivity can be achieved through actinide† transmutation [13,14]. The actinides should then be

† An actinide is an element with an atom number of 90 or more (Th, Pa, U, Np, ... For the definition of a transurane see the footnote on page 118. HLW does not contain thorium (Th) and protactinium (Pa). Consequently, the uranium isotopes plus the transuranes (group b + group c) are, for HLW, identical with the actinides.

brought in a dedicated nuclear reactor and subsequently "transmuted", by means of a nuclear process, into other, shorter living, nuclides or into stable nuclides. At present it is not clear whether the drawbacks of actinide transmutation (complication and extension of the nuclear fuel cycle) are compensated by the advantage (i.e. the large reduction in long-term radioactivity) [13]. We can benefit, however, from knowledge already gathered in studies on actinide transmutation, which always encompasses separation of HLW in different waste categories as a necessary prerequisite.

The first step in the actinide transmutation process is isolation of the actinide fraction. This first step consists of two phases: (i) isolation of the combined actinide/lanthanide[†] fraction from the HLW followed by (ii) separation of actinides and lanthanides. The lanthanides are not radioactive and form a part of group e of the non-radioactive materials (see table 6.3). In the reprocessing plant the HLW is present in dissolved form, in nitric acid. The HLW remains in this dissolved state until its solidification with glass. The combined actinide/lanthanide fraction can be separated from the nitric acid solution with liquid-liquid extraction, with a suitable organic solvent. Such solvents are TBP[††], HDEHP[††], CMP[††] and HDEHP/TBP-mixtures [13].

The second phase of actinide isolation for the actinide transmutation process, the separation of actinides and lanthanides, is much more difficult. The only known way starts with "sequestration" of the actinides with certain negative ions, resulting in negatively charged complex ions to be formed. These complex ions can be separated from the lanthanide ions by means of - for example - ion exchange, provided that the lanthanide ions do not form complex ions. The only suitable complexing reagent is DPTA[††] [13]. The problems that make the separation of actinides and lanthanides so difficult are connected with radiation damage, gassing, heat generation and the liberation of large amounts of sodium from the DTPA (this affects the

---

[†] A lanthanide is an element between lanthanium and hafnium in the periodic system, atom number 58 (Ce), 59 (Pr), ..., 71 (Lu).

[††] TBP: tri-n-butyl phosphate.
HDEHP: di-(2-ethylhexyl) phosphoric acid.
CMP: dihexyl-N,N-diethylcarbamylmethylene phosphonate.
DTPA: di-ethylenetriamine-penta acetic acid.

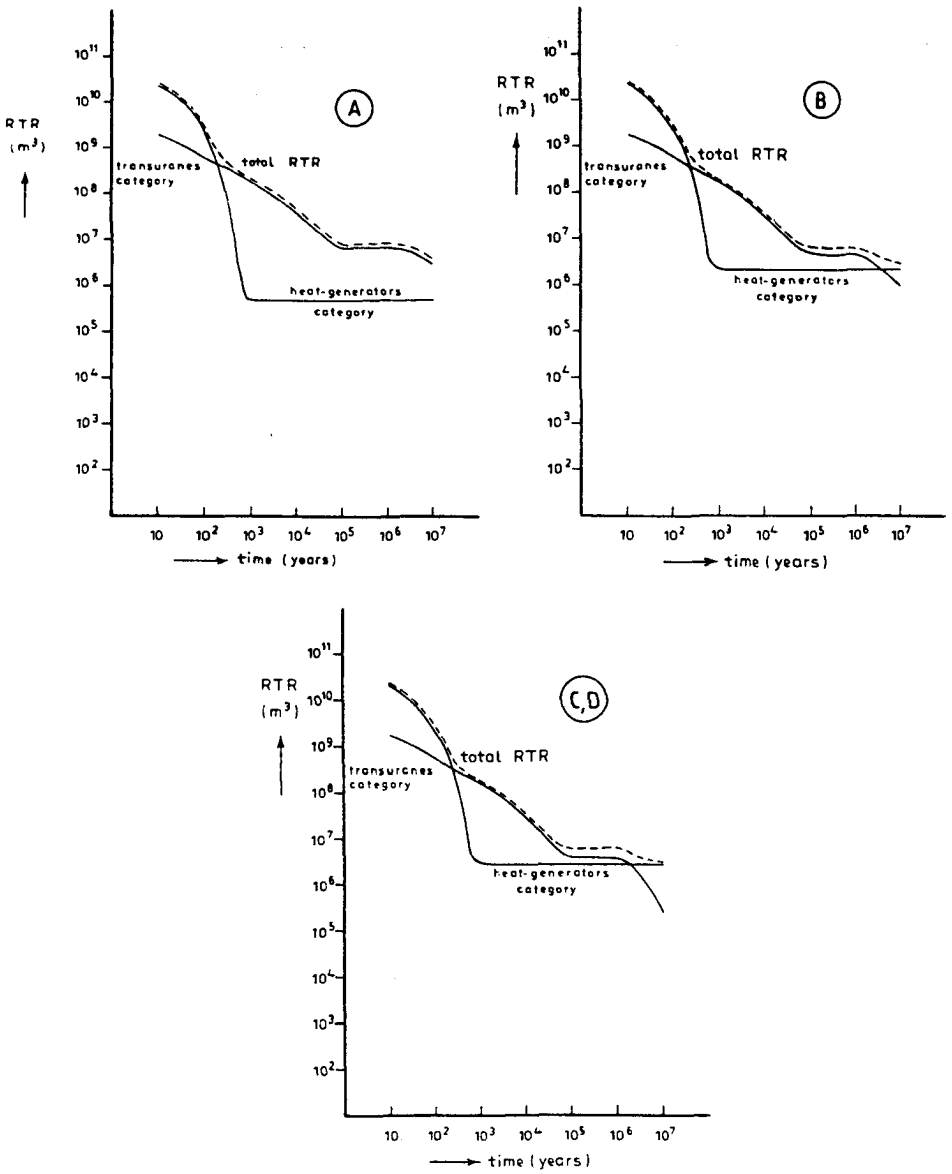

Figure 6.6 The relative total-toxic risks, RTR's, of both HLW-categories for the extreme separation schemes A and D and for the intermediate separation schemes B and C (for the category classifications of the schemes see table 6.4).
The RTR's are given per 1000 kg reactor fuel.

solidification, later on, of the HLW). More information about the isolation of the actinides can be found in the IAEA-report on actinide transmutation [13].

6.6.2 Chemical aspects of separation into two waste categories

From the chemical separation point of view the simplest separation scheme for our specific purposes is the isolation of a combined actinide/lanthanide fraction. This leads to a category classification as in separation scheme B. Effectuation of the much more difficult chemical separation of actinides and lanthanides would make a category classification according to separation scheme C possible. Schemes B and C are presented in table 6.4. The RTR's are drawn in figure 6.6 (numerical values in table 6.7). Also schemes B and C lead to an increase of the number of waste canisters. Scheme B: one canister of unseparated HLW corresponds with one canister of the heat-generators category and 0.275 canister of the transuranes category (total: 1.275 canisters). Scheme C: one canister of unseparated HLW corresponds with one canister of the heat-generators category and 0.140 canister of the transuranes category (total: 1.140 canisters).

Separation schemes B and C are based on already developed chemical separation techniques. For our purposes also scheme A is attractive, in which the heat-generators category contains only the heat generators. Most probably a separation procedure for this scheme can be developed, because the chemical properties of the heat generators, Sr-90 and Cs-137, differ in many respects from those of the other metals present in the HLW (with the exception, of course, of the nuclide Cs-135 of the other radioactive nuclides). Thus a chemical separation according to scheme A, with very few extra components in the heat-generators category, may well be feasible. The development of a separation process for this scheme is beyond the scope of this thesis. Scheme D, finally, is similar to scheme C, but with the uranium isotopes in the heat-generators category and <u>not</u> in the transuranes category. As the chemical properties of uranium and the transuranes are similar, such a separation would pose serious separation-technology difficulties. Moreover, the uranium isotopes have low toxicities and their separation from the transuranes would offer very few advantages. Scheme D is therefore inferior to scheme C.

Table 6.7 The relative total-toxic risks, RTR's, for separation schemes A, B, C and D.
The RTR's are given per 1000 kg reactor fuel.

separation scheme/ category	RTR (m^3) at different points in time						
	(10 y)	(10^2 y)	(10^3 y)	(10^4 y)	(10^5 y)	(10^6 y)	(10^7 y)
separation scheme A:							
- heat-generators category (groups a + f + g)	2.15×10^{10}	2.44×10^{9}	4.35×10^{8}	4.35×10^{8}	4.35×10^{8}	4.35×10^{8}	4.35×10^{8}
- transuranes category {groups b + c + d + e + + 0.965 (groups f + g)}	1.88×10^{9}	5.75×10^{8}	1.60×10^{8}	3.24×10^{7}	6.48×10^{6}	6.59×10^{6}	2.88×10^{6}
separation scheme B:							
- heat-generators category {groups a + d + e (without lanthanides) + + f + g}	2.15×10^{10}	2.44×10^{9}	2.13×10^{6}	2.13×10^{6}	2.12×10^{6}	2.08×10^{6}	2.07×10^{6}
- transuranes category {groups b + c + e (lanthanides) + + 0.275 (groups f + g)}	1.88×10^{9}	5.73×10^{8}	1.58×10^{8}	3.05×10^{7}	4.53×10^{6}	4.68×10^{6}	9.78×10^{5}
separation scheme C:							
- heat-generators category (groups a + d + e + + f + g)	2.15×10^{10}	2.44×10^{9}	2.79×10^{6}	2.79×10^{6}	2.78×10^{6}	2.74×10^{6}	2.73×10^{6}
- transuranes category {groups c + d + + 0.140 (groups f + g)}	1.88×10^{9}	5.72×10^{8}	1.57×10^{8}	2.98×10^{7}	3.82×10^{6}	3.96×10^{6}	2.65×10^{5}
separation scheme D:							
- heat-generators category (groups a + b + d + + e + f + g)	2.15×10^{10}	2.44×10^{9}	2.79×10^{6}	2.79×10^{6}	2.78×10^{6}	2.74×10^{6}	2.73×10^{6}
- transuranes category {group c + + 0.024 (groups f + g)}	1.88×10^{9}	5.72×10^{8}	1.57×10^{8}	2.97×10^{7}	3.77×10^{6}	3.92×10^{6}	2.20×10^{5}

6.7 Discussion

In our study all the relative toxic risks are given per 1000 kg reactor fuel. A 3500 MWe nuclear power plant scheme requires about 3000 ton reactor fuel. Consequently, the total RTR of the corresponding HLW is about three thousand times as large as the data shown in the figures and tables of this chapter, yielding a largest value of 7×10^{13} m^3, the total RTR of the waste of 3000 ton reactor fuel, ten years after leaving the reactor. The RCR of a $2.5\times2.5\times10$ km^3 host salt dome is more than 4×10^{14} m^3 (see chapter 7). Thus the RTR of the HLW of a 3500 MWe nuclear power plant scheme is large, but still one order of magnitude smaller than the RCR of the salt wherein it is disposed.

Table 6.8 Ranking of separation schemes.

separation scheme	criteria		
	toxicity contrast	volume of the HLW	chemical separation aspects
A	++	--	o
B	+	+	+
C	o	+	-
D	o	++	--

Review of the results for the four separation schemes gives the following characteristics (a ranking is presented in table 6.8):

Separation scheme A

In scheme A the difference in long-term toxicity between the heat-generators category and the transuranes category is the largest of all considered schemes. Consequently, the basic principle of this study is best realized in this scheme. However, scheme A has a very serious drawback: the mitigation of the heat effect of the heat generators leads to an amount of canisters for both categories combined of almost twice the amount for unseparated HLW. This makes scheme A unattractive and unpractical.

Separation schemes C and D

Schemes C and D differ only marginally (see figure 6.6 and table 6.7). For these schemes the difference in long-term toxicity for the two categories is relatively small. Besides, the chemical separation necessary for these schemes is more difficult and more complex than for separation scheme B. Therefore schemes C and D are inferior to scheme B.

Separation scheme B

Scheme B is the most attractive one of the four considered schemes. The difference in long-term toxicity is larger than for separation schemes C and D. Furthermore the separation in two categories is technically feasible and relatively simple. The effects on the nuclear fuel cycle are relatively moderate. Finally, the number of canisters of both categories combined increases with a factor only slightly larger than one (1.275). There is no reason, however, not to permit a modest increase in heat evolution per canister accomodating the heat generators. This would imply

that for this separation scheme (and this holds for schemes C and D as well) any increase in the total number of HLW-canisters may be avoided.

6.8 Conclusions

1. Separation of high-level nuclear waste, HLW, into a heat-generators category and a transuranes category has three advantages compared with unseparated HLW:
   - a considerable reduction of the time required for keeping the heat-generators category isolated;
   - a smaller amount of the waste to be isolated from the biosphere for a very long time (the transuranes category);
   - effects related to heat generation are negligible in the case of disposal of the transuranes category.
2. The initial toxicity of the HLW is completely determined by the radiotoxicity. However, after about 10^4-10^5 years the radiotoxicity has decreased to a level on a par with the chemical toxicity of the non-radioactive components of the HLW. Accounting for the chemical toxicity, as has been done in this analysis, is therefore justified.
3. The most attractive separation scheme of the four schemes considered here, with relatively few consequences for the waste processing and management, is separation scheme B, viz.:

   Heat-generators category (72.5 weight % of the original HLW), comprising heat generators, other radioactive nuclides, non-radioactive materials (with the exception of the lanthanides), glass matrix and stainless-steel cylinders.

   Transuranes category (27.5 weight % of the original HLW), comprising transuranes, uranium isotopes, (non-radioactive) lanthanides, glass matrix and stainless-steel cylinders.

List of abbreviations

ALI annual limit of intake
HLW high-level nuclear waste
IAEA International Atomic Energy Agency
ICRP International Commission on Radiological Protection
MAC maximum allowable concentration

ORNL Oak Ridge National Laboratory

RCR relative chemical-toxic risk

RRR relative radiotoxic risk

RTR relative total-toxic risk

MWe megaWatt (electric)

References

1. Van den Broek, W.M.G.T.: De temperatuurverhoging tengevolge van de opslag van kernsplijtingsafval in steenzout, Report Delft University of Technology, 1979.
2. Hamstra, J.: Mogelijkheden in Nederland voor opberging van vast radioactief afval in een steenzoutformatie, Atoomenergie, 15 (1973) 290.
3. Hamstra, J. and Van der Feer, Y.: Nieuwe ICRP-normen en de ondergrondse berging van radioactief afval, Energiespectrum, 5 (1981) 98.
4. Parker, C.R.: Water analysis by atomic absorption, Varian Techtron, Zug, 1972.
5. Normen voor drinkwater, Publicatieblad van de Europese Gemeenschappen no. C 214/6, 18.9.75, European Community, Brussels, 1975.
6. Luckey, T.D., Vemigopal, B. and Hutcheson, D.: Heavy metal toxicity, safety and hormonology, Georg Thieme Publishers, Stuttgart, 1975.
7. ICRP Publication 30 part 1, International Commission on Radiological Protection, Pergamom Press, Oxford, 1979.
8. ICRP Publication 30 part 2, International Commission on Radiological Protection, Pergamom Press, Oxford, 1980.
9. ICRP Publication 2 (recommendations of the International Commission on Radiological Protection), Pergamom Press, Oxford, 1960.
10. ICRP Publication 6 (recommendations of the International Commission on Radiological Protection), Pergamom Press, Oxford, 1964.
11. Weast, R.C. (editor): Handbook of Chemistry and Physics (62nd edition), CRC Press, Boca Raton, 1981.
12. Siting of fuel reprocessing plants and waste management facilities (ORNL-report 4451), Oak Ridge National Laboratory, 1970.
13. Evaluation of actinide partitioning and transmutation (IAEA technical reports series no. 214), International Atomic Energy Agency, Vienna, 1982.
14. Hage, W., Mannone, F. and Schmidt, E.: Chemical separation and transmutation of by-product actinides, Proceedings First European Community Conference on Radioactive Waste Management and Disposal, Harwood, London, 1980.
15. Characteristics of solidified high-level waste products (IAEA technical reports series no. 187), International Atomic Energy Agency, Vienna, 1979.
16. Jongenburger, P.: Kennis der metalen, deel I, Delftsche Uitgevers Maatschappij, Delft, 1963.

Appendix 6.1

Calculation procedure for the relative radiotoxic risks

According to the new standards for the toxicity of radioactive materials [5,7] the toxicity is no longer defined in terms of "maximum allowable concentration" in drinking-water, MAC, but in terms of "annual limit of intake", ALI. However, with a standard quantity of drinking-water of 0.8 m^3 [3] to be consumed anually by the "standard" human being, the ALI can be converted to the MAC. With the MAC the relative radiotoxic risk, RRR, can be calculated. The calculation procedure for the RRR's has been as follows:

- The RRR's of all radioactive nuclides, except Pu-238, Pu-242 and Cm-244, as given by Hamstra and Van der Feer ([3], cf. table II; the RRR's according to the earlier drinking-water standards) were multiplied by the conversion factor given by the same authors ([3], table I) for the considered nuclides (conversion of the "old" RRR's to the "new" RRR's according to the procedure described above).
- The RRR's of the nuclides Pu-238, Pu-242 and Cm-244 were added to the list (these nuclides are mentioned in [2], but not in [3]). These RRR's were calculated from the RRR's of [2], table II: for Cm-244 by multiplication with the conversion factor given in [3], for Pu-238 and Pu-242 by multiplication with a factor 5, in accordance with the conversion factors for Pu-239 and Pu-240 (for Pu-238 and Pu-242 no conversion factors were given in [3], table I).

The thus calculated RRR's, based on the new drinking-water standards, are collected in table 6.2.

Appendix 6.2

Calculation of the relative chemical-toxic risks

The amounts of non-radioactive materials present in HLW are taken from ORNL-report 4451 [12]. For the chemical toxicity we consider only the non-radioactive metals. Two groups are distinguished:

1. Fission products, the non-radioactive decay products of the nuclear reactions. The amounts of fission products depend on the burn-up, the amount of energy produced before regeneration of the fuel. The ORNL-report gives two lists, for burn-ups of 20,000 and 40,000 MW.day/ton fuel, respectively. In most cases the burn-up is between these two

Table 6.9 The relative chemical-toxic risks, RCR's, of the non-radioactive metals present in HLW.
The RCR's are given per 1000 kg reactor fuel.
Source for the metal amounts: ORNL-report 4451 [12].

metal	amount of metal (g)	MAC-value [5] (mg/m^3)	assumed MAC-value (mg/m^3)	RCR (m^3)
fission products:				
Mo	3536	-	10	3.54×10^5
Tc	842	-	10	8.42×10^4
Sr	853	-	100	8.53×10^3
Ba	1570	100		1.57×10^4
Cs	2838	-	10	2.84×10^5
Rb	339	-	10	3.39×10^4
Zr	3586	-	10	3.59×10^5
Ru	2178	-	10	2.18×10^5
Rh	397	-	10	3.97×10^4
Pd	1207	-	10	1.21×10^5
Ag	49	10		4.89×10^3
Cd	70	5		1.40×10^4
Te	492	-	10	4.92×10^4
lanthanides	6620	-	10	6.62×10^5
total for fission products				2.25×10^6
other metals:				
Fe	10027	300		3.34×10^4
Cr	314	50		6.28×10^3
Ni	170	50		3.40×10^3
Al	10	50		200
Na	3383	100000		34
total for other metals				4.33×10^4
total for non-radioactive metals				2.29×10^6

figures. Therefore we take the mean values of the two columns given in [12]. The resulting amounts of metals are presented in table 6.9.
The lanthanides form 17.2 weight % of the non-radioactive materials (this figure was used for the calculation of the weight percentages of the two waste categories of separation scheme B, see paragraph 6.6).

2. Other non-radioactive metals (from the alloying elements in the fuel, from corrosion of the reprocessing plant and from chemicals added during the chemical reprocessing [15]). We take the average values for the three

composition lists for light-water reactors of [12] (cf. table 4.4, page 4-13). The resulting amounts are presented in table 6.9.

With the maximum allowable concentrations in drinking-water (MAC), known, the relative chemical-toxic risks (RCR), can now be calculated. The calculation procedure is as follows:

- For 11 metals of the fission products group no MAC's could be found. With the exception of Sr these metals belong to the 4^{th} and 5^{th} periods of the periodic system. Metals from these periods can be classified as very toxic [6], therefore a MAC of 10 mg/m^3 for each of these metals was assumed. This value is equal to the value for the very toxic metals Ag, Sb and Se, and lies between the value for the toxic metal Pb (50 mg/m^3) and the values for the highly toxic metals Cd (5 mg/m^3) and Hg (1 mg/m^3). For Sr a MAC of 100 mg/m^3 was assumed, equal to the MAC of Ba [5], a metal with comparable chemical properties.
- The MAC's of Ag, Ba, Cd, Cr and Ni were taken from the standards of the European Community [5].
- The RCR of each metal was calculated according to the definition in paragraph 6.2 (see also the example in this paragraph).

Table 6.9 gives the results of the RCR calculations. The total RCR of the non-radioactive materials amounts to 2.29×10^6 m^3 per 1000 kg of reactor fuel.

The heat generators Sr-90 and Cs-137 are present in amounts of 427 and 1280 grammes respectively, per 1000 kg reactor fuel [2]. With MAC's for the stable decay products Zr-90 and Ba-137 of 10 mg/m^3 (assumed) and 100 mg/m^3 [5] respectively, the RCR of the heat generators after total radioactive decay will amount to 5.55×10^4 m^3.

The stainless-steel cylinders also represent a relative chemical-toxic risk. The HLW resulting from 1000 kg of reactor fuel corresponds with 1.86 standard stainless-steel cylinders of 50 l [2]. With 25 kg stainless steel per cylinder and weight percentages of 8 % Ni, 18 % Cr and 74 % Fe in the steel [16], this yields a RCR for the stainless-steel cylinders of 3.57×10^5 m^3 per 1000 kg reactor fuel (MAC's of Ni, Cr and Fe are included in table 6.9).

Also for the glass matrix we calculated a RCR. According to [5] a maximum increase of 5 g/m^3 is allowed for the Si content of drinking-water. For this analysis a MAC for SiO_2 of 10 g/m^3 has been assumed. This leads to a RCR for

the glass matrix of 2.20×10^{4} m^3 for the amount of glass per 1000 kg reactor fuel, i.e. 1.86 times the amount present in a 50 l standard HLW-canister.

N.B. A RCR for the "insoluble" glass seems illogical. However, glass has a limited solubility: about 10 g/m^3 (see chapter 7). This solubility is equal to the assumed MAC of SiO_2. Consequently, a treatment of glass identical to the treatment of other non-radioactive components is justified.

Chapter Seven

THE DISSOLUTION IN GROUND-WATER OF RADIOACTIVE WASTE IN A GLASS MATRIX[†]

Abstract

Underground disposal of radioactive waste implies having a series of "barriers" safeguarding the biosphere. One such barrier is obtained by melting together high-level nuclear waste (HLW) and glass, the solubility of glass in water being very low. This study tries to quantify this argument. A calculation shows that the dissolution process cannot lead to dangerously high HLW-concentrations in ground-water reaching the biosphere. Further measurements of the solubilities of various glass types (and of synrock) are recommended.

7.1 Introduction

With underground disposal of radioactive waste one aims at keeping the active components outside the biosphere. Of some of the most important components the effective life-time amounts to tens of thousands of years[††].

The best studied scheme for the Netherlands with respect to the most active part, the high-level nuclear waste (HLW), is as follows:

- The waste is mixed with molten glass. This mass is allowed to solidify.
- The mixture of glass and waste is placed in stainless-steel cylinders.

[†] A revision of:
Van den Broek, W.M.G.T., Bruining, J., Dietz, D.N. and Weijdema, J.: Het oplossen in grondwater van radio-actief afval vermengd met glas, i²-Procestechnologie, 3 (1987), Nr. 1, 29 (publisher: Ingenieurspers BV, The Hague).

[††] Some less important components have much longer life-times. Toxic non-radioactive materials can be considered as the extreme case in this respect; of course these materials have the eternal life.

- The cylinders are lowered in bore holes drilled in massive salt formations: salt layers, salt pillows, salt domes. The waste generates heat during a relatively short time. The half-life of the heat-generation rate is about 30 years. After 100 years the heat-generation rate is reduced to 10 % of the original capacity and after 200 years to 1 %. To play safe with respect to heat generation the bore holes with these "stoves" must be spaced at distances of at least some tens of meters (see chapter 4).

Such a scheme provides a number of barriers between the waste and the biosphere.

Barriers:

1. The glass and thus the waste mixed with the glass is practically insoluble in the ground-water.
2. The stainless-steel cylinder protects the glass and the waste against contact with water.
3. The salt has creep properties. Below a certain depth, and thus above a certain pressure, any water-channel present may become sealed off.
4. The chosen salt formation is so massive, that erosion at the periphery of the salt body leaves sufficient salt protection.
5. The penetration depth of the radiation is of the order of only a few decimeters so that influence of the radiation on the wider surroundings need not be feared.
6. The Netherlands are located in a seismically quiet region. Consequently, sudden fracture of the salt body is not to be expected (very slow halokinetic movements can however occur; see chapter 2).
7. In most cases contaminated ground-water will become diluted upon entering the biosphere. Only after dilution, a fraction of the contamination will become concentrated again according to known processes (accumulation of certain elements in fishes).

The barriers, briefly described above in rather absolute terms, have of course been studied critically, one by one as well as in combinations. Curiously enough, relatively little attention has been given to the first barrier, the one related to the poor solubility of glass. A wellcome exception is found in a paper by Harvey and Litke [1]. Our study tries to elucidate exactly this aspect, where especially the ground-water flow is taken into account. We have developed a calculation procedure and we present an example calculation, based on some literature data of the glass

solubility and an assumed configuration of placement of HLW-canisters. For a proper evaluation of a particular barrier, we must introduce the extreme hypothesis that all other barriers have failed. In our case we must therefore assume that all stainless-steel cylinders have corroded away and that the complete salt formation in which the waste has been stored, has been dissolved and upon its disappearance has been replaced by a porous and permeable mass through which water flows. Such complete transformation is very unlikely; the final result is somewhat similar to the situation in the Dutch province of Zeeland, where at a depth of 100 m uranium-containing nodules are present within a sand aquifer. For the further elaboration of our model we shall introduce more data and assumptions, but these can better be presented when treating the separate processes described below. For the amount of waste we base ourselves on the Dutch 3500 MWe scheme for nuclear power plants. This scheme aims at future extension of the existing nuclear power capacity of 500 MWe. Every now and then this scheme has been adjusted and estimates of life-time of the power plants and of their yearly waste production have varied up and down. This does not influence, however, the fundamental considerations presented here.

7.2 The dissolution process

As a physical concept the dissolution rate is exclusively the transition of solid to liquid at the solid/liquid interface. In this sense it is mostly an extremely rapid process. Because of this, the liquid near the interface will become saturated in a very short time, and this will almost prevent further dissolution. The dissolved material will be transported through diffusion and (natural) convection from the boundary layer to the body of the liquid. A resulting decrease in concentration at the boundary layer leads to further dissolution. As a rule diffusion and convection are relatively slow, and this means that the total effect of the dissolution process is governed by the rates of these transport mechanisms. In practice we may assume that at the interface the solution remains almost saturated. In case the assumption of instantaneous saturation at the interface should not be correct this provides for a safety margin. Below, we shall indicate how the amount of dissolved material can be determined.

Here we merely want to obtain a first impression of the glass concentration in a saturated solution. Table 7.1 shows literature data.

Table 7.1 Estimated solubilities of glass and quartz in aqueous liquids.

aqueous liquid type	volume	contact time	temperature (°C)	weight loss (mg)	estimated solubility (g/m³)
		Pyrex glass [2]			
neutral water	200 cm³	24 hours	100	2	10
NaOH 0.5 N	200 cm³	20 min.	100	13	65
		Jena glass [3]			
NaOH 0.5 N	150 cm³	2 hours	20	0.1	0.7
NaOH 0.5 N	150 cm³	2 hours	100	9.4	63
		"Glass 843" (aluminosilicate glass) [1]			
neutral water	-	120 days	100	-	64
		quartz [4]			
neutral water	-	-	20	-	~10
neutral water	-	-	100	-	~70

Firstly we consider extremely pure water, in which case we are inclined to consider the dissolution as a physical process. Water experts also use the word "water" for all types of aqueous solutions, which can contain acids, bases and salts. One speaks of the "water analysis" which lists the dissolved components. If water in this broader sense attacks glass and the glass components are dissolved in the water, then the process resembles primarily a chemical reaction rather than a physical phase transition process. Table 7.1 also gives some strong aqueous solutions which can best be described as etching liquids. Here the chemical nature of the process cannot be denied. The solubility of the glass does not only depend on the

water analysis, but also on the glass composition. Apparently boron-silicate glasses ("Pyrex", "Jena") are only slightly affected. The literature data are from rather early date; the solubility is calculated from the weight decrease related to the contacting volume of water. For the solubilities of aluminosilicate glass and quartz one finds somewhat higher values. Roughly we may put the solubility at 10 g/m^3. Evidently some glass components are very insoluble, while some other components are preferentially dissolved. Then we wonder if, in the course of time, the outer glass layer, stripped of the more soluble components, can form a protecting zone [1], which delays the dissolution of the deeper lying glass (we consider fractions of mm). Similar delayed dissolution processes are also known for double salts and salt mixtures.

We must make a choice with respect to the water analysis and the glass analysis, but we must also adopt a specific temperature. Shallow ground-water has a temperature of 10 °C. As a rule ground-water flow velocities are extremely small. Therefore we expect that solely shallow ground-water can penetrate into the biosphere before the most important effect of the radioactive contamination after tens of thousands of years has disappeared. Thus it is realistic to choose 10 °C as a dissolution temperature. We ignore the effect of a change in climate leading to temperature rise or temperature fall.

Finally we want to mention an additional effect. When ground-water moves through a vast sand bed, it will be in equilibrium with the sand. After only a short travelling distance the water becomes saturated and will not dissolve further amounts of sand, or glass for that matter, in case the glass has a similar composition as the sand. Only in the case of differences between sand and glass compositions may the ground-water dissolve some additional material.

Taking into account the data of table 7.1 and the above considerations we think to be on the very safe side when we assume a saturation concentration of glass in water of 10 g/m^3 for use in our calculation.

Further research will undoubtedly benefit from more specific dissolution experiments. Such experiments may lead to recommendations for the type of glass used for mixing with the HLW, and for the mixing ratio glass/HLW. Similar considerations and recommendations apply for "synrock", developed as an alternative for glass.

7.3 The ground-water flow

When we assume that the salt gets replaced by a water-bearing sand mass, then we can at first instance assume that the positioning of the cylinders with HLW remains roughly the same. In reality such replacement represents a large scale geological process and will bring about an enormous chaos with unpredictable consequences. To enable a calculation to be made we shall nevertheless make some assumptions.

- Within a sufficiently large area the amount of HLW will not change, and we will also assume that the vertical orientation of the columns remains unchanged.
- The ground-water flow will be contaminated where it is in contact with the glass cylinder, and this will lead to a contaminated zone trailing downstream of the cylinder. The dimensions of this zone will not change if the cylinder is tilted perpendicular to the flow direction. Tilting in the flow direction leads to a smaller zone. Consequently, the assumption of vertical columns is on the safe side.

The ultimate amount of HLW to be expected on the basis of a 3500 MWe nuclear power plant scheme corresponds with a total column length of thousands of meters (see chapter 1 and [5]). Numerous configurations are conceivable, but we think it is useful to make a preliminary calculation on the basis of 30 HLW-colums with a diameter of 20 cm (this implies a length of about 450 m for each column [5]), widely spaced in a circular region with a diameter of 2500 m. The columns are assumed to be perpendicular to the direction of a horizontal, parallel ground-water flow. The results can be easily converted to those for other configurations.

Now we will investigate how much glass of a massive cylinder is dissolved in the water. The water flows around the circular circumference and a boundary layer, containing the dissolved glass, is formed. The dispersion of this dissolved glass is, for the extremely low water velocities to be expected [6], mainly governed by diffusion [7]. Only extremely small amounts of material will be dissolved. This can be seen if one realizes that the water/glass contact surface is very small compared with the contact areas normally encountered in porous rocks. This leads us to the suggestion that we do not necessarily have to expect a smooth glass cylinder. We will assume, as a worst case situation, that the glass cylinders have become

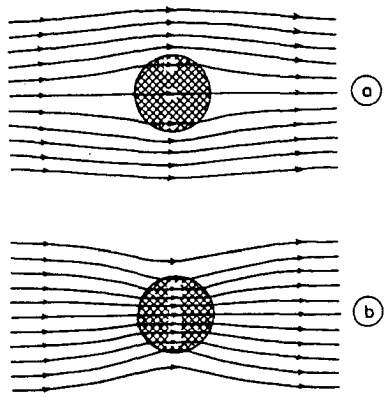

Figure 7.1 Flow perpendicular to the axis of a cylinder, in case the permeability of the cylinder is smaller than that of the surroundings (a), and in case the permeability of the cylinder is larger than that of the surroundings (b).

completely pulverized and do no longer exist in their initial shape and dimensions.

Loose granular material usually consists of two volume parts of solid and one volume part of pore space. Consequently, pulverization leads to a volume increase by a factor 1.5. If the general outer shape - the cylinder - remains unchanged, then its diameter will have increased with a factor $\sqrt{1.5}$ = 1.22.

Starting with a massive glass cylinder of 0.20 m diameter we get a porous cylinder of 0.24 m diameter. Generally the permeability of the pulverized glass will differ from the permeability of the surrounding sand. We have already stated that the general ground-water flow (in an infinite field) is a parallel one and is perpendicular to the cylinder axis. If the cylindrical body is less permeable than the surroundings, then the flow lines will partly avoid the cylinder. If the cylindrical body is more permeable, then extra flow lines will bend towards the cylinder and traverse it, see figures 7.1a and 7.1b. Far downstream and far upstream the flow path through the cylinder posesses the same width, which is in general different from the cylinder diameter. This flow comes into close contact with the pulverized glass with a very large specific contact area and we assume that the water will become saturated with the glass. Downstream, where the flow lines are

parallel again, we can compare the width of the contaminated flow with the column to column distance in order to determine which part of the flowing water becomes contaminated. The degree of widening or narrowing of the flow path can be derived from a combination of the solutions given in [8,9]. For completeness some details are given in appendix 7.1. The result is as follows:

$$\frac{Y}{a} = \frac{2k_2}{k_1+k_2} = \frac{2}{k_1/k_2+1} \qquad (7.1)$$

2Y: width of the flow path, far upstream or downstream;

2a: cylinder diameter;

k_1: permeability outside the cylinder;

k_2: permeability inside the cylinder.

From this solution follows in the first place the evident conclusion that, in case the glass is so finely pulverized that the permeability is small compared with the surroundings, then all the ground-water will circumvent the pulverized glass cylinder. This case is therefore almost equivalent to that of the massive glass cylinder. For the opposite case, where the permeability of the pulverized glass is large compared with that of the surroundings, we find a flow path having a width two times the cylinder diameter of 0.24 m, thus 0.48 m. For the chosen number of columns of 30 and disposal region diameter of 2500 m, a saturation concentration of 10 g/m^3 leads to an average contamination with HLW-containing glass of:

$$\frac{30\times0.48}{2500} \times 10 = 0.058\ g/m^3 \qquad (7.2)$$

Immediately downstream of the cylinders there are sharply outlined bands of water, saturated with glass (10 g/m^3), lying between perfectly "clean" water. At some distance this image will be blurred and the contamination will spread through dispersion perpendicular to the flow direction. The total contamination remains the same, as does the total amount of water and, consequently, also the average contamination.

In the above analysis we have presupposed that all care had been taken to arrive at a state of complete dissolution of the HLW in the cooled-down glass melt. This can be achieved through a proper choice of, for example,

mixing ratio, glass type. Under this provision dissolution of the glass will lead to a HLW-concentration in the ground-water that is proportional to the glass concentration, also in the case of pulverized glass.

7.4 The contamination of the biosphere

Where surface water is fed by ground-water, contamination of the biosphere can occur. The ground-water responsible for the contamination is described above as a strip with a maximum horizontal width of 2500 m (the diameter of the disposal region) with small bands of contaminated water. As a result of dispersion the bands become blurred downstream. The influence of the diffusion-dominated dispersion is only modest: a more or less even distribution of the contamination would only occur after a distance of the order of 1000 km has been covered. In general flowing ground-water will reach surface water somewhere within much smaller travelling distances. In surface water, however, mixing will occur much more readily, and the bands will soon spread.

Furthermore a surface water of some extension will undoubtedly be fed by various other sources. The additional dilution factor will be as a rule a "reasonable" power of 10. A quantitative estimate in this respect would be rather speculative. We disregard this additional dilution factor and consider how much water can be contaminated (up to 0.058 g/m^3) by the total amount of HLW resulting from a 3500 MWe nuclear power plant scheme. A yearly production of 9 m^3 vitrified HLW yields a total of 360 m^3 for a 40 year life-time of the power plants. The specific mass of vitrified HLW is about 3000 kg/m^3. Thus the total mass is $360 \times 3000 = 1{,}080{,}000$ kg.

For dilution down to a strength of 0.058 $g/m^3 = 5.8 \times 10^{-5}$ kg/m^3 the required amount of water is:

$$\frac{1{,}080{,}000}{5.8 \times 10^{-5}} \approx 2 \times 10^{10}\ m^3 \qquad (7.3)$$

Consequently, if in the far future the HLW should be contacted by an aquifer, then the waste would gradually dissolve in the ground-water during a long period of time. This dissolution period would depend on the yearly amount of ground-water that flows by. Ultimately the HLW would be distributed over 2×10^{10} m^3.

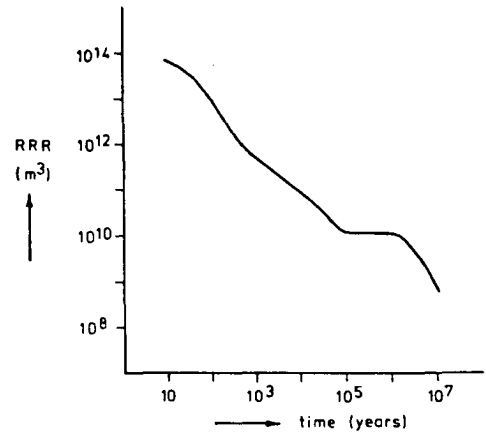

Figure 7.2 The relative radiotoxic risk (RRR) of 3000 ton high-level nuclear waste (HLW) as a function of time. This amount of HLW corresponds with an electric power of 3500 MWe, 40 years in operation.

7.5 Toxicity

The toxicity of an amount of waste, radioactive or otherwise dangerous, can be expressed as the amount of water required to dilute the waste up to the limit allowed for drinking-water. This amount of water is expressed in m^3. Depending on the nature of the toxic material or of the mixture one speaks of Relative Radiotoxic Risk (RRR), Relative Chemical-toxic Risk (RCR) or, in case of a combination, of Relative Total-toxic Risk (RTR).

The RRR for the nuclear power plants is known and is generally given per ton fuel. Through radioactive decay this RRR decreases with time. For its total life-time, a 3500 MWe nuclear power plant scheme requires about 3000 ton fuel. The decay curve of the RRR (based on the data given in chapter 6) is presented in figure 7.2. This figure shows that, in case the waste should come into contact with the ground-water after several tens of thousands of years, then the RRR would be about 2×10^{10} m^3.

At such quantitative considerations on the toxicity a surprising peculiarity arises. Another barrier, preceding the one discussed, consists of the dissolution of the protecting salt in the ground-water; Smith [6] among others has analysed this case. The maximum allowable salt content of drinking water is usually expressed by the chlorine content. Maximum

allowable chlorine contents of 100 to 300 g/m^3 are mentioned. Based on principal dimensions of a salt dome of $2.5 \times 2.5 \times 10$ km^3 (oblong, not round as the word suggests) one finds a RCR of the surrounding salt of more than 4×10^{14} m^3, thus a toxicity due to the familiar household salt of a nearly unimaginably large degree, 20,000 times as much as the toxicity, after tens of thousands of years, of the radioactive waste disposed in the salt. This is in apparent contradiction with our intuition and should bring us to modesty. The concepts RRR and RCR have to be handled with caution. It must be emphasized that the definitions of RRR and RCR are purely theoretical and do not suggest that the billions of m^3 have anything to do with actual consumption.

7.6 Discussion and conclusions

Above we have seen that, owing to the low solubility of the glass and the possible ground-water flow, the HLW could become distributed over 2×10^{10} m^3 of water, in case all other barriers fail.

Furthermore it was shown that, to remain within acceptable drinking-water limits after a period of tens of thousands of years, the HLW should be distributed over at least 2×10^{10} m^3 water.

Combination of both statements leads to the conclusion, that mixing of the waste with the glass leads to a full-fledged safety barrier.

Our calculation is based on a number of assumptions. The most important assumption is that about the solubility of the used glass mass in ground-water in equilibrium with sand. Further measurements on the solubility of glass and also on the solubility of the alternative synrock are recommended.

In sofar as a closer determination of the solubilities should necessitate this, the quality of the HLW fusion mass could be modified. Besides, adaptation of the HLW concentration within a certain margin can be considered.

List of symbols

$2a$	cylinder diameter
k_1	permeability outside the cylinder
k_2	permeability inside the cylinder
r	radial coordinate

v_0 flow velocity far away from the cylinder

x length coordinate, x-direction

y length coordinate, y-direction

2Y width of the flow path, far upstream or downstream

Φ potential outside the cylinder

μ dynamic viscosity of water

Ψ flow function

List of abbreviations

HLW high-level nuclear waste

RCR relative chemical-toxic risk

RRR relative radiotoxic risk

RTR relative total-toxic risk

MWe megaWatt (electric)

References

1. Harvey, K.B. and Litke, C.D.: Model for leaching behavior of aluminosilicate glasses developed as matrices for immobilizing high-level wastes, J. Am. Ceram. Soc., 67 (1984) 553.
2. Walker, P.H. and Smither, F.W.: Comparitive tests of chemical glassware, Ind. Eng. Chem., 9 (1917) 1090.
3. Moser, L. and Maxymowicz, W.: Erfahrungen über die Verwendbarkeit der Glasfiltertiegel in der Gewichtsanalyse, Chem. Ztg., 48 (1924) 693.
4. Van Lier, J.A.: The solubility of quartz, Thesis (State University of Utrecht), v/h Kemink & Zn., Utrecht, 1959.
   See also Siever, R.: Silica solubility 0-200 °C and the diagenesis of silicium sediments, J. Geology (Chicago), 70 (1962) 127.
5. Van den Broek, W.M.G.T.: De temperatuurverhoging tengevolge van de opslag van kernsplijtingsafval in steenzout, Report Delft University of Technology, 1979.
6. Smith, J.M.: Estimations of the rate of penetration of rock salt by fresh water, Report Delft University of Technology, 1977.
7. Stalkup, F.I.: Miscible displacement, Society of Petroleum Engineers of AIME, New York, 1984.
8. Carslaw, H.S. and Jaeger, J.C.: Conduction of heat in solids (second edition), Oxford University Press, London, 1959.
9. Hughes, W.F. and Brighton, J.A.: Fluid dynamics (Schaum's outline series), McGraw-Hill, New York, 1967.

Appendix 7.1

Width of the flow path

The cylinder $0 \leq r \leq a$ with a permeability k_2 has its axis perpendicular to the x-y plane. The dynamic viscosity of the water and its flow velocity far away from the cylinder are denoted as μ and v_0 respectively. The region outside the cylinder has a permeability k_1, and the potential, Φ, is $-\mu v_0 x/k_1$ far away from the cylinder. The y-coordinate is perpendicular to the direction of flow. The potential Φ outside the cylinder is given by Carslaw and Jaeger ([9], p. 426):

$$\Phi = - \frac{\mu v_0 x}{k_1} \{1 + \frac{(k_1-k_2)a^2}{(k_1+k_2)r^2}\} \qquad (7.4)$$

This potential is the real part of the complex potential. The imaginary part of this potential is given by the flow function Ψ (Hughes and Brighton [10], chapter 6, p. 119):

$$\Psi = - \frac{\mu v_0 y}{k_1} \{1 - \frac{(k_1-k_2)a^2}{k_1+k_2)r^2}\} \qquad (7.5)$$

The flow function for the flow line that touches the cylinder is satisfied by the point of contact, where y=r=a, and thus:

$$\Psi = - 2\mu v_0 a \frac{k_2}{k_1(k_1+k_2)} \qquad (7.6)$$

From this equation it can be deduced that the y-position (Y) of this flow line far away from the cylinder is given by:

$$\frac{Y}{a} = \frac{2k_2}{k_1+k_2} \qquad (7.7)$$

In other words, Y/a gives the ratio between the width of the flow path that flows, after widening or narrowing, through the cylinder and the diameter of this cylinder.

Chapter Eight

UNDERGROUND DISPOSAL OF HIGH-LEVEL NUCLEAR WASTE IN ROCK SALT

Abstract

In this last chapter of the thesis some aspects of disposal of high-level nuclear waste (HLW) in rock salt are shortly reviewed, viz. increase in temperature, brine migration, separation of HLW, dissolution of HLW-containing glass, radiation damage of rock salt and salt deformation. The main conclusion that can be drawn is, that HLW may cause some effects in the rock salt that can be unfavourable for disposal, but that methods are available to reduce these effects to acceptable levels. There are no indications that a safe disposal of HLW in rock salt is not technically feasible.

The chapter is concluded with some recommendations for further study.

8.1 Introduction

Radioactive waste consists of various waste types (see chapter 1). The by far most active type is high-level nuclear waste (HLW). In the case of the "salt mine disposal option" this waste is buried in bore holes from the mine galleries, in the case of the "bore holes/cavity disposal option" in bore holes from the surface (see chapter 3). The amount of HLW is small compared with the other waste types (low-, medium- and high-active solid waste: LAW, MAW and HAW). The characteristics of HLW, however, are such that disposal of this waste poses much more difficulties than disposal of LAW, MAW and HAW. If a technical solution for the safe disposal of HLW can be made available, then a safe disposal of LAW, MAW and HAW will certainly be possible too, despite the much larger amounts of these waste types. As a consequence, the effects resulting from HLW-disposal form much more frequently a subject of study in investigations on radioactive waste disposal than the effects resulting from disposal of LAW, MAW and HAW. This also applies to this

thesis: by far the largest part pertains to disposal of HLW. This chapter reviews some relevant aspects of underground disposal of HLW in rock salt.

8.2 HLW-disposal aspects

8.2.1 Increase in temperature

The increase in temperature in pure rock salt (halite) due to the presence of HLW can be accurately calculated. Impurities in rock salt can lead to deviations from the calculated values, but these deviations will generally not be large (see chapter 4). The increase in temperature can therefore be predicted with sufficient precision. A consequence of the HLW heat generation is, that temperature gradients will develop and that the salt will deform to some extent. In case a salt with a low melting point is present (kainite, bischofite or carnallite, melting points at atmospheric pressure 85 °C, 117 °C and 167.5 °C respectively [1]), the temperature in the disposal region should preferably stay below the melting point of the salt in question. When this condition cannot be met, the option of storage of HLW at the surface for a sufficiently long period is available. Another option is to refrain from disposal of HLW in rock salt containing a salt with a low melting point.

Whether the HLW is disposed in a salt mine or in bore holes from the surface does not influence the increase in temperature. A slight advantage of bore holes from the surface is, that there are no negative consequences in the case very widely spaced HLW-columns are considered (this leads to reduction of the increases in temperature).

8.2.2 Brine migration

In chapter 5 the phenomenon of thermal migration of brine inclusions to a heat source was treated:

- A calculation based on very conservative assumptions resulted in an amount, per meter HLW-canister, of about 2 liter brine which may ultimately be attracted by the HLW. There may be a tendency for this brine to rise in the salt and this could eventually lead to a substantial amount of brine near the upper HLW-canisters (there is also a tendency for the HLW-canister to sink, but this effect is negligible - see paragraph 8.2.6). The amount of brine will increase with increasing HLW-column length. A separate study will be required to analyse whether a

considerable amount of brine around the upper end of a heat-generating HLW-column poses a threat to the long-term isolation of the HLW in the rock salt.

- There are strong indications that the brine migration phenomenon does not occur in case the temperature gradients are very small, of the order of 0.5 °C/cm or less. As the temperature gradients decrease with time and with increasing distance to the HLW-canister, it is probable that the amount of brine that assembles around a HLW-column will be much smaller than the calculated amount, or even negligible. Relevant data in the low temperature-gradient range will be required to arrive at a more accurate estimate of the brine influx. As natural rock salt is subjected to the natural geothermal gradient, investigation of rock salt sampled from appropriate locations may provide useful information about brine migration at extremely low temperature gradients.

In case the brine migration phenomenon should prove to be a threat to the isolation of the HLW (e.g. because of corrosive attack), or in case the possibility of a dangerous situation otherwise cannot be ruled out, then measures will have to be taken against the occurrence of brine migration. The most effective measure is reduction of the driving force for migration, the temperature gradient. This reduction can be achieved by allowing the HLW to give off a large part of its heat at surface prior to underground disposal. The general temperature level will then be lower than in the case of disposal of "fresh" HLW material. Because propagation velocities of brine inclusions decrease with decreasing temperature, this provides an additional advantage. Another approach is to hinder reaction between HLW and brine through corrosion-prevention measures or through the introduction of an extra barrier by encapsulating HLW-canisters in concrete (see also paragraph 8.2.5).

The bore holes in a salt mine for the HLW are drilled dry. Bore holes from the surface are drilled with mud, which may contain brine. In case it is necessary to keep the amount of brine near HLW-canisters as small as possible, the use of water-free mud should be considered.

8.2.3 Separation of the HLW

A possibility for a more efficient and more safe disposal of the HLW is separation of HLW into two waste categories (see chapter 6), viz.:

- The heat-generators category, with the same heat-generation rate as the original HLW, but containing only small amounts of long-living radioactive nuclides. A comparatively short period of isolation from the biosphere will therefore suffice. Such isolation period can easily be guaranteed. Consequently, a safe disposal of this waste category can almost certainly be realized. Temporary storage at the surface may not be necessary.
- The transuranes-category containing most of the long-living radioactive nuclides, and with a negligible heat-generation rate. Due to the absence of temperature effects unfavourable for disposal, efficient disposal of this category should present less difficulties than in the case of unseparated HLW. Moreover, temporary storage at the surface is not necessary.

Separation of HLW into two waste categories provides for some advantages in disposal methods. But it bears the disadvantage that the nuclear fuel cycle (the complete cycle of the management and processing of the nuclear fuel and nuclear waste) will be affected. The advantages for the underground disposal operation may, however, outweigh the disadvantage for the waste management operations at the surface.

8.2.4 Dissolution of HLW-containing glass

Safe disposal of radioactive waste implies isolation of the waste from the biosphere for a sufficiently long period. Deposition in a deep rock formation, far away from ground-water channels which are in contact with the biosphere, has many advantages. As in rock-salt formations no ground-water channels are present, this rock type is more suited for disposal purposes than most other rock types. An analysis in chapter 7 shows, however, that even in case the rock-salt formation should break down after only a very limited period, any radioactive contamination by the HLW in ground-water contacting the biosphere after tens of thousands of years will remain within acceptable limits. This is due to the very low solubility of the cylindric glass matrix containing the HLW. This glass cylinder is a full-fledged safety barrier in itself. Disposal of a HLW-canister in rock salt provides therefore two strong safety barriers: the rock-salt formation as well as the cylinder with poorly soluble glass.

In the case of bore holes drilled from the surface the HLW can be buried very deep, far from the biosphere. Also a relatively wide spacing of the

HLW-columns can be easily realized. Deep burial and wide column spacing lead to maximum benificial effects of the glass matrix barrier. In the case of the salt mine option deep burial is not possible and very wide spacing presents difficulties. Consequently, with respect to the glass matrix barrier, disposal of HLW in bore holes drilled from the surface is to be preferred above disposal in a salt mine.

8.2.5 Radiation damage of rock salt

The γ-radiation of the radioactive waste penetrates into the rock salt for a distance of a few decimeters [2] and causes radiation damage. F-centres (anion vacancies) and H-centres (kation vacancies) are formed. The free Na-atoms combine to colloidal sodium atom clusters, the Cl-atoms to chlorine molecules. Colloidal sodium as well as chlorine molecules are entrapped in the sodium chloride crystal lattice and at irregularities in the crystal. The breakdown of sodium chloride into separate components implies the build-up of stored energy, because the reverse reaction (the formation of sodium chloride from sodium and chlorine) is exothermal. It has been suggested by Van Opbroek and Den Hartog [3] that the sudden release of stored radiation energy may lead to a very large increase in temperature in the rock salt. However, the heat-generation rate caused by the reverse reaction is small. Moreover, due to the relatively high thermal conductivity of the salt, the developed heat will be conducted effectively away from the heat-generation zone. This is shown in appendix 8.1. Here an estimate of the extra increase in temperature (due to the reverse reaction) is presented for a specific disposal configuration. The extra increase in temperature proved to be relatively insignificant (a very short-living "first phase" increase of maximally 14 °C about a month after disposal, and a small, gradual, "second phase" increase with a maximum value of about 0.2 °C after 10-12 years). Further analyses will be necessary, but the occurrence of a large increase in temperature caused by the reverse reaction heat is very unlikely.

Another effect mentioned by Van Opbroek and Den Hartog is, that there is a tendency for increasing radiation damage (for a given radiation dose) with decreasing radiation dose rate. This effect may lead to an underestimation of the radiation damage of rock salt. Although a discussion about this effect is outside the scope of this thesis, it should be pointed out that rock salt is by nature frequently subjected to irradiation by the γ-rays of

the potassium isotope K-40 [4]. Investigation of suitable rock-salt samples may provide useful information about radiation damage at extremely low radiation dose rates.

In case the possibility of undesirable processes in the rock salt due to irradiation cannot be ruled out, then there is the option (suggested by ECN, the Netherlands Energy Research Foundation) to enclose the HLW-canisters with a radiation shield to almost completely prevent γ-radiation to reach the rock salt. Consequently, technical measures can be taken to avoid the build-up of energy through radiation damage. Therefore this effect need not pose an obstacle in achieving a safe disposal of the HLW.

8.2.6 Salt deformation

The disposal of HLW-canisters will lead to some deformation of the rock salt. We distinguish short-term deformation and long-term deformation.

The short-term deformation of rock salt results from the heat-generation of the HLW. This heat generation brings about temperature gradients, causing thermal stresses in the salt. These thermal stresses will decrease with time, not primarily as a result of the decay of the HLW heat generation rate, but mainly because rock salt deforms plastically as well as elastically. The presence of limited amounts of water promotes this non-elastic behaviour through salt recrystallization [5,6]. The most important cause for short-term salt displacement, however, is expansion as a result of warming-up by the HLW-heat. The resulting displacement of the salt in the disposal zone will be limited, maximally of the order of a few meters [7,8].

After the increases in temperature caused by the HLW-heat have died out, thus after a period of about 1000 years [9], movements in the salt will gradually die down to the movements that occur by nature in salt formations. The possibility exists that that HLW-canisters will move slightly under the influence of the density difference between canister and rock salt. A calculation similar to the one on the movement of a brine inclusion under the influence of the density difference with salt (this calculation was presented in appendix 5.3), shows that the distance travelled by a HLW-canister (50 l, 20 cm diameter) in one million years will be of the order of one decimeter. This effect is therefore of very limited importance. A second remark on long-term deformation concerns halokinesis (see chapter 2). The development of heat in the disposal zone disturbs to some extent the equilibrium in the salt formation. In view of the - on a geological time

scale - extremely short period of heat generation, it seems extremely unlikely that this heat generation should pose a threat to this equilibrium and give rise to significant long-term salt deformation. However, more knowledge on the halokinesis phenomenon and on salt deformation on a geological time-scale would be necessary for a thorough analysis.

We conclude with two remarks on radiation damage in connection with salt deformation:

- A favourable side-effect of salt recrystallization is annealing of radiation damage. Research on this subject is in progress at the Institute of Earth Sciences of the State University of Utrecht.
- γ-radiation can cause alterations of the mechanical properties of salt [10]. For some analyses it will be necessary to take this effect into account.

8.3 Conclusion

Effects unfavourable for disposal of HLW in rock salt (relatively large increases in temperature, migration of substantial amounts of brine) can occur. There is, however, a simple measure that can be taken to minimize the occurrence of these effects: an extra period of storage at surface allowing the HLW to give off a part of its heat prior to disposal underground. Separation of HLW into two waste categories is an alternative which for the long-living radioactive nuclides does not give rise to thermal effects. The HLW heat generation causes not only negative effects, however; a favourable one is recrystallization, leading to annealing of radiation damage.

For most of the studied subjects the chosen disposal method for the HLW, a salt mine or a bore hole drilled from the surface, is not of great importance. An notable exception is formed by the functioning of the glass matrix barrier. The protective quality of this barrier will be considerable for HLW buried in very deep and widely spaced bore holes. Very deep bore holes can only be constructed from the surface, not from within a salt mine.

A preliminary estimate reveals that, partly because of the relatively high thermal conductivity of rock salt, release of stored radiation energy resulting from irradiation by γ-rays does not lead to significant temperature effects. But even in case this irradiation should form a disposal risk, then this risk can be minimized or even reduced to an insignificant level by a radiation shield between HLW and rock salt.

The main conclusion that can be drawn from our study of underground disposal of high-level nuclear waste in rock salt as presented in this thesis is, that disposal may cause undesired effects. In designing a disposal configuration these effects should be fully taken into account. In the case the effects will reach an unacceptable level, then a method can be used to reduce the effects. Separation of HLW provides additional possibilities for safe and efficient HLW-disposal. With respect to the aspects studied in this thesis there are no indications that a safe disposal of HLW in rock salt is not technically feasible. Further study on some subjects is however recommended.

8.4 Recommendations for further study of HLW-disposal

1. The study of thermal migration of brine inclusions should be continued; more attention should be directed to migration under the influence of extremely small temperature gradients, to the gathering of experimental data on natural rock-salt samples, and to the consequences for HLW-disposal. Furthermore both brine migration and salt deformation occur as a result of the heat generation of the HLW and, consequently, brine migration and salt deformation may take place simultaneously. Deformation of salt should therefore be incorporated in the study of the brine migration phenomenon.
2. We recommend to study the feasibility of separation of HLW into two waste categories. Such study must provide a detailed nuclear-fuel-cycle process scheme and an estimate of the costs of this alternative scheme.
3. For the prediction of very-long-term effects resulting from disposal of radioactive waste in rock salt, investigation of phenomena occurring under natural geological circumstances (natural geological temperature gradient, natural irradiation by the potassium isotope K-40, natural underground stress distribution) can provide very useful information. Study of these phenomena is therefore recommended. The gathered information can be combined with data from laboratory experiments carried out in the respective fields of investigation.
4. It is very unlikely that significant extra increases in temperature as a result of release of stored radiation energy will occur. However, as the effects of irradiation of rock salt by γ-rays are dependent on salt type, and as knowledge of the radiation damage and heat release processes is

rather incomplete, a definite analysis is not yet possible. More experimental data on these processes should therefore be acquired.

List of symbols

c_s specific heat of rock salt
I_0 symbol of the zero-order modified Bessel function
r radial coordinate
r_1 radius of the cylindrical surface source
Q'_c cylindrical surface source strength
Q'_l line source strength
t time since the start of the heat generation
T absolute temperature
θ_b salt temperature at the canister/salt-boundary
θ_e extra increase in temperature
λ_s thermal conductivity of rock salt
ρ_s specific mass of rock salt
κ_s thermal diffusivity of rock salt

List of abbreviations

ECN *Stichting Energieonderzoek Centrum Nederland* (Netherlands Energy Research Foundation)
HAW high-active solid waste
HLW high-level nuclear waste
LAW low-active solid waste
MAW medium-active solid waste

References

1. Dietz, D.N.: Het phasegedrag van carnalliet bij enige temperaturen, dicht onder en op zijn smeltpunt; smeltpunten van kaïniet, bischofiet en carnalliet als functies van de druk, Report Delft University of Technology, 1977.
2. Bergsma, J. and Heijboer, R.J.: Radiation dose deposition and energy accumulation in a rock salt waste repository, Report Netherlands Energy Research Foundation, ECN-144, Petten, 1983.
3. Van Opbroek, G. and Den Hartog, H.W.: Straling en zout, Report State University of Groningen, 1984.
4. Weijdema, J. (retired research engineer Koninklijke/Shell Exploratie en Produktie Laboratorium, Rijswijk): personal communication.

5. Urai, J.L.: Deformation of wet salt rocks, Thesis State University of Utrecht, 1983.
6. Spiers, C.J., Urai, J.L., Peach, C.J. and Zwart, H.J.: The effect of brine (inherent and added) on rheology and deformation mechanisms in salt rock, Second Conference on the Mechanical Behavior of Salt, Hannover, 1984.
7. Ehlert, C. and Winske, P.: Estimation of the thermomechanical response of salt formations to high-level radioactive waste by means of simple geometrical bodies, Proceedings Fifth Symposium on Salt, Vol. 2, 189, The Northern Ohio Geological Society, Cleveland, 1980.
8. Dawson, P.R. and Tillerson, J.R.: Nuclear waste canister thermally induced motion, Sandia Laboratories Report (Sand-78-0566), 1978.
9. Van den Broek, W.M.G.T.: De temperatuurverhoging tengevolge van de opslag van kernsplijtingsafval in steenzout, Report Delft University of Technology, 1979.
10. Lerner, I. and Kohlstedt, D.L.: Effect of γ-radiation on plastic flow of NaCl, J. Am. Cer. Soc., 64 (1981) 105.
11. Jenks, G.H. and Bopp, C.D.: Storage and release of radiation energy in salt in radiation waste repositories, Report Oak Ridge National Laboratory, ORNL-5058, 1977.
12. Van den Broek, W.M.G.T.: Fysische constanten van steenzout en van kernsplijtingsafval ten behoeve van temperatuurberekeningen, Report Delft University of Technology, 1978.
13. Carslaw, H.S. and Jaeger, J.C.: Conduction of heat in solids (second edition), Oxford University Press, London, 1959.

Appendix 8.1

Estimate of the extra increase in temperature caused by the release of stored radiation energy in a specific disposal situation

Data for the calculations

Recombination of colloidal sodium and free chlorine, the products of irradiation of sodium chloride by γ-rays, gives rise to release of heat. We will analyse the consequences of release of this stored radiation energy for the increase in temperature, for the following disposal configuration:

- diameter HLW-canisters: 30 cm;
- length HLW-columns: 50 m;
- distance between the HLW-columns: 50 m (hexagonal disposal pattern);
- number of HLW-columns: infinite (simultaneous placement of all columns);
- original salt temperature: 40 °C (corresponds with a depth of about 1000 m).

The increase in temperature in the salt as a result of the HLW heat generation is given by Van den Broek [9]. Table 8.1 presents the resulting temperatures. The release of stored radiation energy leads to an extra increase in temperature. The resulting temperature distribution is the

Table 8.1 Temperature at the canister/salt-boundary, as a result of the heat generation of the HLW, for the considered disposal configuration. Source: Van den Broek [9].

time (years)	temperature (°C)	time (years)	temperature (°C)	time (years)	temperature (°C)
0.1	118.58	7	152.26	60	109.10
0.2	126.61	10	151.55	80	96.58
0.3	131.21	15	148.56	100	87.34
0.5	136.79	20	144.41	150	73.51
0.7	140.26	25	139.78	200	66.63
1	143.60	30	134.95	300	60.32
2	148.55	35	130.17	500	52.86
3	150.41	40	125.52		
5	151.92	50	116.83		

superposition of (i) the HLW-heat temperature field and (ii) the temperature field caused by the release of the stored radiation energy.

Jenks and Bopp [11] measured the release of stored radiation energy. They investigated three irradiated salt samples, one (synthetic) sodium chloride single crystal and two natural rock-salt samples from the Lyons mine in Kansas. Their results can be summerized as follows:

1. For a rising temperature a rapid release of heat occurs in the temperature region 115-120 °C, with a maximum of 2 to 3 cal/g: the "first phase" release of stored radiation energy.
2. The remaining heat is released according to a zero-order reaction (independent of the concentration): the "second phase" release of stored radiation energy. For the three investigated salt samples the expressions for the heat release were found to be (with T as the absolute temperature):

   Lyons salt 1: $1.92\times10^{16}.\exp(-19{,}600/T)$ cal/g.hour;

   Harshaw salt: $4.97\times10^{16}.\exp(-19{,}600/T)$ cal/g.hour;

   Lyons salt 2: $11.68\times10^{16}.\exp(-19{,}600/T)$ cal/g.hour.

For the calculations we base ourselves on the results of Jenks and Bopp, with a release of heat in the second phase according to the last expression, i.e. according to the most rapid reaction. Further we assume that the radiation damage is limited to distances up to 33 cm from the canister wall. At this distance the stored radiation energy level has decreased to 1 % of the level at the canister wall (see the figures 4a and 4b of Bergsma and

Heyboer [2]). With a specific mass of rock salt, ρ_s, of 2138 kg/m^3 at 115 °C [12], the amount of salt with radiation damage is $\pi(0.48^2-0.15^2)$ = 0.6531 m^3 = 0.6531×2138 = 1396 kg, per meter HLW-column.

First phase temperature effect

After disposal of a HLW-column the increase in temperature will at first be determined by the HLW heat generation. After about one month the salt temperature at the canister wall will reach the 115-120 °C region. Then the first phase release of stored radiation energy will start. We assume a worst case situation:

- in the considered region the radiation damage after this short period is at least 3 cal/g;
- after reaching a temperature of 115 °C the 3 cal/g stored radiation energy is released instantaneously.

The instantaneous release of the first phase heat implies an amount of heat of 3×4.1868×1000 = 12,560 J/kg salt. With a specific heat of rock salt, c_s, at 115 °C of 903 J/kg.°C [12], this leads to a increase in temperature of 12,560/903 = 13.91 °C. The total amount of heat is 12,560×1396 = 17.53×10^6 J per meter column (this amount of heat corresponds roughly with 7 hours initial HLW heat generation). The heat of the heat pulse flows away relatively rapid. If we assume that the heat is released instantaneously along a cylindrical surface source (in solid salt), then the extra increase in temperature, θ_e, is, according to Carslaw and Jaeger [13]:

$$\theta_e = \frac{Q'_c}{4\pi\kappa_s t} \exp\{-(r^2+r_1^2)/4\kappa_s t\}.I_0(rr_1/2\kappa_s t) \qquad (8.1)$$

Q'_c: cylindrical surface source strength (amount of heat generated per unit length: $Q'_c\rho_s c_s$);
r: radial coordinate;
r_1: radius of the cylindrical surface source;
κ_s: thermal diffusivity of rock salt;
I_0: symbol of the zero-order modified Bessel function;
t: time since the start of the heat generation.

For r_1 we chose 35 cm, the weighted average of 15 and 48 cm. Table 8.2 gives the calculated extra increase in temperature as a result of the heat

Table 8.2 Extra increase in temperature, in °C, as a result of the first phase release of stored radiation energy (3 cal/g). Assumed model: instantaneous release as a cylindrical surface source (in solid salt) with a radius of 35 cm.

time	radial coordinate (m)									
	0.00	0.15	0.25	0.35	0.50	0.70	1.00	1.50	2.00	3.00
1 hour	1.61	5.64	11.68	13.70	0.36	0.16	--	--	--	--
2 hours	6.23	8.27	10.13	9.80	5.60	0.88	--	--	--	--
3 hours	8.22	8.79	9.03	8.27	5.60	1.44	0.04	--	--	--
6 hours	8.14	7.81	7.20	6.27	4.45	2.09	0.32	--	--	--
12 hours	5.72	5.50	5.10	4.56	3.57	2.23	0.78	0.05	--	--
1 day	3.40	3.31	3.16	2.95	2.54	1.92	1.06	0.24	0.03	--
2 days	1.85	1.83	1.78	1.71	1.58	1.35	0.98	0.44	0.14	0.01
5 days	0.78	0.77	0.77	0.75	0.73	0.68	0.59	0.42	0.27	0.07
10 days	0.40	0.39	0.39	0.39	0.38	0.37	0.35	0.29	0.23	0.12

Table 8.3 Second phase rate of release of stored radiation energy as a function of salt temperature.

temperature (°C)	heat-generation rate (W/m)	temperature (°C)	heat-generation rate (W/m)
100	0.003	155	2.45
105	0.006	160	4.16
110	0.011	165	6.98
115	0.022	170	11.6
120	0.042	175	18.9
125	0.078	180	30.7
130	0.143	185	49.2
135	0.260	190	78.2
140	0.465	195	123
145	0.820	200	191
150	1.43		

pulse. We see that after 10 days this increase in temperature has decreased to below 0.4 °C.

Second_phase_temperature_effect

We find for the second phase release of stored radiation energy: $11.68 \times 10^{16}\{\exp(-19{,}600/T)\} \times 4.1868 \times 1396 \times 1000/3600 = 1.896 \times 10^{20} \times \exp(-19{,}600/T)$ W/m. Table 8.3 gives the heat release rates at different temperatures. For the temperatures resulting from the HLW heat generation in our disposal

configuration (table 8.1) the rate of release of stored radiation energy is very small compared with the original HLW heat-generation rate, 675 W/m.

The extra increase in temperature as a result of this second phase temperature effect was calculated according to the following procedure:

1. The time was divided in periods of 1 year.
2. The temperatures, constant for each period, were assumed to be equal to the HLW heat generation temperatures at 0.5, 1.5, 2.5 ... years after disposal.
3. The stored radiation energy was assumed to be released as instantantaneous line sources at 0.5, 1.5, 2.5 ... years after disposal, with strengths of $1.896\times10^{20}\exp\{-19{,}600(273+\theta_b)\}\times3600\times24\times365$ J/m (with θ_b the temperature at the canister/salt-boundary as a result of the HLW heat generation).
4. The contribution of each line source, at the canister/salt-boundary, was calculated according to the equation given by Carslaw and Jaeger [13]:

$$\theta_e = \frac{Q_l'}{4\pi\lambda_s t}\exp(-r^2/4\kappa_s t) \qquad (8.2)$$

Q_l': line source strength;
λ_s: thermal conductivity of rock salt.

The thermal properties were taken at 140 °C, the average temperature in the area of interest (ρ_s=2132 kg/m^3; c_s=913 J/kg.°C; λ_s=3.70 W/m.°C [12]). The θ_e-values were rounded off at 0.001 °C.

5. The contributions of the different line sources for each year, for 1 to 50 years, were added up.

Table 8.4 presents the results. The extra increase in temperature is, in first approximation, proportional to the the HLW-heat increase in temperature. It is very small: the maximum calculated value is 0.154 °C.

In principle the given procedure should be repeated a number of times with the corrected values of θ_b ($\theta_{b,new}=\theta_{b,old}+\theta_e$), until a constant extra increase in temperature is obtained. As the value of θ_e was very small, and as only an estimate of the extra increase in temperature was sought, this extended procedure was judged to be unnecessary.

Table 8.4 Extra increase in temperature at the canister/salt-boundary, as a result of the second phase release of stored radiation energy, for the considered disposal configuration.

time (years)	increase in temperature (°C)	time (years)	increase in temperature (°C)	time (years)	increase in temperature (°C)
1	0.014	18	0.120	35	0.043
2	0.044	19	0.118	36	0.042
3	0.071	20	0.111	37	0.041
4	0.096	21	0.106	38	0.042
5	0.118	22	0.099	39	0.042
6	0.128	23	0.092	40	0.042
7	0.137	24	0.090	41	0.039
8	0.144	25	0.083	42	0.032
9	0.149	26	0.077	43	0.030
10	0.154	27	0.072	44	0.027
11	0.151	28	0.069	45	0.026
12	0.153	29	0.069	46	0.024
13	0.149	30	0.066	47	0.024
14	0.141	31	0.062	48	0.023
15	0.139	32	0.052	49	0.022
16	0.133	33	0.048	50	0.020
17	0.126	34	0.045		

Evaluation

The extra increase in temperature as a result of the release of stored radiation energy was calculated for a specific disposal configuration. The calculations were based on the data of Jenks and Bopp. The extra increase in temperature of the "first phase" as well as that of the "second phase" was relatively small. The limited amounts of heat that are released are effectively conducted away from the heat generation zone by the rock salt.

SAMENVATTING

Dit proefschrift, "Aspecten van ondergrondse berging van radio-actief afval in steenzout", beschrijft onderzoek dat is verricht naar een aantal effecten die zullen optreden bij berging van radio-actief afval in steenzout. In de inleiding wordt de huidige stand van het onderzoek besproken, worden de probleem-gebieden aangeduid, en wordt aangegeven op welke wijze het proefschrift is opgezet.

De eerste drie hoofdstukken geven van belang zijnde achtergrond-informatie en zijn gebaseerd op literatuurgegevens. Hoofdstuk 1 handelt over radio-actief afval: soorten afval, eigenschappen van het afval, hoeveelheden afval in de Nederlandse situatie. Betreffende de soorten afval is het nodig onderscheid te maken tussen kernsplijtingsafval (KSA), dat vrijkomt bij opwerking van uitgeputte reactorstaven, en het overige, minder actieve, afval. Hoofdstuk 2 geeft informatie over het steenzout: soorten zoutformaties, samenstelling en eigenschappen van het steenzout, beschikbare formaties in de Nederlandse ondergrond. Hoofdstuk 3 bespreekt de mijnbouwtechnieken die nodig zijn voor berging van het afval. Hierbij zijn twee bergingsopties te onderscheiden, te weten een zoutmijn voor al het radio-actieve afval (optie 1) en de combinatie van boorgaten vanaf het aardoppervlak voor het KSA verpakt in cylinders plus een zoutholte voor het overige afval (optie 2).

Hoofdstuk 4 geeft een beschrijving van de temperatuurverhoging die in het steenzout optreedt als gevolg van de warmteontwikkeling van het KSA. Deze temperatuurverhoging hangt vooral af van de bergingsparameters: diameter van de KSA-cylinders, lengte van de kolommen met op elkaar gestapelde cylinders, onderlinge afstand van de kolommen. Voor een aantal configuraties is de temperatuurverhoging berekend: (i) voor één kolom en voor een oneindig aantal gelijktijdig geplaatste kolommen bij verschillende waarden van bergingsparameters en (ii) voor twee gevallen van niet-gelijktijdige plaatsing. Het blijkt dat de maximale temperatuurverhoging met name wordt bepaald door de diameter van de KSA-cylinders: voor niet te korte onderlinge afstanden van de KSA-kolommen bedraagt deze maximale temperatuurverhoging: ca. 30, ca. 50 en ca. 110 °C voor cylinderdiameters van resp. 15, 20 en 30 cm. Het hoofdstuk wordt besloten met een analyse van de invloed van verontreinigingen in het steenzout op de temperatuurverhoging. Verontreinigingen met een lage warmtegeleidingscoëfficiënt kunnen een

ongunstige invloed op de temperatuurverhoging hebben; hiermee zal mogelijk rekening moeten worden gehouden.

Hoofstuk 5 handelt over beweging van pekelinsluitsels. De KSA-warmte-ontwikkeling veroorzaakt niet alleen een temperatuurverhoging in steenzout maar ook een temperatuurgradiënt. Van nature in steenzout aanwezige pekelinsluitsels kunnen zich, onder andere vanwege de bij stijgende temperatuur toenemende oplosbaarheid van zout, gaan begeven naar de warmtebron, de KSA-cylinder. Voortplantingssnelheden van een groot aantal kunstmatige insluitsels in natriumchloride éénkristallen werden experimenteel bepaald, bij verschillende temperaturen en verschillende temperatuurgradiënten. Vergelijking met waarden uit de literatuur leverde dat voortplantingssnelheden in steenzout ten hoogste van dezelfde grootte-orde zijn. Berekening van de uiteindelijk door een KSA-kolom aan te trekken hoeveelheid pekel voor een aangenomen bergingsconfiguratie leidde tot een waarde van ongeveer 2 liter per meter KSA-kolom. Deze waarde moet worden gezien als een bovengrens, de in werkelijkheid optredende waarde zal vermoedelijk veel kleiner zijn. Voor een nauwkeurige voorspelling zijn betrouwbare gegevens nodig betreffende de voortplantingssnelheden van pekelinsluitsels in steenzout bij zeer lage temperatuurgradiënten.

Hoofdstuk 6 geeft een beschouwing over scheiding van KSA in twee categorieën afval. KSA bevat zowel radio-actieve componenten die gedurende een relatief korte tijd veel warmte produceren (de warmteproducenten) als componenten die nauwelijks warmte produceren maar wel zeer langdurig radio-actief blijven (voornamelijk transuranen). De aanwezigheid van elk van de twee groepen componenten leidt tot specifieke eisen met betrekking tot de berging. Scheiding van KSA in twee categorieën afval, een warmteproducenten-categorie en een transuranen-categorie, heeft voordelen: het aantal randvoorwaarden in verband met berging is voor elk van de twee categorieën kleiner dan het aantal voor het oorspronkelijke KSA. Dit kan leiden tot een veiliger en meer efficiënte berging. De scheiding heeft echter ook een nadeel: het KSA-opwerkingsproces wordt complexer. Bij de beoordeling van het effect van de scheiding werden zowel de radiotoxiciteit als de chemische toxiciteit van het KSA in de beschouwing betrokken. Het hoofdstuk wordt besloten met de presentatie van een KSA-scheidingsschema met relatief beperkte gevolgen voor het opwerkingsproces.

In KSA-cylinders bevindt zich in glas ingesmolten kernsplijtingsafval. Doordat glas zeer slecht in water oplosbaar is, kan dit worden beschouwd als

een extra veiligheidsbarrière tegen verspreiding van het KSA. Hoofdstuk 7 geeft een analyse van de sterkte van het glas als barrière. Voor deze analyse werd verondersteld dat de gehele zoutformatie na korte tijd is verdwenen, en dat het glas met kernsplijtingsafval in rechtstreeks contact is met grondwater. Voor een aangenomen bergingsconfiguratie bleek, dat desondanks de radio-actieve verontreiniging van het grondwater zeer beperkt zal blijven. Vanwege de zeer geringe oplosbaarheid vormt het glas een volwaardige veiligheidsbarrière.

In het laatste hoofdstuk, hoofdstuk 8, worden een aantal aspecten van ondergrondse berging van kernsplijtingsafval in steenzout in samenhang beschouwd. Berging van KSA leidt tot effecten in het zout die mogelijk ongunstig zijn. In het geval van temperatuurverhoging kan een goede voorspelling van de omvang van het effect worden gegeven. Voor beweging van pekelinsluitsels en voor de extra temperatuurverhoging tengevolge van het vrijkomen van opgeslagen stralingsenergie is dit niet het geval; wèl is het maken van een schatting van de effecten die maximaal kunnen optreden mogelijk.

De voornaamste conclusie die kan worden getrokken uit de studie is: er zijn geen aanwijzingen gevonden dat een veilige berging in steenzout van het meest actieve soort afval, het kernsplijtingsafval, niet mogelijk is.

Andere conclusies zijn:

- Er zijn methoden beschikbaar om het optreden van voor berging mogelijk nadelige effecten te beperken, zoals bovengrondse opslag van kernsplijtingsafval voor een periode van enige tientallen jaren.
- Scheiding van kernsplijtingsafval in twee categorieën afval leidt tot extra flexibiliteit bij de berging.
- De samensmelting van kernsplijtingsafval met glas levert een volwaardige veiligheidsbarrière.
- Juist door het snel dichtvloeien van diepgelegen zoutholten zouden deze zeer geschikt kunnen zijn voor berging van radio-actief afval; een studie naar de haalbaarheid van berging van radio-actief afval in een diepe zoutholte wordt aanbevolen.

SUMMARY

This thesis describes research carried out on a number of effects resulting from underground disposal of radioactive waste in rock salt. In the introduction the state of the art of investigations on disposal of radioactive waste in rock salt is discussed, the problem areas are defined, and the way in which the thesis is organized is explained.

The first three chapters give relevant background information and are based on literature data. Chapter 1 deals with radioactive waste: waste types, waste properties, waste amounts in the Dutch situation. As to the waste types it is necessary to distinguish between high-level nuclear waste (HLW), the waste resulting from the reprocessing of the spent fuel elements, and the other, less active, waste types. Chapter 2 gives information about rock salt: salt-formation types, composition and properties of rock salt, salt formations accessible underground in the Netherlands. Chapter 3 discusses the mining techniques necessary for waste disposal. Two disposal options can be distinguished, viz. a salt mine repository for all the radioactive waste (option 1) and the combination of bore holes drilled from the surface for the HLW plus a salt cavity for the other waste types (option 2).

Chapter 4 presents a description of the increase in temperature in the rock salt resulting from the heat generation of the HLW. This increase in temperature depends mainly on the disposal parameters: diameter of the HLW-canisters, length of the columns of stacked canisters, distance between the columns. The increase in temperature has been calculated for a number of configurations: (i) for a single column and for an infinite number of simultaneously placed columns, for varying values of disposal parameters, and (ii) for two cases of non-simultaneous placement. It appears that the maximum increase in temperature is mainly determined by the diameter of the HLW-canisters: for not too short distances between the HLW-columns these maximum increases in temperature are: ca. 30, ca. 50 and ca. 110 °C for canister diameters of 15, 20 and 30 cm respectively. The chapter is concluded with an analysis of the influence of impurities in the rock salt on the increase in temperature. Impurities with a low thermal conductivity can enhance this increase; this effect may have to be taken into account.

Chapter 5 treats migration of brine inclusions. The heat generation of the HLW leads not only to an increase in temperature in rock salt but also

to a temperature gradient. As a consequence of, among others, the increase in solubility with increasing temperature, brine inclusions (by nature present in rock salt) can migrate towards the heat source, the HLW-canister. Propagation velocities of a large number of artificial inclusions in sodium chloride single crystals were determined experimentally, at varying temperatures and temperature gradients. Comparison with literature data showed that propagation velocities in rock-salt samples are at most of the same order of magnitude. For an assumed disposal configuration the amount of brine that will ultimately be attracted by each HLW-column was calculated as about 2 liter per meter HLW-column. This value must be apprehended as an upper limit, in practice a much smaller amount will presumably be attracted. For an accurate prediction reliable data on propagation velocities of brine inclusions in rock salt at very low temperature gradients will be necessary.

Chapter 6 gives an analysis of separation of HLW in two waste categories. HLW contains radioactive components generating heat during a relatively short period (the heat generators) as well as very long-living radioactive components with no significant heat generation (mainly transuranes). The presence of each of the two groups leads to specific demands in disposal operations. Separation of HLW into two waste categories, a heat-generators category and a transuranes category, has advantages: there are less restrictions for disposal of each of the categories seperately than in case of the original undivided HLW. This will enable a safer and more efficient disposal. The separation has as a drawback the necessity of a more complex HLW-reprocessing. In the analysis radiotoxicity as well as chemical toxicity were taken into account. The chapter is concluded with the presentation of a HLW separation scheme with relatively limited consequences for the reprocessing.

In the HLW-containers high-level nuclear waste is present in a glass matrix. As the solubility of glass in water is very low, this glass can be considered as an extra safety barrier against the spreading of the HLW. Chapter 7 analyses the strength of the glass barrier. For this analysis it was presumed that after a short period the salt formation had completely disappeared, and that the glass with the high-level nuclear waste is in direct contact with ground-water. For an assumed disposal configuration it could be shown that nevertheless the radioactive contamination of any ground-water reaching the biosphere will be very limited. As a result of the low solubility the glass forms a full-fledged safety barrier.

The last chapter, chapter 8, presents a combined treatment of a number of aspects of underground disposal of high-level nuclear waste in rock salt. Disposal of HLW leads to effects in the salt that can be unfavourable. In the case of increase in temperature an accurate prediction of the level of the effect can be given. For migration of brine inclusions and for the extra increase in temperature caused by the release of stored radiation energy this is not possible; an estimate of the maximum level of these effects can however be derived.

The main conclusion that can be drawn from this study is: there are no indications that a safe disposal in rock salt of the most active waste type, the high-level nuclear waste, is not possible.

Other conclusions are:

- Methods are available to reduce the level of effects that can be unfavourable for disposal, such as surface storage of high-level nuclear waste for a period of some tens of years.
- Separation of high-level nuclear waste into two waste categories leads to extra flexibility at disposal operations.
- The melting together of high-level nuclear waste and glass provides for a full-fledged safety barrier.
- The rapid convergence of deep-lying salt cavities may prove to be a very favourable property for disposal of radioactive waste; a study on the feasibility of disposal of radioactive waste in a deep salt cavity is recommended.

NAWOORD

De basis van dit proefschrift werd gelegd tijdens het TH-project "Ondergrondse berging van radio-actief afval in steenzout", dat onder leiding stond van prof.ir. D.N. Dietz. Vlak voordat hij de TH vanwege het bereiken van de leeftijdsgrens verliet, werd besloten om een deel van de bereikte resultaten te gebruiken voor het samenstellen van een proefschrift. Tot eind 1987 heeft prof. Dietz mij als promotor begeleid en heeft als zodanig veel bijgedragen aan de totstandkoming van dit proefschrift. Hiervoor ben ik hem veel dank verschuldigd. Helaas heeft hij het bereiken van het eindresultaat niet meer mogen meemaken.

Prof.dr.ir. J. Hagoort volgde prof. Dietz in het begin van 1988 op als promotor. Zeer snel maakte hij zich de problematiek van ondergrondse afvalberging - een voor hem toch enigszins vreemd terrein - eigen. De wijzigingen die zijn aangebracht naar aanleiding van zijn commentaar op de afzonderlijke hoofdstukken en op het proefschrift als geheel zijn de kwaliteit van het proefschrift zeer ten goede gekomen. Hiervoor, en voor het op zich nemen van het promotorschap, ben ik hem zeer erkentelijk.

Bijzonder veel heb ik ook te danken aan ir. J. Weijdema, die de taak op zich had genomen om de tekst te "editen". Door zijn zeer nauwgezette correctiewerkzaamheden en suggesties voor verbeteringen werd de engelse tekst zoals die oorspronkelijk aanwezig was getransformeerd tot presentabel engels. Echter ook op inhoudelijk gebied heeft hij veel bijgedragen aan dit proefschrift, onder meer als mede-auteur van het artikel over het oplossen van radio-actief afval vermengd met glas.

Prof.dr.ir. G.M. van Rosmalen dank ik voor de waardevolle suggesties die zij gaf naar aanleiding van een voorlopige versie van het hoofdstuk over thermische migratie van pekelinsluitsels. Deze suggesties zijn uiteraard ter harte genomen.

Verder dank ik ir. P. Sonneveld (Faculteit Technische Wiskunde en Informatica) en mijn collega's dr. J. Bruining en dr. C.J. de Pater voor hun bijdragen aan dit proefschrift: de eerste voor het schrijven van het rekenprogramma waarmee ik temperatuurvelden kon berekenen, de tweede als mede-auteur van het artikel over het oplossen van radio-actief afval vermengd met glas en de derde voor het met het rekenprogramma MARC berekenen van het temperatuurveld in een oneindig lange rechthoekige staaf.

Het merendeel van de gepresenteerde figuren is van de bekwame hand van J.J. Swanink. R. Ephraïm hielp mij bij het nemen van foto's van pekelinsluitsels via de microscoop. A. Steenhuis fotografeerde nauwgezet de figuren voor de definitieve versie van het proefschrift. Ook naar hen gaat mijn dank uit.

Tenslotte bedank ik Izaak Dekker, Martijn Groenendijk, Bert Meijer en Bas van de Ven die mij hielpen de concept-versie van het proefschrift in ijltempo te vermenigvuldigen.

CURRICULUM VITAE

18 dec. 1943: Geboren te Heerlen.

1961: Eindexamen HBS-B.
St.-Bernardinuscollege, Heerlen.

1965: Eindexamen HTS chemische techniek.
Hogere Technische School, Heerlen.

1965-1967: Vervulling militaire dienstplicht.

1967-1977: Technisch ambtenaar Technische Hogeschool Delft, Afdeling Scheikundige Technologie (Vakgroep Analytische Scheikunde).

1977: Doctoraal examen technische natuurkunde (afstudeerrichting: fysische technologie).
Technische Hogeschool Delft.

1977-1984: Wetenschappelijk ambtenaar Technische Hogeschool Delft bij het TH-project "Ondergrondse berging van radio-actief afval in steenzout".

vanaf 1984: Universitair docent Technische Universiteit Delft, Faculteit Mijnbouwkunde en Petroleumwinning (Vakgroep Petroleumwinning en Technische Geofysica) met als taken:
- onderwijs (colleges "oplosmijnen" en "stromingsleer en warmteoverdracht bij de petroleumwinning");
- onderzoek (projecten "berging van radio-actief afval in steenzout" en "olie-water scheiding").